Flavour physics and CP violation

R. Fleischer
CERN, Geneva, Switzerland

Abstract
The starting point of these lectures is an introduction to the weak interactions of quarks and the Standard-Model description of CP violation, where the central role is played by the Cabibbo–Kobayashi–Maskawa matrix and the corresponding unitarity triangles. Since the B-meson system will govern the stage of (quark) flavour physics and CP violation in this decade, it will be our main focus. We shall classify B-meson decays, introduce the theoretical tools to deal with them, investigate the requirements for non-vanishing CP-violating asymmetries, and discuss the main strategies to explore CP violation and the preferred avenues to enter for physics beyond the Standard Model. This formalism is then applied to discuss the status of important B-factory benchmark modes, where we focus on puzzling patterns in the data that may indicate new-physics effects, as well as the prospects for B-decay studies at the LHC.

1 Introduction

The history of CP violation, i.e., the non-invariance of the weak interactions with respect to a combined charge-conjugation (C) and parity (P) transformation, goes back to 1964 when this phenomenon was discovered through the observation of $K_{\rm L} \to \pi^+\pi^-$ decays [1] which exhibit a branching ratio at the 10^{-3} level. This surprising effect is a manifestation of *indirect* CP violation, which arises from the fact that the mass eigenstates $K_{\rm L,S}$ of the neutral kaon system, which shows K^0–$\bar{K}^0$ mixing, are not eigenstates of the CP operator. In particular, the $K_{\rm L}$ state is governed by the CP-odd eigenstate, but has also a tiny admixture of the CP-even eigenstate, which may decay through CP-conserving interactions into the $\pi^+\pi^-$ final state. These CP-violating effects are described by the following observable:

$$\varepsilon_K = (2.280 \pm 0.013) \times 10^{-3} \times e^{i\pi/4} \,. \tag{1}$$

On the other hand, CP-violating effects may also arise directly at the decay-amplitude level, thereby yielding *direct* CP violation. This phenomenon, which leads to a non-vanishing value of a quantity ${\rm Re}(\varepsilon'_K/\varepsilon_K)$, was established in 1999 through the NA48 (CERN) and KTeV (FNAL) Collaborations [2]; the final results of the corresponding measurements are given by

$${\rm Re}(\varepsilon'_K/\varepsilon_K) = \begin{cases} (14.7 \pm 2.2) \times 10^{-4} & \text{(NA48 [3])} \\ (20.7 \pm 2.8) \times 10^{-4} & \text{(KTeV [4])} \,. \end{cases} \tag{2}$$

In this decade, there are huge experimental efforts to further explore CP violation and the quark-flavour sector of the Standard Model (SM). In these studies, the main actor is the B-meson system, where we distinguish between charged and neutral B mesons, which are characterized by the following valence-quark contents:

$$\begin{array}{llll} B^+ \sim u\bar{b}, & B_c^+ \sim c\bar{b}, & B_d^0 \sim d\bar{b}, & B_s^0 \sim s\bar{b}, \\ B^- \sim \bar{u}b, & B_c^- \sim \bar{c}b, & \bar{B}_d^0 \sim \bar{d}b, & \bar{B}_s^0 \sim \bar{s}b \,. \end{array} \tag{3}$$

In contrast to the charged B mesons, their neutral counterparts B_q ($q \in \{d, s\}$) show —in analogy to K^0–$\bar{K}^0$ mixing—the phenomenon of B_q^0–$\bar{B}_q^0$ mixing. The asymmetric e^+e^- B factories at SLAC and KEK with their detectors BaBar and Belle, respectively, can only produce B^+ and B_d^0 mesons (and

their anti-particles) since they operate at the $\Upsilon(4S)$ resonance, and have already collected $\mathcal{O}(10^8)$ $B\bar{B}$ pairs of this kind. Moreover, first B-physics results from Run II of the Tevatron were reported from the CDF and D0 Collaborations, including also B_c^+ and B_s^0 studies, and second-generation B-decay studies will become possible at the Large Hadron Collider (LHC) at CERN, in particular thanks to the LHCb experiment, starting in the autumn of 2007. For the more distant future, an e^+–e^- 'super-B factory' is under consideration, with an increase of luminosity by up to two orders of magnitude with respect to the currently operating machines. Moreover, there are plans to measure the very 'rare' kaon decays $K^+ \to \pi^+\nu\bar{\nu}$ and $K_{\rm L} \to \pi^0\nu\bar{\nu}$, which are absent at the tree level in the Standard Model (SM), at CERN and KEK/J-PARC.

In 2001, CP-violating effects were discovered in B decays with the help of $B_d \to J/\psi K_{\rm S}$ modes by the BaBar and Belle Collaborations [5], representing the first observation of CP violation outside the kaon system. This particular kind of CP violation, which is by now well established, originates from the interference between B_d^0–$\bar{B}_d^0$ mixing and $B_d^0 \to J/\psi K_{\rm S}$, $\bar{B}_d^0 \to J/\psi K_{\rm S}$ decay processes, and is referred to as 'mixing-induced' CP violation. In the summer of 2004, direct CP violation was detected in $B_d \to \pi^\mp K^\pm$ decays [6], thereby complementing the measurement of a non-zero value of ${\rm Re}(\varepsilon'_K/\varepsilon_K)$.

Studies of CP violation and flavour physics are particularly interesting since 'new physics' (NP), i.e., physics lying beyond the SM, typically leads to new sources of flavour and CP violation. Furthermore, the origin of the fermion masses, flavour mixing, CP violation etc. lies completely in the dark and is expected to involve NP, too. Interestingly, CP violation offers also a link to cosmology. One of the key features of our Universe is the cosmological baryon asymmetry of $\mathcal{O}(10^{-10})$. As was pointed out by Sakharov [7], the necessary conditions for the generation of such an asymmetry include also the requirement that elementary interactions violate CP (and C). Model calculations of the baryon asymmetry indicate, however, that the CP violation present in the SM seems to be too small to generate the observed asymmetry [8]. On the one hand, the required new sources of CP violation could be associated with very high energy scales, as in 'leptogenesis', where new CP-violating effects appear in decays of heavy Majorana neutrinos [9]. On the other hand, new sources of CP violation could also be accessible in the laboratory, as they arise naturally when going beyond the SM.

Before searching for NP, it is essential to understand first the picture of flavour physics and CP violation arising in the framework of the SM, where the Cabibbo–Kobayashi–Maskawa (CKM) matrix—the quark-mixing matrix—plays the key role [10, 11]. The corresponding phenomenology is extremely rich [12]. In general, the key problem for the theoretical interpretation is related to strong interactions, i.e., to 'hadronic' uncertainties. A famous example is ${\rm Re}(\varepsilon'_K/\varepsilon_K)$, where we have to deal with a subtle interplay between different contributions which largely cancel [13]. Although the non-vanishing value of this quantity has unambiguously ruled out 'superweak' models of CP violation [14], it currently does not allow a stringent test of the SM.

In the B-meson system, there are various strategies to eliminate the hadronic uncertainties in the exploration of CP violation (simply speaking, there are many B decays). Moreover, we may also search for relations and/or correlations that hold in the SM but could well be spoiled by NP. These topics will be the focus of this lecture, which is complemented by the dedicated lectures on the experimental aspects of K- and B-meson decays in Refs. [15] and [16], respectively. The outline is as follows: in Section 2, we discuss the quark mixing in the SM by having a closer look at the CKM matrix and the associated unitarity triangles. The main actors of this lecture—the B mesons and their weak decays—will then be introduced in Section 3. There we shall also move towards studies of CP violation and shall classify the main strategies for its exploration, using amplitude relations and the phenomenon of B_q^0–$\bar{B}_q^0$ mixing ($q \in \{d, s\}$). In Section 4, we illustrate the former kind of methods by having a closer look at clean amplitude relations between $B^\pm \to K^\pm D$ and $B_c^\pm \to D_s^\pm D$ decays, whereas we discuss features of neutral B_q mesons in Section 5. In Section 6, we address the question of how NP could enter, and then apply these considerations in Section 7 to the B-factory benchmark modes $B_d^0 \to J/\psi K_{\rm S}$, $B_d^0 \to \phi K_{\rm S}$ and $B_d^0 \to \pi^+\pi^-$. Since the data for certain $B \to \pi K$ decays have shown a puzzling pattern for several

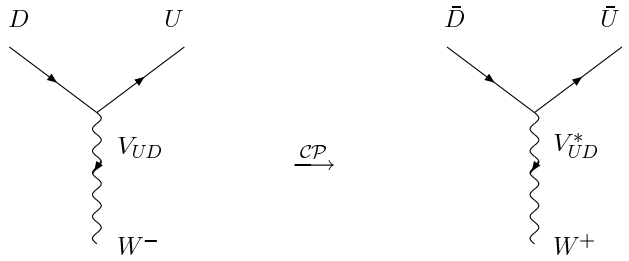

Fig. 1: CP-conjugate charged-current quark-level interaction processes in the SM

years, we have devoted Section 8 to a detailed discussion of this '$B \to \pi K$ puzzle' and its interplay with rare K and B decays. In Section 9, we focus on $b \to d$ penguin processes, which are now coming within experimental reach at the B factories, thereby offering an exciting new playground. Finally, in Section 10, we discuss B-decay studies at the LHC, where the physics potential of the B_s^0-meson system can be fully exploited. The conclusions and a brief outlook are given in Section 11.

For detailed discussions and textbooks dealing with flavour physics and CP violation, the reader is referred to Refs. [17]– [21], alternative lecture notes can be found in Refs. [22, 23], and a selection of more compact recent reviews is given in Refs. [24]– [26]. The data used in these lectures refer to the situation in the spring of 2006.

2 CP violation in the Standard Model

2.1 Weak interactions of quarks and the quark-mixing matrix

In the framework of the Standard Model of electroweak interactions [27, 28], which is based on the spontaneously broken gauge group

$$SU(2)_{\rm L} \times U(1)_{\rm Y} \stackrel{\rm SSB}{\longrightarrow} U(1)_{\rm em} \,, \tag{4}$$

CP-violating effects may originate from the charged-current interactions of quarks, having the structure

$$D \to U W^- \,. \tag{5}$$

Here $D \in \{d, s, b\}$ and $U \in \{u, c, t\}$ denote down- and up-type quark flavours, respectively, whereas the W^- is the usual $SU(2)_{\rm L}$ gauge boson. From a phenomenological point of view, it is convenient to collect the generic 'coupling strengths' V_{UD} of the charged-current processes in (5) in the form of the following matrix:

$$\hat{V}_{\rm CKM} = \left(\begin{array}{ccc} V_{ud} & V_{us} & V_{ub} \\ V_{cd} & V_{cs} & V_{cb} \\ V_{td} & V_{ts} & V_{tb} \end{array} \right) , \tag{6}$$

which is referred to as the Cabibbo–Kobayashi–Maskawa (CKM) matrix [10, 11].

From a theoretical point of view, this matrix connects the electroweak states (d', s', b') of the down, strange and bottom quarks with their mass eigenstates (d, s, b) through the following unitary transformation [27]:

$$\left(\begin{array}{c} d' \\ s' \\ b' \end{array} \right) = \left(\begin{array}{ccc} V_{ud} & V_{us} & V_{ub} \\ V_{cd} & V_{cs} & V_{cb} \\ V_{td} & V_{ts} & V_{tb} \end{array} \right) \cdot \left(\begin{array}{c} d \\ s \\ b \end{array} \right) . \tag{7}$$

Consequently, $\hat{V}_{\rm CKM}$ is actually a *unitary* matrix. This feature ensures the absence of flavour-changing neutral-current (FCNC) processes at the tree level in the SM, and is hence at the basis of the famous

Glashow–Iliopoulos–Maiani (GIM) mechanism [29]. We shall return to the unitarity of the CKM matrix in Section 2.6, discussing the 'unitarity triangles'. If we express the non-leptonic charged-current interaction Lagrangian in terms of the mass eigenstates appearing in (7), we arrive at

$$\mathcal{L}_{\rm int}^{\rm CC} = -\frac{g_2}{\sqrt{2}} \left(\begin{array}{ccc} \bar{u}_{\rm L}, & \bar{c}_{\rm L}, & \bar{t}_{\rm L} \end{array} \right) \gamma^\mu \hat{V}_{\rm CKM} \left(\begin{array}{c} d_{\rm L} \\ s_{\rm L} \\ b_{\rm L} \end{array} \right) W_\mu^\dagger \; + \; \text{h.c.}, \tag{8}$$

where the gauge coupling g_2 is related to the gauge group $SU(2)_{\rm L}$, and the $W_\mu^{(\dagger)}$ field corresponds to the charged W bosons. Looking at the interaction vertices following from (8), we observe that the elements of the CKM matrix describe in fact the generic strengths of the associated charged-current processes, as we have noted above.

In Fig. 1, we show the $D \to UW^-$ vertex and its CP conjugate. Since the corresponding CP transformation involves the replacement

$$V_{UD} \stackrel{\mathcal{CP}}{\longrightarrow} V_{UD}^* \, , \tag{9}$$

CP violation could—in principle—be accommodated in the SM through complex phases in the CKM matrix. The crucial question in this context is, of course, whether we may actually have physical complex phases in that matrix.

2.2 Phase structure of the CKM matrix

We have the freedom to redefine the up- and down-type quark fields in the following manner:

$$U \to \exp(i\xi_U) U, \quad D \to \exp(i\xi_D) D \, . \tag{10}$$

If we perform such transformations in (8), the invariance of the charged-current interaction Lagrangian implies the following phase transformations of the CKM matrix elements:

$$V_{UD} \to \exp(i\xi_U) V_{UD} \exp(-i\xi_D) \, . \tag{11}$$

Using these transformations to eliminate unphysical phases, it can be shown that the parametrization of the general $N \times N$ quark-mixing matrix, where N denotes the number of fermion generations, involves the following parameters:

$$\underbrace{\frac{1}{2} N(N-1)}_{\text{Euler angles}} + \underbrace{\frac{1}{2}(N-1)(N-2)}_{\text{complex phases}} = (N-1)^2 . \tag{12}$$

If we apply this expression to the case of $N = 2$ generations, we observe that only one rotation angle—the Cabibbo angle $\theta_{\rm C}$ [10]—is required for the parametrization of the 2×2 quark-mixing matrix, which can be written in the following form:

$$\hat{V}_{\rm C} = \left(\begin{array}{cc} \cos\theta_{\rm C} & \sin\theta_{\rm C} \\ -\sin\theta_{\rm C} & \cos\theta_{\rm C} \end{array} \right) , \tag{13}$$

where $\sin\theta_{\rm C} = 0.22$ can be determined from $K \to \pi \ell \bar{\nu}$ decays. On the other hand, in the case of $N = 3$ generations, the parametrization of the corresponding 3×3 quark-mixing matrix involves three Euler-type angles and a single *complex* phase. This complex phase allows us to accommodate CP violation in the SM, as was pointed out by Kobayashi and Maskawa in 1973 [11]. The corresponding picture is referred to as the Kobayashi–Maskawa (KM) mechanism of CP violation.

In the 'standard parametrization' advocated by the Particle Data Group (PDG) [30], the three-generation CKM matrix takes the following form:

$$\hat{V}_{\rm CKM} = \begin{pmatrix} c_{12}c_{13} & s_{12}c_{13} & s_{13}e^{-i\delta_{13}} \\ -s_{12}c_{23} - c_{12}s_{23}s_{13}e^{i\delta_{13}} & c_{12}c_{23} - s_{12}s_{23}s_{13}e^{i\delta_{13}} & s_{23}c_{13} \\ s_{12}s_{23} - c_{12}c_{23}s_{13}e^{i\delta_{13}} & -c_{12}s_{23} - s_{12}c_{23}s_{13}e^{i\delta_{13}} & c_{23}c_{13} \end{pmatrix}, \tag{14}$$

where $c_{ij} \equiv \cos\theta_{ij}$ and $s_{ij} \equiv \sin\theta_{ij}$. Performing appropriate redefinitions of the quark-field phases, the real angles θ_{12}, θ_{23} and θ_{13} can all be made to lie in the first quadrant. The advantage of this parametrization is that the generation labels $i, j = 1, 2, 3$ are introduced in such a manner that the mixing between two chosen generations vanishes if the corresponding mixing angle θ_{ij} is set to zero. In particular, for $\theta_{23} = \theta_{13} = 0$, the third generation decouples, and the 2×2 submatrix describing the mixing between the first and second generations takes the same form as (13).

Another interesting parametrization of the CKM matrix was proposed by Fritzsch and Xing [31]:

$$\hat{V}_{\rm CKM} = \begin{pmatrix} s_{\rm u}s_{\rm d}c + c_{\rm u}c_{\rm d}e^{-i\varphi} & s_{\rm u}c_{\rm d}c - c_{\rm u}s_{\rm d}e^{-i\varphi} & s_{\rm u}s \\ c_{\rm u}s_{\rm d}c - s_{\rm u}c_{\rm d}e^{-i\varphi} & c_{\rm u}c_{\rm d}c + s_{\rm u}s_{\rm d}e^{-i\varphi} & c_{\rm u}s \\ -s_{\rm d}s & -c_{\rm d}s & c \end{pmatrix}. \tag{15}$$

It is inspired by the hierarchical structure of the quark-mass spectrum and is particularly useful in the context of models for fermion masses and mixings. The characteristic feature of this parametrization is that the complex phase arises only in the 2×2 submatrix involving the up, down, strange and charm quarks.

Let us finally note that physical observables, for instance CP-violating asymmetries, *cannot* depend on the chosen parametrization of the CKM matrix, i.e., have to be invariant under the phase transformations specified in (11).

2.3 Further requirements for CP violation

As we have just seen, in order to be able to accommodate CP violation within the framework of the SM through a complex phase in the CKM matrix, at least three generations are required. However, this feature is not sufficient for observable CP-violating effects. To this end, further conditions have to be satisfied, which can be summarized as follows [32, 33]:

$$(m_t^2 - m_c^2)(m_t^2 - m_u^2)(m_c^2 - m_u^2)(m_b^2 - m_s^2)(m_b^2 - m_d^2)(m_s^2 - m_d^2) \times J_{\rm CP} \neq 0, \tag{16}$$

where

$$J_{\rm CP} = |{\rm Im}(V_{i\alpha}V_{j\beta}V_{i\beta}^*V_{j\alpha}^*)| \quad (i \neq j,\, \alpha \neq \beta)\,. \tag{17}$$

The mass factors in (16) are related to the fact that the CP-violating phase of the CKM matrix could be eliminated through an appropriate unitary transformation of the quark fields if any two quarks with the same charge had the same mass. Consequently, the origin of CP violation is closely related to the 'flavour problem' in elementary particle physics, and cannot be understood in a deeper way, unless we have fundamental insights into the hierarchy of quark masses and the number of fermion generations.

The second element of (16), the 'Jarlskog parameter' $J_{\rm CP}$ [32], can be interpreted as a measure of the strength of CP violation in the SM. It does not depend on the chosen quark-field parametrization, i.e., it is invariant under (11), and the unitarity of the CKM matrix implies that all combinations $|{\rm Im}(V_{i\alpha}V_{j\beta}V_{i\beta}^*V_{j\alpha}^*)|$ are equal to one another. Using the standard parametrization of the CKM matrix introduced in (14), we obtain

$$J_{\rm CP} = s_{12}s_{13}s_{23}c_{12}c_{23}c_{13}^2 \sin\delta_{13}\,. \tag{18}$$

The experimental information on the CKM parameters implies $J_{\rm CP} = \mathcal{O}(10^{-5})$, so that CP-violating phenomena are hard to observe. However, new complex couplings are typically present in scenarios for NP [34]. Such additional sources for CP violation could be detected through flavour experiments.

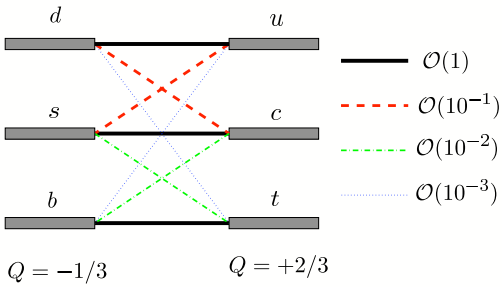

Fig. 2: Hierarchy of the quark transitions mediated through charged-current processes

2.4 Experimental information on $|V_{\rm CKM}|$

In order to determine the magnitudes $|V_{ij}|$ of the elements of the CKM matrix, we may use the following tree-level processes:

- Nuclear beta decays, neutron decays $\Rightarrow |V_{ud}|$.
- $K \to \pi\ell\bar{\nu}$ decays $\Rightarrow |V_{us}|$.
- ν production of charm off valence d quarks $\Rightarrow |V_{cd}|$.
- Charm-tagged W decays (as well as ν production and semileptonic D decays) $\Rightarrow |V_{cs}|$.
- Exclusive and inclusive $b \to c\ell\bar{\nu}$ decays $\Rightarrow |V_{cb}|$.
- Exclusive and inclusive $b \to u\ell\bar{\nu}$ decays $\Rightarrow |V_{ub}|$.
- $\bar{t} \to \bar{b}\ell\bar{\nu}$ processes $\Rightarrow$ (crude direct determination of) $|V_{tb}|$.

If we use the corresponding experimental information, together with the CKM unitarity condition, and assume that there are only three generations, we arrive at the following 90% C.L. limits for the $|V_{ij}|$ [30]:

$$|\hat{V}_{\rm CKM}| = \begin{pmatrix} 0.9739\text{–}0.9751 & 0.221\text{–}0.227 & 0.0029\text{–}0.0045 \\ 0.221\text{–}0.227 & 0.9730\text{–}0.9744 & 0.039\text{–}0.044 \\ 0.0048\text{–}0.014 & 0.037\text{–}0.043 & 0.9990\text{–}0.9992 \end{pmatrix} . \tag{19}$$

In Fig. 2, we have illustrated the resulting hierarchy of the strengths of the charged-current quark-level processes: transitions within the same generation are governed by CKM matrix elements of $\mathcal{O}(1)$, those between the first and the second generation are suppressed by CKM factors of $\mathcal{O}(10^{-1})$, those between the second and the third generation are suppressed by $\mathcal{O}(10^{-2})$, and the transitions between the first and the third generation are even suppressed by CKM factors of $\mathcal{O}(10^{-3})$. In the standard parametrization (14), this hierarchy is reflected by

$$s_{12} = 0.22 \gg s_{23} = \mathcal{O}(10^{-2}) \gg , s_{13} = \mathcal{O}(10^{-3}) . \tag{20}$$

2.5 Wolfenstein parametrization of the CKM matrix

For phenomenological applications, it would be useful to have a parametrization of the CKM matrix available that makes the hierarchy arising in (19)—and illustrated in Fig. 2—explicit [35]. In order to derive such a parametrization, we introduce a set of new parameters, λ, A, ρ and η, by imposing the following relations [36]:

$$s_{12} \equiv \lambda = 0.22, \quad s_{23} \equiv A\lambda^2, \quad s_{13}e^{-i\delta_{13}} \equiv A\lambda^3(\rho - i\eta) . \tag{21}$$

If we now go back to the standard parametrization (14), we obtain an *exact* parametrization of the CKM matrix as a function of λ (and A, ρ, η), allowing us to expand each CKM element in powers of the small

parameter λ. If we neglect terms of $\mathcal{O}(\lambda^4)$, we arrive at the famous 'Wolfenstein parametrization' [35]:

$$\hat{V}_{\rm CKM} = \begin{pmatrix} 1-\frac{1}{2}\lambda^2 & \lambda & A\lambda^3(\rho-i\eta) \\ -\lambda & 1-\frac{1}{2}\lambda^2 & A\lambda^2 \\ A\lambda^3(1-\rho-i\eta) & -A\lambda^2 & 1 \end{pmatrix} + \mathcal{O}(\lambda^4)\,, \tag{22}$$

which makes the hierarchical structure of the CKM matrix very transparent and is an important tool for phenomenological considerations, as we shall see throughout these lectures.

For several applications, next-to-leading order corrections in λ play an important role. Using the exact parametrization following from (14) and (21), they can be calculated straightforwardly by expanding each CKM element to the desired accuracy in λ [36, 37]:

$$\begin{gathered} V_{ud} = 1 - \frac{1}{2}\lambda^2 - \frac{1}{8}\lambda^4 + \mathcal{O}(\lambda^6)\,, \quad V_{us} = \lambda + \mathcal{O}(\lambda^7)\,, \quad V_{ub} = A\lambda^3(\rho - i\,\eta)\,, \\ V_{cd} = -\lambda + \frac{1}{2}A^2\lambda^5\left[1 - 2(\rho + i\eta)\right] + \mathcal{O}(\lambda^7)\,, \\ V_{cs} = 1 - \frac{1}{2}\lambda^2 - \frac{1}{8}\lambda^4(1+4A^2) + \mathcal{O}(\lambda^6)\,, \\ V_{cb} = A\lambda^2 + \mathcal{O}(\lambda^8)\,, \quad V_{td} = A\lambda^3\left[1 - (\rho+i\eta)\left(1 - \frac{1}{2}\lambda^2\right)\right] + \mathcal{O}(\lambda^7)\,, \\ V_{ts} = -A\lambda^2 + \frac{1}{2}A(1-2\rho)\lambda^4 - i\eta A\lambda^4 + \mathcal{O}(\lambda^6)\,, \quad V_{tb} = 1 - \frac{1}{2}A^2\lambda^4 + \mathcal{O}(\lambda^6)\,. \end{gathered} \tag{23}$$

It should be noted that

$$V_{ub} \equiv A\lambda^3(\rho - i\eta) \tag{24}$$

receives *by definition* no power corrections in λ within this prescription. If we follow Ref. [36] and introduce the generalized Wolfenstein parameters

$$\bar{\rho} \equiv \rho\left(1 - \frac{1}{2}\lambda^2\right), \quad \bar{\eta} \equiv \eta\left(1 - \frac{1}{2}\lambda^2\right), \tag{25}$$

we may simply write, up to corrections of $\mathcal{O}(\lambda^7)$,

$$V_{td} = A\lambda^3(1 - \bar{\rho} - i\,\bar{\eta})\,. \tag{26}$$

Moreover, we have to an excellent accuracy

$$V_{us} = \lambda \quad \text{and} \quad V_{cb} = A\lambda^2\,, \tag{27}$$

as these quantities receive only corrections at the λ^7 and λ^8 levels, respectively. In comparison with other generalizations of the Wolfenstein parametrization found in the literature, the advantage of (23) is the absence of relevant corrections to V_{us} and V_{cb}, and that V_{ub} and V_{td} take forms similar to those in (22). As far as the Jarlskog parameter introduced in (17) is concerned, we obtain the simple expression

$$J_{\rm CP} = \lambda^6 A^2 \eta\,, \tag{28}$$

which should be compared with (18).

2.6 Unitarity triangles of the CKM matrix

The unitarity of the CKM matrix, which is described by

$$\hat{V}_{\rm CKM}^{\dagger}\cdot\hat{V}_{\rm CKM}=\hat{1}=\hat{V}_{\rm CKM}\cdot\hat{V}_{\rm CKM}^{\dagger}\,, \tag{29}$$

leads to a set of 12 equations, consisting of 6 normalization and 6 orthogonality relations. The latter can be represented as 6 triangles in the complex plane [38], all having the same area, $2A_\Delta = J_{\rm CP}$ [39]. Let us now have a closer look at these relations: those describing the orthogonality of different columns of the CKM matrix are given by

$$\underbrace{V_{ud}V_{us}^*}_{\mathcal{O}(\lambda)}+\underbrace{V_{cd}V_{cs}^*}_{\mathcal{O}(\lambda)}+\underbrace{V_{td}V_{ts}^*}_{\mathcal{O}(\lambda^5)} = 0 \tag{30}$$

$$\underbrace{V_{us}V_{ub}^*}_{\mathcal{O}(\lambda^4)}+\underbrace{V_{cs}V_{cb}^*}_{\mathcal{O}(\lambda^2)}+\underbrace{V_{ts}V_{tb}^*}_{\mathcal{O}(\lambda^2)} = 0 \tag{31}$$

$$\underbrace{V_{ud}V_{ub}^*}_{(\rho+i\eta)A\lambda^3}+\underbrace{V_{cd}V_{cb}^*}_{-A\lambda^3}+\underbrace{V_{td}V_{tb}^*}_{(1-\rho-i\eta)A\lambda^3} = 0\,, \tag{32}$$

whereas those associated with the orthogonality of different rows take the following form:

$$\underbrace{V_{ud}^*V_{cd}}_{\mathcal{O}(\lambda)}+\underbrace{V_{us}^*V_{cs}}_{\mathcal{O}(\lambda)}+\underbrace{V_{ub}^*V_{cb}}_{\mathcal{O}(\lambda^5)} = 0 \tag{33}$$

$$\underbrace{V_{cd}^*V_{td}}_{\mathcal{O}(\lambda^4)}+\underbrace{V_{cs}^*V_{ts}}_{\mathcal{O}(\lambda^2)}+\underbrace{V_{cb}^*V_{tb}}_{\mathcal{O}(\lambda^2)} = 0 \tag{34}$$

$$\underbrace{V_{ud}^*V_{td}}_{(1-\rho-i\eta)A\lambda^3}+\underbrace{V_{us}^*V_{ts}}_{-A\lambda^3}+\underbrace{V_{ub}^*V_{tb}}_{(\rho+i\eta)A\lambda^3} = 0\,. \tag{35}$$

Here we have also indicated the structures that arise if we apply the Wolfenstein parametrization by keeping just the leading, non-vanishing terms. We observe that only in (32) and (35), which describe the orthogonality of the first and third columns and of the first and third rows, respectively, are all three sides of comparable magnitude, $\mathcal{O}(\lambda^3)$, while in the remaining relations, one side is suppressed with respect to the others by factors of $\mathcal{O}(\lambda^2)$ or $\mathcal{O}(\lambda^4)$. Consequently, we have to deal with only *two* non-squashed unitarity triangles in the complex plane. However, as we have already indicated in (32) and (35), the corresponding orthogonality relations agree with each other at the λ^3 level, yielding

$$\left[(\rho+i\eta)+(-1)+(1-\rho-i\eta)\right]A\lambda^3=0\,. \tag{36}$$

Consequently, they describe the same triangle, which is usually referred to as *the* unitarity triangle of the CKM matrix [39,40].

Concerning second-generation B-decay studies in the LHC era, the experimental accuracy will be so tremendous that we shall also have to take the next-to-leading order terms of the Wolfenstein expansion into account, and shall have to distinguish between the unitarity triangles following from (32) and (35). Let us first have a closer look at the former relation. Including terms of $\mathcal{O}(\lambda^5)$, we obtain the following generalization of (36):

$$\left[(\bar\rho+i\bar\eta)+(-1)+(1-\bar\rho-i\bar\eta)\right]A\lambda^3+\mathcal{O}(\lambda^7)=0\,, \tag{37}$$

where $\bar\rho$ and $\bar\eta$ are as defined in (25). If we divide this relation by the overall normalization factor $A\lambda^3$, and introduce

$$R_b\equiv\sqrt{\overline{\rho}^2+\overline{\eta}^2}=\left(1-\frac{\lambda^2}{2}\right)\frac{1}{\lambda}\left|\frac{V_{ub}}{V_{cb}}\right| \tag{38}$$

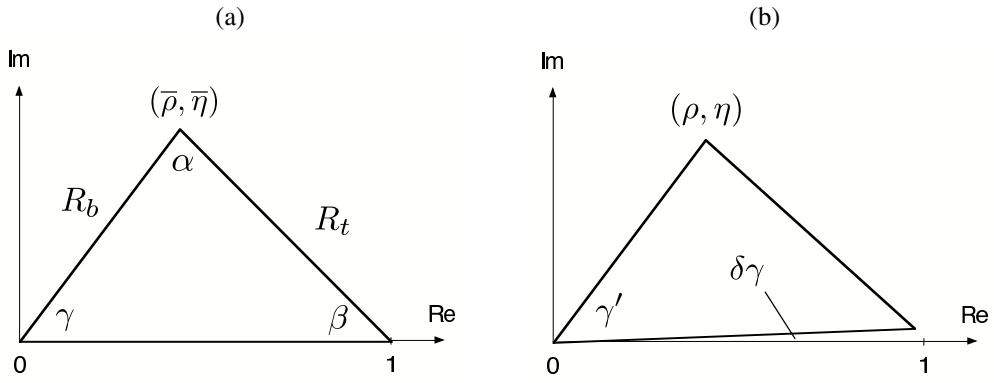

Fig. 3: The two non-squashed unitarity triangles of the CKM matrix, as explained in the text: (a) and (b) correspond to the orthogonality relations (32) and (35), respectively. In Asia, the notation $\phi_1 \equiv \beta$, $\phi_2 \equiv \alpha$, and $\phi_3 \equiv \gamma$ is used for the angles of the triangle shown in (a).

$$R_t \equiv \sqrt{(1-\overline{\rho})^2+\overline{\eta}^2} = \frac{1}{\lambda}\left|\frac{V_{td}}{V_{cb}}\right| , \tag{39}$$

we arrive at the unitarity triangle illustrated in Fig. 3 (a). It is a straightforward generalization of the leading-order case described by (36): instead of (ρ,η), the apex is now simply given by $(\bar{\rho},\bar{\eta})$ [36]. The two sides R_b and R_t, as well as the three angles α, β and γ, will show up at several places throughout these lectures. Moreover, the relations

$$V_{ub} = A\lambda^3\left(\frac{R_b}{1-\lambda^2/2}\right)e^{-i\gamma}, \quad V_{td} = A\lambda^3 R_t e^{-i\beta} \tag{40}$$

are also useful for phenomenological applications, since they make the dependences of γ and β explicit; they correspond to the phase convention chosen both in the standard parametrization (14) and in the generalized Wolfenstein parametrization (23). Finally, if we take also (21) into account, we obtain

$$\delta_{13} = \gamma \, . \tag{41}$$

Let us now turn to (35). Here we arrive at an expression that is more complicated than (37):

$$\left[\left\{1-\frac{\lambda^2}{2}-(1-\lambda^2)\rho - i(1-\lambda^2)\eta\right\}+\left\{-1+\left(\frac{1}{2}-\rho\right)\lambda^2 - i\eta\lambda^2\right\}+\{\rho+i\eta\}\right]A\lambda^3+\mathcal{O}(\lambda^7)=0. \tag{42}$$

If we divide again by $A\lambda^3$, we obtain the unitarity triangle sketched in Fig. 3 (b), where the apex is given by (ρ,η) and *not* by $(\bar{\rho},\bar{\eta})$. On the other hand, we encounter a tiny angle

$$\delta\gamma \equiv \lambda^2\eta = \mathcal{O}(1^\circ) \tag{43}$$

between real axis and basis of the triangle, which satisfies

$$\gamma = \gamma' + \delta\gamma \, , \tag{44}$$

where γ coincides with the corresponding angle in Fig. 3 (a).

Whenever we refer to a 'unitarity triangle' (UT) in the following discussion, we mean the one illustrated in Fig. 3 (a), which is the generic generalization of the leading-order case described by (36). As we shall see below, the UT is the central target of the experimental tests of the SM description of CP violation. Interestingly, the tiny angle $\delta\gamma$ also can be probed directly through certain CP-violating effects that can be explored at hadron colliders, in particular at the LHC.

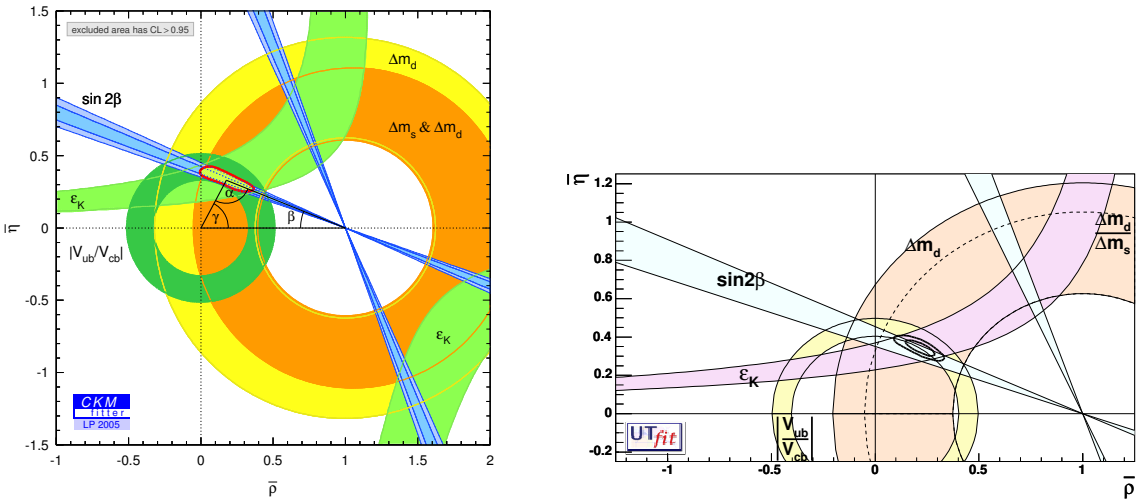

Fig. 4: Analyses of the CKMfitter and UTfit Collaborations [41, 42]

2.7 The determination of the unitarity triangle

The next obvious question is how to determine the UT. There are two conceptually different avenues that we may follow:

(i) In the 'CKM fits', theory is used to convert experimental data into contours in the $\bar{\rho}$–$\bar{\eta}$ plane. In particular, semi-leptonic $b \to u\ell\bar{\nu}_\ell$, $c\ell\bar{\nu}_\ell$ decays and B_q^0–$\bar{B}_q^0$ mixing ($q \in \{d, s\}$) allow us to determine the UT sides R_b and R_t, respectively, i.e., to fix two circles in the $\bar{\rho}$–$\bar{\eta}$ plane. Furthermore, the indirect CP violation in the neutral kaon system described by ε_K can be transformed into a hyperbola.

(ii) Theoretical considerations allow us to convert measurements of CP-violating effects in B-meson decays into direct information on the UT angles. The most prominent example is the determination of $\sin 2\beta$ through CP violation in $B_d^0 \to J/\psi K_S$ decays, but several other strategies were proposed.

The goal is to 'overconstrain' the UT as much as possible. In the future, additional contours can be fixed in the $\bar{\rho}$–$\bar{\eta}$ plane through the measurement of rare decays.

In Fig. 4, we show examples of the comprehensive analyses of the UT that are performed (and continuously updated) by the 'CKM Fitter Group' [41] and the 'UTfit Collaboration' [42]. In these figures, we can nicely see the circles that are determined through the semi-leptonic B decays and the ε_K hyperbolas. Moreover, the straight lines following from the direct measurement of $\sin 2\beta$ with the help of $B_d^0 \to J/\psi K_S$ modes are also shown. We observe that the global consistency is very good. However, looking closer, we also see that the most recent average for $(\sin 2\beta)_{\psi K_S}$ is now on the lower side, so that the situation in the $\bar{\rho}$–$\bar{\eta}$ plane is no longer 'perfect'. As we shall discuss in detail in the course of these lectures, there are certain puzzles in the B-factory data, and several important aspects have not yet been addressed experimentally and are hence still essentially unexplored. Consequently, we may hope that flavour studies will eventually establish deviations from the SM description of CP violation. Since B mesons play a key role in these explorations, let us next have a closer look at them.

3 Decays of B mesons

The B-meson system consists of charged and neutral B mesons, which are characterized by the valence quark contents in (3). The characteristic feature of the neutral B_q ($q \in \{d, s\}$) mesons is the phenomenon of B_q^0–$\bar{B}_q^0$ mixing, which will be discussed in Section 5. As far as the weak decays of B mesons are concerned, we distinguish between leptonic, semileptonic, and non-leptonic transitions.

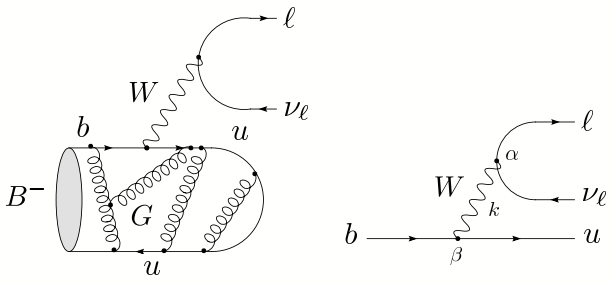

Fig. 5: Feynman diagrams contributing to the leptonic decay $B^- \to \ell\bar{\nu}_\ell$

3.1 Leptonic decays

The simplest B-meson decay class is given by leptonic decays of the kind $B^- \to \ell\bar{\nu}_\ell$, as illustrated in Fig. 5. If we evaluate the corresponding Feynman diagram, we arrive at the following transition amplitude:

$$T_{fi} = -\frac{g_2^2}{8} V_{ub} \underbrace{[\bar{u}_\ell \gamma^\alpha (1-\gamma_5) v_\nu]}_{\text{Dirac spinors}} \left[\frac{g_{\alpha\beta}}{k^2 - M_W^2}\right] \underbrace{\langle 0|\bar{u}\gamma^\beta(1-\gamma_5)b|B^-\rangle}_{\text{hadronic ME}} , \tag{45}$$

where g_2 is the $SU(2)_{\rm L}$ gauge coupling, V_{ub} the corresponding element of the CKM matrix, α and β are Lorentz indices, and M_W denotes the mass of the W gauge boson. Since the four-momentum k that is carried by the W satisfies $k^2 = M_B^2 \ll M_W^2$, we may write

$$\frac{g_{\alpha\beta}}{k^2 - M_W^2} \quad \longrightarrow \quad -\frac{g_{\alpha\beta}}{M_W^2} \equiv -\left(\frac{8 G_{\rm F}}{\sqrt{2} g_2^2}\right) g_{\alpha\beta} , \tag{46}$$

where $G_{\rm F}$ is Fermi's constant. Consequently, we may 'integrate out' the W boson in (45), which yields

$$T_{fi} = \frac{G_{\rm F}}{\sqrt{2}} V_{ub} \, [\bar{u}_\ell \gamma^\alpha (1-\gamma_5) v_\nu] \, \langle 0|\bar{u}\gamma_\alpha(1-\gamma_5)b|B^-\rangle . \tag{47}$$

In this simple expression, *all* the hadronic physics is encoded in the *hadronic matrix element*

$$\langle 0|\bar{u}\gamma_\alpha(1-\gamma_5)b|B^-\rangle ,$$

i.e., there are no other strong-interaction QCD effects (for a detailed discussion of QCD, see Ref. [43]). Since the B^- meson is a pseudoscalar particle, we have

$$\langle 0|\overline{u}\gamma_\alpha b|B^-\rangle = 0 , \tag{48}$$

and may write

$$\langle 0|\bar{u}\gamma_\alpha\gamma_5 b|B^-(q)\rangle = i f_B q_\alpha , \tag{49}$$

where f_B is the B-meson *decay constant*, which is an important input for phenomenological studies. In order to determine this quantity, which is a very challenging task, non-perturbative techniques, such as QCD sum-rule analyses [44] or lattice studies, where a numerical evaluation of the QCD path integral is performed with the help of a space-time lattice, [45]– [47], are required. If we use (47) with (48) and (49), and perform the corresponding phase-space integrations, we obtain the following decay rate:

$$\Gamma(B^- \to \ell\bar{\nu}_\ell) = \frac{G_{\rm F}^2}{8\pi} M_B m_\ell^2 \left(1 - \frac{m_\ell^2}{M_B^2}\right)^2 f_B^2 |V_{ub}|^2 , \tag{50}$$

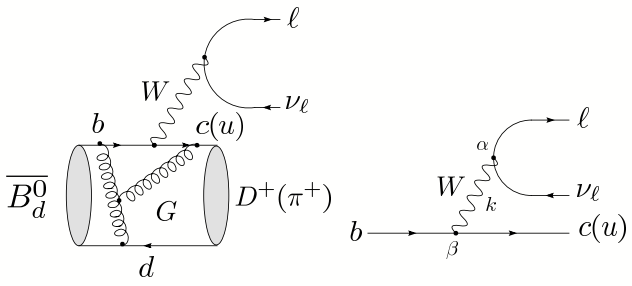

Fig. 6: Feynman diagrams contributing to semileptonic $\bar{B}^0_d \to D^+(\pi^+)\ell\bar{\nu}_\ell$ decays

where M_B and m_ℓ denote the masses of the B^- and ℓ, respectively. Because of the tiny value of $|V_{ub}| \propto \lambda^3$ and a helicity-suppression mechanism, we obtain unfortunately very small branching ratios of $\mathcal{O}(10^{-10})$ and $\mathcal{O}(10^{-7})$ for $\ell = e$ and $\ell = \mu$, respectively [48]. The helicity suppression is not effective for $\ell = \tau$, but—because of the required τ reconstruction—these modes are also very challenging from an experimental point of view. Nevertheless, the Belle experiment has recently reported the first evidence for the purely leptonic decay $B^- \to \tau^-\bar{\nu}_\tau$, with the following branching ratio [49]:

$$\mathrm{BR}(B^- \to \tau^-\bar{\nu}_\tau) = \left[1.06^{+0.34}_{-0.28}\,,(\mathrm{stat})\,^{+0.18}_{-0.16}\,(\mathrm{syst})\right] \times 10^{-4}\,, \tag{51}$$

which corresponds to a significance of 4.2 standard deviations. Using the SM expression for this branching ratio and the measured values of $G_{\rm F}$, M_B, m_τ and the B-meson lifetime, the product of the B-meson decay constant f_B and the magnitude of the CKM matrix element $|V_{ub}|$ is obtained as

$$f_B|V_{ub}| = \left[7.73^{+1.24}_{-1.02}\,(\mathrm{stat})\,^{+0.66}_{-0.58}\,(\mathrm{syst})\right] \times 10^{-4}\,\mathrm{GeV}\,. \tag{52}$$

The determination of this quantity is very interesting, as knowledge of $|V_{ub}|$ allows us to extract f_B, thereby providing tests of non-perturbative calculations of this important parameter.

Before discussing the determination of $|V_{ub}|$ from semileptonic B decays in the next subsection, let us have a look at the leptonic D-meson decay $D^+ \to \mu^+\nu$. It is governed by the CKM factor

$$|V_{cd}| = |V_{us}| + \mathcal{O}(\lambda^5) = \lambda[1 + \mathcal{O}(\lambda^4)]\,, \tag{53}$$

whereas $B^- \to \mu^-\bar{\nu}$ involves $|V_{ub}| = \lambda^3 R_b$. Consequently, we win a factor of $\mathcal{O}(\lambda^4)$ in the decay rate, so that $D^+ \to \mu^+\nu$ is accessible at the CLEO-c experiment [50]. Since the corresponding CKM factor is well known, the decay constant f_{D^+} defined in analogy to (49) can be extracted, allowing another interesting testing ground for lattice calculations. Thanks to recent progress in these techniques [51], the 'quenched' approximation, which had to be applied for many many years and ingnores quark loops, is no longer required for the calculation of f_{D^+}. In the summer of 2005, there was a first showdown between the corresponding theoretical prediction and experiment: the lattice result of $f_{D^+} = (201 \pm 3 \pm 17)$MeV was reported [52], while CLEO-c announced the measurement of $f_{D^+} = (222.6 \pm 16.7^{+2.8}_{-3.4})$ MeV [53]. Both numbers agree well within the uncertainties, and it will be interesting to stay tuned for future results.

3.2 Semileptonic decays

3.2.1 General structure

Semileptonic B-meson decays of the kind shown in Fig. 6 have a structure that is more complicated than the one of the leptonic transitions. If we evaluate the corresponding Feynman diagram for the $b \to c$ case, we obtain

$$T_{fi} = -\frac{g_2^2}{8} V_{cb} \underbrace{[\bar{u}_\ell \gamma^\alpha (1-\gamma_5) v_\nu]}_{\text{Dirac spinors}} \left[\frac{g_{\alpha\beta}}{k^2 - M_W^2}\right] \underbrace{\langle D^+|\bar{c}\gamma^\beta(1-\gamma_5)b|\bar{B}^0_d\rangle}_{\text{hadronic ME}}\,. \tag{54}$$

Because of $k^2 \sim M_B^2 \ll M_W^2$, we may again—as in (45)—integrate out the W boson with the help of (46), which yields

$$T_{fi} = \frac{G_{\rm F}}{\sqrt{2}} V_{cb} \left[\bar{u}_\ell \gamma^\alpha (1-\gamma_5) v_\nu\right] \langle D^+ | \bar{c} \gamma_\alpha (1-\gamma_5) b | \bar{B}_d^0 \rangle \,, \tag{55}$$

where *all* the hadronic physics is encoded in the hadronic matrix element

$$\langle D^+ | \bar{c} \gamma_\alpha (1-\gamma_5) b | \bar{B}_d^0 \rangle \,,$$

i.e., there are *no* other QCD effects. Since the $\bar{B}_d^0$ and D^+ are pseudoscalar mesons, we have

$$\langle D^+ | \bar{c} \gamma_\alpha \gamma_5 b | \bar{B}_d^0 \rangle = 0 \,, \tag{56}$$

and may write

$$\langle D^+(k) | \bar{c} \gamma_\alpha b | \bar{B}_d^0(p) \rangle = F_1(q^2) \left[(p+k)_\alpha - \left(\frac{M_B^2 - M_D^2}{q^2}\right) q_\alpha\right] + F_0(q^2) \left(\frac{M_B^2 - M_D^2}{q^2}\right) q_\alpha \,, \tag{57}$$

where $q \equiv p - k$, and the $F_{1,0}(q^2)$ denote the *form factors* of the $\bar{B} \to D$ transitions. Consequently, in contrast to the simple case of the leptonic transitions, semileptonic decays involve *two* hadronic form factors instead of the decay constant f_B. In order to calculate these parameters, which depend on the momentum transfer q, again non-perturbative techniques (QCD sum rules, lattice, etc.) are required.

3.2.2 Aspects of the heavy-quark effective theory

If the mass m_Q of a quark Q is much larger than the QCD scale parameter $\Lambda_{\rm QCD} = \mathcal{O}(100\,\text{MeV})$ [43], it is referred to as a 'heavy' quark. Since the bottom and charm quarks have masses at the level of 5 GeV and 1 GeV, respectively, they belong to this important category. As far as the extremely heavy top quark, with $m_t \sim 170\,\text{GeV}$ is concerned, it decays unfortunately through weak interactions before a hadron can be formed. Let us now consider a heavy quark that is bound inside a hadron, i.e., a bottom or a charm quark. The heavy quark then moves almost with the hadron's four velocity v and is almost on-shell, so that

$$p_Q^\mu = m_Q v^\mu + k^\mu \,, \tag{58}$$

where $v^2 = 1$ and $k \ll m_Q$ is the 'residual' momentum. Owing to the interactions of the heavy quark with the light degrees of freedom of the hadron, the residual momentum may only change by $\Delta k \sim \Lambda_{\rm QCD}$, and $\Delta v \to 0$ for $\Lambda_{\rm QCD}/m_Q \to 0$.

It is now instructive to have a look at the elastic scattering process $\bar{B}(v) \to \bar{B}(v')$ in the limit of $\Lambda_{\rm QCD}/m_b \to 0$, which is characterized by the following matrix element:

$$\frac{1}{M_B} \langle \bar{B}(v') | \bar{b}_{v'} \gamma_\alpha b_v | \bar{B}(v) \rangle = \xi(v'\cdot v)(v+v')_\alpha \,. \tag{59}$$

Since the contraction of this matrix element with $(v-v')^\alpha$ has to vanish because of $\not{v} b_v = b_v$ and $\overline{b}_{v'} \not{v}' = \overline{b}_{v'}$, no $(v-v')_\alpha$ term arises in the parametrization in (59). On the other hand, the $1/M_B$ factor is related to the normalization of states, i.e., the right-hand side of

$$\left(\frac{1}{\sqrt{M_B}} \langle \bar{B}(p') |\right) \left(|\bar{B}(p)\rangle \frac{1}{\sqrt{M_B}}\right) = 2v^0 (2\pi)^3 \delta^3(\vec{p} - \vec{p}') \tag{60}$$

does not depend on M_B. Finally, current conservation implies the following normalization condition:

$$\xi(v'\cdot v = 1) = 1 \,, \tag{61}$$

where the 'Isgur–Wise' function $\xi(v' \cdot v)$ does *not* depend on the flavour of the heavy quark (heavy-quark symmetry) [54]. Consequently, for $\Lambda_{\rm QCD}/m_{b,c} \to 0$, we may write

$$\frac{1}{\sqrt{M_D M_B}} \langle D(v')|\bar{c}_{v'} \gamma_\alpha b_v|\bar{B}(v)\rangle = \xi(v' \cdot v)(v + v')_\alpha \,, \tag{62}$$

and observe that this transition amplitude is governed—in the heavy-quark limit—by *one* hadronic form factor $\xi(v' \cdot v)$, which satisfies $\xi(1) = 1$. If we now compare (62) with (57), we obtain

$$F_1(q^2) = \frac{M_D + M_B}{2\sqrt{M_D M_B}} \xi(w) \tag{63}$$

$$F_0(q^2) = \frac{2\sqrt{M_D M_B}}{M_D + M_B} \left[\frac{1+w}{2}\right] \xi(w) \,, \tag{64}$$

with

$$w \equiv v_D \cdot v_B = \frac{M_D^2 + M_B^2 - q^2}{2 M_D M_B} \,. \tag{65}$$

Similar relations hold for the $\bar{B} \to D^*$ form factors because of the heavy-quark spin symmetry, since the D^* is related to the D by a rotation of the heavy-quark spin. A detailed discussion of these interesting features and the associated 'heavy-quark effective theory' (HQET) is beyond the scope of these lectures. For a detailed overview, we refer the reader to Ref. [55], where also a comprehensive list of original references can be found. For a more phenomenological discussion, Ref. [56] is very useful.

3.2.3 Applications

An important application of the formalism sketched above is the extraction of the CKM element $|V_{cb}|$. To this end, $\bar{B} \to D^* \ell \bar{\nu}$ decays are particularly promising. The corresponding rate can be written as

$$\frac{{\rm d}\Gamma}{{\rm d}w} = G_{\rm F}^2 K(M_B, M_{D^*}, w) F(w)^2 |V_{cb}|^2 \,, \tag{66}$$

where $K(M_B, M_{D^*}, w)$ is a known kinematic function, and $F(w)$ agrees with the Isgur–Wise function, up to perturbative QCD corrections and $\Lambda_{\rm QCD}/m_{b,c}$ terms. The form factor $F(w)$ is a non-perturbative quantity. However, it satisfies the following normalization condition:

$$F(1) = \eta_A(\alpha_s) \left[1 + \frac{0}{m_c} + \frac{0}{m_b} + \mathcal{O}(\Lambda_{\rm QCD}^2/m_{b,c}^2)\right] , \tag{67}$$

where $\eta_A(\alpha_s)$ is a perturbatively calculable short-distance QCD factor, and the $\Lambda_{\rm QCD}/m_{b,c}$ corrections *vanish* [55, 57]. The important latter feature is an implication of Luke's theorem [58]. Consequently, if we extract $F(w)|V_{cb}|$ from a measurement of (66) as a function of w and extrapolate to the 'zero-recoil point' $w = 1$ (where the rate vanishes), we may determine $|V_{cb}|$. In the case of $\bar{B} \to D \ell \bar{\nu}$ decays, we have $\mathcal{O}(\Lambda_{\rm QCD}/m_{b,c})$ corrections to the corresponding rate ${\rm d}\Gamma/{\rm d}w$ at $w = 1$. In order to determine $|V_{cb}|$, inclusive $B \to X_c \ell \bar{\nu}$ decays offer also very attractive avenues. As becomes obvious from (27) and the considerations in Section 2.6, $|V_{cb}|$ fixes the normalization of the UT. Moreover, this quantity is an important input parameter for various theoretical calculations. The CKM matrix element $|V_{cb}|$ is currently known with 2% precision; performing an analysis of leptonic and hadronic moments in inclusive $b \to c \ell \bar{\nu}$ processes [59], the following value was extracted from the B-factory data [60]:

$$|V_{cb}| = (42.0 \pm 0.7) \times 10^{-3} \,, \tag{68}$$

which agrees with that from exclusive decays.

Let us now turn to $\bar{B} \to \pi \ell \bar{\nu}, \rho \ell \bar{\nu}$ decays, which originate from $b \to u \ell \bar{\nu}$ quark-level processes, as can be seen in Fig. 6, and provide access to $|V_{ub}|$. If we complement this CKM matrix element with $|V_{cb}|$,

we may determine the side R_b of the UT with the help of (38). The determination of $|V_{ub}|$ is hence a very important aspect of flavour physics. Since the π and ρ are 'light' mesons, the HQET symmetry relations cannot be applied to the $\bar{B} \to \pi\ell\bar{\nu}, \rho\ell\bar{\nu}$ modes. Consequently, in order to determine $|V_{ub}|$ from these exclusive channels, the corresponding heavy-to-light form factors have to be described by models. An important alternative is provided by inclusive decays. The corresponding decay rate takes the following form:

$$\Gamma(\bar{B} \to X_u\ell\bar{\nu}) = \frac{G_{\rm F}^2|V_{ub}|^2}{192\pi^3} m_b^5 \left[1 - 2.41\frac{\alpha_s}{\pi} + \frac{\lambda_1 - 9\lambda_2}{2m_b^2} + \ldots\right], \tag{69}$$

where λ_1 and λ_2 are non-perturbative parameters, which describe the hadronic matrix elements of certain 'kinetic' and 'chromomagnetic' operators appearing within the framework of the HQET. Using the heavy-quark expansions

$$M_B = m_b + \bar{\Lambda} - \frac{\lambda_1 + 3\lambda_2}{2m_b} + \ldots, \quad M_{B^*} = m_b + \bar{\Lambda} - \frac{\lambda_1 - \lambda_2}{2m_b} + \ldots \tag{70}$$

for the $B^{(*)}$-meson masses, where $\bar{\Lambda} \sim \Lambda_{\rm QCD}$ is another non-perturbative parameter that is related to the light degrees of freedom, the parameter λ_2 can be determined from the measured values of the $M_{B^{(*)}}$. The strong dependence of (69) on m_b is a significant source of uncertainty. On the other hand, the $1/m_b^2$ corrections can be better controlled than in the exclusive case (67), where we have, moreover, to deal with $1/m_c^2$ corrections. From an experimental point of view, we have to struggle with large backgrounds, which originate from $b \to c\ell\bar{\nu}$ processes and require also a model-dependent treatment. The determination of $|V_{ub}|$ from B-meson decays caused by $b \to u\ell\bar{\nu}$ quark-level processes is therefore a very challenging issue, and the situation is less favourable than with $|V_{cb}|$: there is a $1\,\sigma$ discrepancy between the values from inclusive and exclusive transitions [61]:

$$|V_{ub}|_{\rm incl} = (4.4 \pm 0.3) \times 10^{-3}\,, \quad |V_{ub}|_{\rm excl} = (3.8 \pm 0.6) \times 10^{-3}\,, \tag{71}$$

which has to be settled in the future. The error on $|V_{ub}|_{\rm excl}$ is dominated by the theoretical uncertainty of lattice and light-cone sum rule calculations of $B \to \pi$ and $B \to \rho$ transition form factors [62, 63], whereas for $|V_{ub}|_{\rm incl}$ experimental and theoretical errors are at par. Using the values of $|V_{cb}|$ and $|V_{ub}|$ given above and $\lambda = 0.225 \pm 0.001$ [64], we obtain

$$R_b^{\rm incl} = 0.45 \pm 0.03\,, \qquad R_b^{\rm excl} = 0.39 \pm 0.06\,, \tag{72}$$

where the labels 'incl' and 'excl' refer to the determinations of $|V_{ub}|$ through inclusive and exclusive $b \to u\ell\bar{\nu}_\ell$ transitions, respectively.

For a much more detailed discussion of the determinations of $|V_{cb}|$ and $|V_{ub}|$, addressing also various recent developments and the future prospects, we refer the reader to Ref. [12], where also the references to the vast original literature can be found. Another excellent presentation is given in Ref. [56].

3.3 Non-leptonic decays

3.3.1 Classification

The most complicated B decays are the non-leptonic transitions, which are mediated by $b \to q_1\,\bar{q}_2\,d\,(s)$ quark-level processes, with $q_1, q_2 \in \{u, d, c, s\}$. There are two kinds of topologies contributing to such decays: tree-diagram-like and 'penguin' topologies. The latter consist of gluonic (QCD) and electroweak (EW) penguins. In Fig. 7, the corresponding leading-order Feynman diagrams are shown. Depending on the flavour content of their final states, we may classify $b \to q_1\,\bar{q}_2\,d\,(s)$ decays as follows:

- $q_1 \neq q_2 \in \{u, c\}$: *only* tree diagrams contribute.
- $q_1 = q_2 \in \{u, c\}$: tree *and* penguin diagrams contribute.
- $q_1 = q_2 \in \{d, s\}$: *only* penguin diagrams contribute.

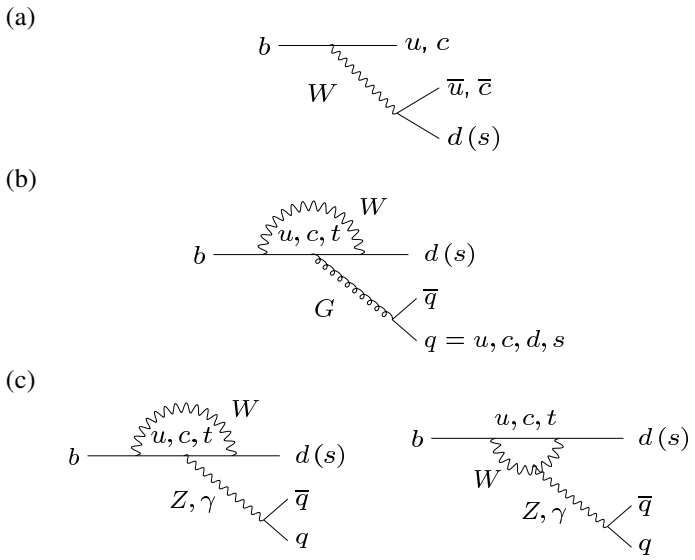

Fig. 7: Feynman diagrams of the topologies characterizing non-leptonic B decays: (a) trees, (b) QCD penguins, and (c) electroweak penguins

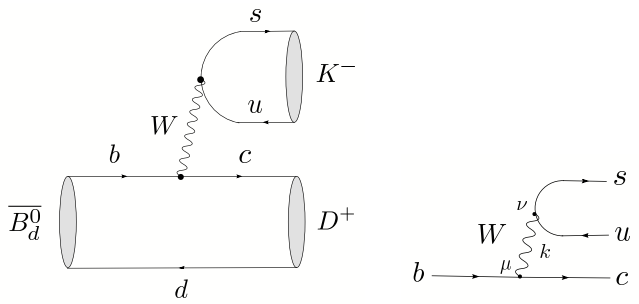

Fig. 8: Feynman diagrams contributing to the non-leptonic $\bar{B}^0_d \to D^+K^-$ decay

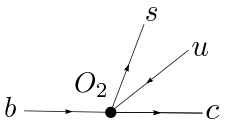

Fig. 9: The description of the $b \to d\bar{u}s$ process through the four-quark operator O_2 in the effective theory after the W boson has been integrated out

3.3.2 Low-energy effective Hamiltonians

In order to analyse non-leptonic B decays theoretically, one uses low-energy effective Hamiltonians, which are calculated by making use of the 'operator product expansion', yielding transition matrix elements of the following structure:

$$\langle f|\mathcal{H}_{\rm eff}|i\rangle = \frac{G_{\rm F}}{\sqrt{2}}\lambda_{\rm CKM}\sum_k C_k(\mu)\langle f|Q_k(\mu)|i\rangle\,. \tag{73}$$

The technique of the operator product expansion allows us to separate the short-distance contributions to this transition amplitude from the long-distance ones, which are described by perturbative quantities $C_k(\mu)$ ('Wilson coefficient functions') and non-perturbative quantities $\langle f|Q_k(\mu)|i\rangle$ ('hadronic matrix elements'), respectively. As before, $G_{\rm F}$ is the Fermi constant, whereas $\lambda_{\rm CKM}$ is a CKM factor and μ

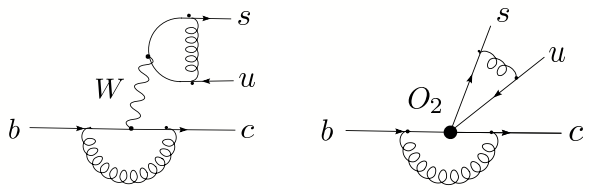

Fig. 10: Factorizable QCD corrections in the full and effective theories

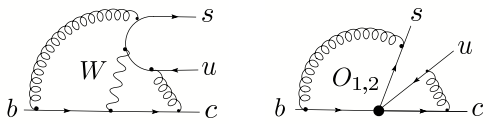

Fig. 11: Non-factorizable QCD corrections in the full and effective theories

denotes an appropriate renormalization scale. The Q_k are local operators, which are generated by electroweak interactions and QCD, and govern 'effectively' the decay in question. The Wilson coefficients $C_k(\mu)$ can be considered as scale-dependent couplings related to the vertices described by the Q_k.

In order to illustrate this rather abstract formalism, let us consider the decay $\bar{B}^0_d \to D^+K^-$, which allows a transparent discussion of the evaluation of the corresponding low-energy effective Hamiltonian. Since this transition originates from a $b \to c\bar{u}s$ quark-level process, it is—as we have seen in our classification in Subsection 3.3.1—a pure 'tree' decay, i.e., we do not have to deal with penguin topologies, which simplifies the analysis considerably. The leading-order Feynman diagram contributing to $\bar{B}^0_d \to D^+K^-$ can straightforwardly be obtained from Fig. 6 by substituting ℓ and ν_ℓ by s and u, respectively, as can be seen in Fig. 8. Consequently, the lepton current is simply replaced by a quark current, which will have important implications shown below. Evaluating the corresponding Feynman diagram yields

$$-\frac{g_2^2}{8}V_{us}^*V_{cb}\left[\bar{s}\gamma^\nu(1-\gamma_5)u\right]\left[\frac{g_{\nu\mu}}{k^2-M_W^2}\right]\left[\bar{c}\gamma^\mu(1-\gamma_5)b\right]\,. \tag{74}$$

Because of $k^2 \sim m_b^2 \ll M_W^2$, we may—as in (54)—'integrate out' the W boson with the help of (46), and arrive at

$$\begin{aligned}\mathcal{H}_{\text{eff}} &= \frac{G_{\text{F}}}{\sqrt{2}}V_{us}^*V_{cb}\left[\bar{s}_\alpha\gamma_\mu(1-\gamma_5)u_\alpha\right]\left[\bar{c}_\beta\gamma^\mu(1-\gamma_5)b_\beta\right]\\ &= \frac{G_{\text{F}}}{\sqrt{2}}V_{us}^*V_{cb}(\bar{s}_\alpha u_\alpha)_{\text{V-A}}(\bar{c}_\beta b_\beta)_{\text{V-A}} \equiv \frac{G_{\text{F}}}{\sqrt{2}}V_{us}^*V_{cb}O_2\,,\end{aligned} \tag{75}$$

where α and β denote the colour indices of the $SU(3)_{\text{C}}$ gauge group of QCD. Effectively, our $b \to c\bar{u}s$ decay process is now described by the 'current–current' operator O_2, as is illustrated in Fig. 9.

So far, we neglected QCD corrections. Their important impact is twofold: thanks to *factorizable* QCD corrections as shown in Fig. 10, the Wilson coefficient C_2 acquires a renormalization-scale dependence, i.e., $C_2(\mu) \neq 1$. On the other hand, *non-factorizable* QCD corrections as illustrated in Fig. 11 generate a second current–current operator through 'operator mixing', which is given by

$$O_1 \equiv \left[\bar{s}_\alpha\gamma_\mu(1-\gamma_5)u_\beta\right]\left[\bar{c}_\beta\gamma^\mu(1-\gamma_5)b_\alpha\right]. \tag{76}$$

Consequently, we eventually arrive at a low-energy effective Hamiltonian of the following structure:

$$\mathcal{H}_{\text{eff}} = \frac{G_{\text{F}}}{\sqrt{2}}V_{us}^*V_{cb}\left[C_1(\mu)O_1 + C_2(\mu)O_2\right]. \tag{77}$$

In order to evaluate the Wilson coefficients $C_1(\mu) \neq 0$ and $C_2(\mu) \neq 1$ [65], we must first calculate the QCD corrections to the decay processes both in the full theory, i.e., with W exchange, and in the effective theory, where the W is integrated out (see Figs. 10 and 11), and have then to express the QCD-corrected transition amplitude in terms of QCD-corrected matrix elements and Wilson coefficients as in (73). This procedure is called 'matching' between the full and the effective theory. The results for the $C_k(\mu)$ thus obtained contain terms of $\log(\mu/M_W)$, which become large for $\mu = \mathcal{O}(m_b)$, the scale governing the hadronic matrix elements of the O_k. Making use of the renormalization group, which exploits the fact that the transition amplitude (73) cannot depend on the chosen renormalization scale μ, we may sum up the following terms of the Wilson coefficients:

$$\alpha_s^n \left[\log\left(\frac{\mu}{M_W}\right)\right]^n \text{ (LO)}, \quad \alpha_s^n \left[\log\left(\frac{\mu}{M_W}\right)\right]^{n-1} \text{ (NLO)}, \quad \ldots \quad ; \tag{78}$$

detailed discussions of these rather technical aspects can be found in Refs. [66, 67].

For the exploration of CP violation, the class of non-leptonic B decays that receives contributions both from tree and from penguin topologies plays a key role. In this important case, the operator basis is much larger than in our example (77), where we considered a pure 'tree' decay. If we apply the relation

$$V_{ur}^* V_{ub} + V_{cr}^* V_{cb} + V_{tr}^* V_{tb} = 0 \quad (r \in \{d, s\}), \tag{79}$$

which follows from the unitarity of the CKM matrix, and 'integrate out' the top quark (which enters through the penguin loop processes) and the W boson, we may write

$$\mathcal{H}_{\text{eff}} = \frac{G_{\text{F}}}{\sqrt{2}} \left[\sum_{j=u,c} V_{jr}^* V_{jb} \left\{\sum_{k=1}^{2} C_k(\mu)\, Q_k^{jr} + \sum_{k=3}^{10} C_k(\mu)\, Q_k^{r}\right\}\right]. \tag{80}$$

Here we have introduced another quark-flavour label $j \in \{u, c\}$, and the Q_k^{jr} can be divided as follows:

– Current–current operators:

$$\begin{array}{rcl} Q_1^{jr} & = & (\bar{r}_\alpha j_\beta)_{\text{V-A}} (\bar{j}_\beta b_\alpha)_{\text{V-A}} \\ Q_2^{jr} & = & (\bar{r}_\alpha j_\alpha)_{\text{V-A}} (\bar{j}_\beta b_\beta)_{\text{V-A}}. \end{array} \tag{81}$$

– QCD penguin operators:

$$\begin{array}{rcl} Q_3^{r} & = & (\bar{r}_\alpha b_\alpha)_{\text{V-A}} \sum_{q'} (\bar{q}'_\beta q'_\beta)_{\text{V-A}} \\ Q_4^{r} & = & (\bar{r}_\alpha b_\beta)_{\text{V-A}} \sum_{q'} (\bar{q}'_\beta q'_\alpha)_{\text{V-A}} \\ Q_5^{r} & = & (\bar{r}_\alpha b_\alpha)_{\text{V-A}} \sum_{q'} (\bar{q}'_\beta q'_\beta)_{\text{V+A}} \\ Q_6^{r} & = & (\bar{r}_\alpha b_\beta)_{\text{V-A}} \sum_{q'} (\bar{q}'_\beta q'_\alpha)_{\text{V+A}}. \end{array} \tag{82}$$

– EW penguin operators (the $e_{q'}$ denote the electrical quark charges):

$$\begin{array}{rcl} Q_7^{r} & = & \frac{3}{2} (\bar{r}_\alpha b_\alpha)_{\text{V-A}} \sum_{q'} e_{q'} (\bar{q}'_\beta q'_\beta)_{\text{V+A}} \\ Q_8^{r} & = & \frac{3}{2} (\bar{r}_\alpha b_\beta)_{\text{V-A}} \sum_{q'} e_{q'} (\bar{q}'_\beta q'_\alpha)_{\text{V+A}} \\ Q_9^{r} & = & \frac{3}{2} (\bar{r}_\alpha b_\alpha)_{\text{V-A}} \sum_{q'} e_{q'} (\bar{q}'_\beta q'_\beta)_{\text{V-A}} \\ Q_{10}^{r} & = & \frac{3}{2} (\bar{r}_\alpha b_\beta)_{\text{V-A}} \sum_{q'} e_{q'} (\bar{q}'_\beta q'_\alpha)_{\text{V-A}}. \end{array} \tag{83}$$

The current–current, QCD and EW penguin operators are related to the tree, QCD and EW penguin processes shown in Fig. 7. At a renormalization scale $\mu = \mathcal{O}(m_b)$, the Wilson coefficients of the current–current operators are $C_1(\mu) = \mathcal{O}(10^{-1})$ and $C_2(\mu) = \mathcal{O}(1)$, whereas those of the penguin operators are $\mathcal{O}(10^{-2})$ [66, 67]. Note that penguin topologies with internal charm- and up-quark exchanges [68] are described in this framework by penguin-like matrix elements of the corresponding current–current operators [69], and may also have important phenomenological consequences [70, 71].

Since the ratio $\alpha/\alpha_s = \mathcal{O}(10^{-2})$ of the QED and QCD couplings is very small, we would expect naïvely that EW penguins should play a minor role in comparison with QCD penguins. This would actually be the case if the top quark was not 'heavy'. However, since the Wilson coefficient C_9 increases strongly with m_t, we obtain interesting EW penguin effects in several B decays: $B \to K\phi$ modes are affected significantly by EW penguins, whereas $B \to \pi\phi$ and $B_s \to \pi^0\phi$ transitions are even *dominated* by such topologies [72, 73]. EW penguins also have an important impact on the $B \to \pi K$ system [74].

The low-energy effective Hamiltonians discussed above apply to all B decays that are caused by the same quark-level transition, i.e., they are 'universal'. Consequently, the differences between the various exclusive modes of a given decay class arise within this formalism only through the hadronic matrix elements of the relevant four-quark operators. Unfortunately, the evaluation of such matrix elements is associated with large uncertainties and is a very challenging task. In this context, 'factorization' is a widely used concept, which is our next topic.

3.3.3 Factorization of hadronic matrix elements

In order to discuss 'factorization', let us consider once more the decay $\bar{B}^0_d \to D^+K^-$. Evaluating the corresponding transition amplitude, we encounter the hadronic matrix elements of the $O_{1,2}$ operators between the $\langle K^-D^+|$ final and the $|\bar{B}^0_d\rangle$ initial states. If we use the well-known $SU(N_{\rm C})$ colour-algebra relation

$$T^a_{\alpha\beta}T^a_{\gamma\delta} = \frac{1}{2}\left(\delta_{\alpha\delta}\delta_{\beta\gamma} - \frac{1}{N_{\rm C}}\delta_{\alpha\beta}\delta_{\gamma\delta}\right) \tag{84}$$

to rewrite the operator O_1, we obtain

$$\begin{aligned}\langle K^-D^+|\mathcal{H}_{\rm eff}|\bar{B}^0_d\rangle = \frac{G_{\rm F}}{\sqrt{2}}V^*_{us}V_{cb}\Big[a_1\langle K^-D^+|(\bar{s}_\alpha u_\alpha)_{\rm V\text{–}A}(\bar{c}_\beta b_\beta)_{\rm V\text{–}A}|\bar{B}^0_d\rangle \\ +2\,C_1\langle K^-D^+|(\bar{s}_\alpha\,T^a_{\alpha\beta}\,u_\beta)_{\rm V\text{–}A}(\bar{c}_\gamma\,T^a_{\gamma\delta}\,b_\delta)_{\rm V\text{–}A}|\bar{B}^0_d\rangle\Big],\end{aligned}$$

with

$$a_1 = C_1/N_{\rm C} + C_2 \sim 1\,. \tag{85}$$

It is now straightforward to 'factorize' the hadronic matrix elements in (85):

$$\begin{aligned}&\langle K^-D^+|(\bar{s}_\alpha u_\alpha)_{\rm V\text{–}A}(\bar{c}_\beta b_\beta)_{\rm V\text{–}A}|\bar{B}^0_d\rangle\big|_{\rm fact} \\ &\quad= \langle K^-|\,[\bar{s}_\alpha\gamma_\mu(1-\gamma_5)u_\alpha]\,|0\rangle\langle D^+|\,[\bar{c}_\beta\gamma^\mu(1-\gamma_5)b_\beta]\,|\bar{B}^0_d\rangle \\ &\quad= \underbrace{if_K}_{\text{decay constant}} \times \underbrace{F_0^{(BD)}(M_K^2)}_{B\to D\text{ form factor}} \times \underbrace{(M_B^2 - M_D^2)}_{\text{kinematical factor}},\end{aligned} \tag{86}$$

$$\langle K^-D^+|(\bar{s}_\alpha\,T^a_{\alpha\beta}\,u_\beta)_{\rm V\text{–}A}(\bar{c}_\gamma\,T^a_{\gamma\delta}\,b_\delta)_{\rm V\text{–}A}|\bar{B}^0_d\rangle\big|_{\rm fact} = 0\,. \tag{87}$$

The quantity a_1 is a phenomenological 'colour factor', which governs 'colour-allowed' decays; the decay $\bar{B}^0_d \to D^+K^-$ belongs to this category, since the colour indices of the K^- meson and the $\bar{B}^0_d$–D^+ system run independently from each other in the corresponding leading-order diagram shown in Fig. 8. On the other hand, in the case of 'colour-suppressed' modes, for instance $\bar{B}^0_d \to \pi^0D^0$, where only one colour index runs through the whole diagram, we have to deal with the combination

$$a_2 = C_1 + C_2/N_{\rm C} \sim 0.25\,. \tag{88}$$

The concept of factorizing the hadronic matrix elements of four-quark operators into the product of hadronic matrix elements of quark currents has a long history [75], and can be justified, for example, in the large-$N_{\rm C}$ limit [76]. Interesting recent developments are the following:

– 'QCD factorization' [77], which is in accordance with the old picture that factorization should hold for certain decays in the limit of $m_b \gg \Lambda_{\rm QCD}$ [78], provides a formalism to calculate the relevant amplitudes at the leading order of a $\Lambda_{\rm QCD}/m_b$ expansion. The resulting expression for the transition amplitudes incorporates elements both of the naïve factorization approach sketched above and of the hard-scattering picture. Let us consider a decay $\bar{B} \to M_1 M_2$, where M_1 picks up the spectator quark. If M_1 is either a heavy (D) or a light (π, K) meson, and M_2 a light (π, K) meson, QCD factorization gives a transition amplitude of the following structure:

$$A(\bar{B} \to M_1 M_2) = [\text{'naïve factorization'}] \times [1 + \mathcal{O}(\alpha_s) + \mathcal{O}(\Lambda_{\rm QCD}/m_b)]\,. \tag{89}$$

While the $\mathcal{O}(\alpha_s)$ terms, i.e., the radiative non-factorizable corrections, can be calculated systematically, the main limitation of the theoretical accuracy originates from the $\mathcal{O}(\Lambda_{\rm QCD}/m_b)$ terms.

– Another QCD approach to deal with non-leptonic B-meson decays—the 'perturbative hard-scattering approach' (PQCD)—was developed independently in Ref. [79], and differs from the QCD factorization formalism in some technical aspects.

– An interesting technique for 'factorization proofs' is provided by the framework of the 'soft collinear effective theory' (SCET) [80], which has received a lot of attention in the recent literature and led to various applications.

– Non-leptonic B decays can also be studied within QCD light-cone sum-rule approaches [81].

A detailed presentation of these topics would be very technical and is beyond the scope of these lectures. However, for the discussion of the CP-violating effects in the B-meson system, we must only be familiar with the general structure of the non-leptonic B decay amplitudes and not enter the details of the techniques to deal with the corresponding hadronic matrix elements. Let us finally note that the B-factory data will eventually decide how well factorization and the new concepts sketched above are actually working. For example, data on the $B \to \pi\pi$ system point towards large non-factorizable corrections [82, 83], to which we shall return in Section 8.2.

3.4 Towards studies of CP violation

As we have seen above, leptonic and semileptonic B-meson decays involve only a single weak (CKM) amplitude. On the other hand, the structure of non-leptonic transitions is considerably more complicated. Let us consider a non-leptonic decay $\bar{B} \to \bar{f}$ that is described by the low-energy effective Hamiltonian in (80). The corresponding decay amplitude is then given as follows:

$$\begin{aligned} A(\bar{B} \to \bar{f}) &= \langle \bar{f}|\mathcal{H}_{\rm eff}|\bar{B}\rangle \\ &= \frac{G_{\rm F}}{\sqrt{2}} \left[\sum_{j=u,c} V_{jr}^* V_{jb} \left\{\sum_{k=1}^{2} C_k(\mu)\langle \bar{f}|Q_k^{jr}(\mu)|\bar{B}\rangle + \sum_{k=3}^{10} C_k(\mu)\langle \bar{f}|Q_k^{r}(\mu)|\bar{B}\rangle\right\}\right]. \end{aligned} \tag{90}$$

Concerning the CP-conjugate process $B \to f$, we have

$$\begin{aligned} A(B \to f) &= \langle f|\mathcal{H}_{\rm eff}^{\dagger}|B\rangle \\ &= \frac{G_{\rm F}}{\sqrt{2}} \left[\sum_{j=u,c} V_{jr} V_{jb}^* \left\{\sum_{k=1}^{2} C_k(\mu)\langle f|Q_k^{jr\dagger}(\mu)|B\rangle + \sum_{k=3}^{10} C_k(\mu)\langle f|Q_k^{r\dagger}(\mu)|B\rangle\right\}\right]. \end{aligned} \tag{91}$$

If we use now that strong interactions are invariant under CP transformations, insert $(\mathcal{CP})^\dagger(\mathcal{CP}) = \hat{1}$ both after the $\langle f|$ and in front of the $|B\rangle$, and take the relation

$$(\mathcal{CP})Q_k^{jr\dagger}(\mathcal{CP})^\dagger = Q_k^{jr} \tag{92}$$

into account, we arrive at

$$A(B \to f) = e^{i[\phi_{\rm CP}(B) - \phi_{\rm CP}(f)]} \times \frac{G_{\rm F}}{\sqrt{2}} \left[\sum_{j=u,c} V_{jr} V_{jb}^* \left\{ \sum_{k=1}^{2} C_k(\mu) \langle \bar{f} | Q_k^{jr}(\mu) | \bar{B} \rangle + \sum_{k=3}^{10} C_k(\mu) \langle \bar{f} | Q_k^{r}(\mu) | \bar{B} \rangle \right\} \right], \tag{93}$$

where the convention-dependent phases $\phi_{\rm CP}(B)$ and $\phi_{\rm CP}(f)$ are defined through

$$(\mathcal{CP})|B\rangle = e^{i\phi_{\rm CP}(B)}|\bar{B}\rangle, \quad (\mathcal{CP})|f\rangle = e^{i\phi_{\rm CP}(f)}|\bar{f}\rangle. \tag{94}$$

Consequently, we may write

$$A(\bar{B} \to \bar{f}) = e^{+i\varphi_1}|A_1|e^{i\delta_1} + e^{+i\varphi_2}|A_2|e^{i\delta_2} \tag{95}$$

$$A(B \to f) = e^{i[\phi_{\rm CP}(B) - \phi_{\rm CP}(f)]} \left[e^{-i\varphi_1}|A_1|e^{i\delta_1} + e^{-i\varphi_2}|A_2|e^{i\delta_2} \right]. \tag{96}$$

Here the CP-violating phases $\varphi_{1,2}$ originate from the CKM factors $V_{jr}^* V_{jb}$, and the CP-conserving 'strong' amplitudes $|A_{1,2}|e^{i\delta_{1,2}}$ involve the hadronic matrix elements of the four-quark operators. In fact, these expressions are the most general forms of any non-leptonic B-decay amplitude in the SM, i.e., they do not only refer to the $\Delta C = \Delta U = 0$ case described by (80). Using (95) and (96), we obtain the following CP asymmetry:

$$\begin{aligned} \mathcal{A}_{\rm CP} &\equiv \frac{\Gamma(B \to f) - \Gamma(\bar{B} \to \bar{f})}{\Gamma(B \to f) + \Gamma(\bar{B} \to \bar{f})} = \frac{|A(B \to f)|^2 - |A(\bar{B} \to \bar{f})|^2}{|A(B \to f)|^2 + |A(\bar{B} \to \bar{f})|^2} \\ &= \frac{2|A_1||A_2|\sin(\delta_1 - \delta_2)\sin(\varphi_1 - \varphi_2)}{|A_1|^2 + 2|A_1||A_2|\cos(\delta_1 - \delta_2)\cos(\varphi_1 - \varphi_2) + |A_2|^2}\,. \end{aligned} \tag{97}$$

We observe that a non-vanishing value can be generated through the interference between the two weak amplitudes, provided both a non-trivial weak phase difference $\varphi_1 - \varphi_2$ and a non-trivial strong phase difference $\delta_1 - \delta_2$ are present. This kind of CP violation is referred to as 'direct' CP violation, as it originates directly at the amplitude level of the considered decay. It is the B-meson counterpart of the effects that are probed through ${\rm Re}(\varepsilon'/\varepsilon)$ in the neutral kaon system[1], and could recently be established with the help of $B_d \to \pi^\mp K^\pm$ decays [6], as we shall see in Section 7.3.

Since $\varphi_1 - \varphi_2$ is in general given by one of the UT angles—usually γ—the goal is to extract this quantity from the measured value of $\mathcal{A}_{\rm CP}$. Unfortunately, hadronic uncertainties affect this determination through the poorly known hadronic matrix elements in (90). In order to deal with this problem, we may proceed along one of the following two avenues:

(i) Amplitude relations can be used to eliminate the hadronic matrix elements. We distinguish between exact relations, using pure 'tree' decays of the kind $B^\pm \to K^\pm D$ [84, 85] or $B_c^\pm \to D_s^\pm D$ [86], and relations which follow from the flavour symmetries of strong interactions, i.e., isospin or $SU(3)_{\rm F}$, and involve $B_{(s)} \to \pi\pi, \pi K, KK$ modes [87].

(ii) In decays of neutral B_q mesons, interference effects between B_q^0–$\bar{B}_q^0$ mixing and decay processes may induce 'mixing-induced CP violation'. If a single CKM amplitude governs the decay, the hadronic matrix elements cancel in the corresponding CP asymmetries; otherwise we again have to use amplitude relations. The most important example is the decay $B_d^0 \to J/\psi K_{\rm S}$ [88].

Before discussing the features of neutral B_q mesons and B_q^0–$\bar{B}_q^0$ mixing in detail in Section 5, let us illustrate the use of amplitude relations for clean extractions of the UT angle γ from decays of charged B_u and B_c mesons.

[1] In order to calculate this quantity, an approriate low-energy effective Hamiltonian having the same structure as (80) is used. The large theoretical uncertainties mentioned in Section 1 originate from a strong cancellation between the contributions of the QCD and EW penguins (caused by the large top-quark mass) and the associated hadronic matrix elements.

4 Amplitude relations

4.1 $B^\pm \to K^\pm D$

The prototype of the strategies using theoretically clean amplitude relations is provided by $B^\pm \to K^\pm D$ decays [84]. Looking at Fig. 12, we observe that $B^+ \to K^+\bar{D}^0$ and $B^+ \to K^+D^0$ are pure 'tree' decays. If we consider, in addition, the transition $B^+ \to D_+^0 K^+$, where D_+^0 denotes the CP eigenstate of the neutral D-meson system with eigenvalue $+1$,

$$|D_+^0\rangle = \frac{1}{\sqrt{2}}\left[|D^0\rangle + |\bar{D}^0\rangle\right], \tag{98}$$

we obtain interference effects, which are described by

$$\sqrt{2}A(B^+ \to K^+ D_+^0) = A(B^+ \to K^+D^0) + A(B^+ \to K^+\bar{D}^0) \tag{99}$$

$$\sqrt{2}A(B^- \to K^- D_+^0) = A(B^- \to K^-\bar{D}^0) + A(B^- \to K^-D^0)\,. \tag{100}$$

These relations can be represented as two triangles in the complex plane. Since we have only to deal with tree-diagram-like topologies, we have moreover

$$A(B^+ \to K^+\bar{D}^0) = A(B^- \to K^-D^0) \tag{101}$$

$$A(B^+ \to K^+D^0) = A(B^- \to K^-\bar{D}^0) \times e^{2i\gamma}\,, \tag{102}$$

allowing a *theoretically clean* extraction of γ, as shown in Fig. 13. Unfortunately, these triangles are very squashed, since $B^+ \to K^+D^0$ is colour-suppressed with respect to $B^+ \to K^+\bar{D}^0$:

$$\left|\frac{A(B^+ \to K^+D^0)}{A(B^+ \to K^+\bar{D}^0}\right| = \left|\frac{A(B^- \to K^-\bar{D}^0)}{A(B^- \to K^-D^0}\right| \approx \frac{1}{\lambda}\frac{|V_{ub}|}{|V_{cb}|} \times \frac{a_2}{a_1} \approx 0.4 \times 0.3 = \mathcal{O}(0.1)\,, \tag{103}$$

where the phenomenological 'colour' factors were introduced in Subsection 3.3.3.

Another—more subtle—problem is related to the measurement of BR$(B^+ \to K^+D^0)$. From the theoretical point of view, $D^0 \to K^-\ell^+\nu$ would be ideal to measure this tiny branching ratio. However, because of the huge background from semileptonic B decays, we must rely on Cabibbo-allowed hadronic $D^0 \to f_{\rm NE}$ decays, such as $f_{\rm NE} = \pi^+K^-$, ρ^+K^-, ..., i.e., have to measure

$$B^+ \to K^+D^0\,[\to f_{\rm NE}]\,. \tag{104}$$

Unfortunately, we then encounter another decay path into the *same* final state $K^+f_{\rm NE}$ through

$$B^+ \to K^+\bar{D}^0\,[\to f_{\rm NE}]\,, \tag{105}$$

where BR$(B^+ \to K^+\bar{D}^0)$ is *larger* than BR$(B^+ \to K^+D^0)$ by a factor of $\mathcal{O}(10^2)$, while $\bar{D}^0 \to f_{\rm NE}$ is doubly Cabibbo-suppressed, i.e., the corresponding branching ratio is suppressed with respect to the one of $D^0 \to f_{\rm NE}$ by a factor of $\mathcal{O}(10^{-2})$. Consequently, we obtain interference effects of $\mathcal{O}(1)$ between the decay chains in (104) and (105). However, if two different final states $f_{\rm NE}$ are considered, γ can be extracted [85], although this determination is then more involved than the original triangle approach presented in [84].

The angle γ can be determined in a variety of ways through CP-violating effects in pure tree decays of type $B \to D^{(*)}K^{(*)}$ [89]. Using the present B-factory data, the following results were obtained through a combination of various methods:

$$\gamma|_{D^{(*)}K^{(*)}} = \begin{cases} (62^{+35}_{-25})^\circ & \text{(CKMfitter Collaboration [41])}\,, \\ (65 \pm 20)^\circ & \text{(UTfit Collaboration [42])}\,. \end{cases} \tag{106}$$

Here we have discarded a second solution given by $180^\circ + \gamma|_{D^{(*)}K^{(*)}}$ in the third quadrant of the $\bar{\rho}$–$\bar{\eta}$ plane, as it is disfavoured by the global fits of the UT, and by the data for mixing-induced CP violation in pure tree decays of type $B_d \to D^\pm\pi^\mp, D^{*\pm}\pi^\mp, ...$ [90]. A similar comment applies to the information from $B \to \pi\pi, \pi K$ modes [91].

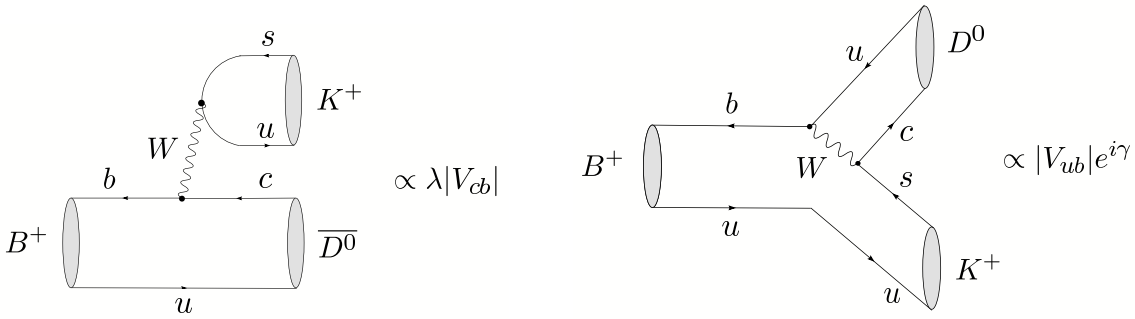

Fig. 12: Feynman diagrams contributing to $B^+ \to K^+\bar{D}^0$ and $B^+ \to K^+D^0$

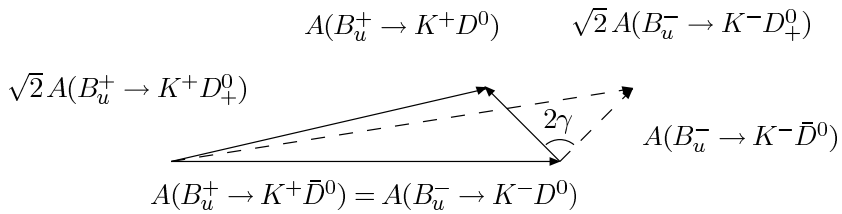

Fig. 13: The extraction of γ from $B^\pm \to K^\pm\{D^0, \bar{D}^0, D_+^0\}$ decays

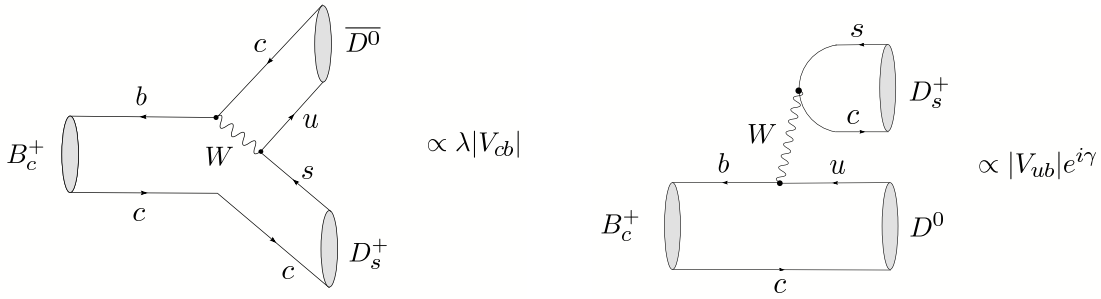

Fig. 14: Feynman diagrams contributing to $B_c^+ \to D_s^+\bar{D}^0$ and $B^+ \to D_s^+D^0$

4.2 $B_c^\pm \to D_s^\pm D$

In addition to the 'conventional' $B_u^\pm$ mesons, there is yet another species of charged B mesons, the B_c-meson system, which consists of $B_c^+ \sim c\bar{b}$ and $B_c^- \sim b\bar{c}$. These mesons were observed by the CDF Collaboration through their decay $B_c^+ \to J/\psi\ell^+\nu$, with the following mass and lifetime [92]:

$$M_{B_c} = (6.40 \pm 0.39 \pm 0.13)\,\text{GeV}, \quad \tau_{B_c} = (0.46^{+0.18}_{-0.16} \pm 0.03)\,\text{ps}\,. \tag{107}$$

Meanwhile, the D0 Collaboration observed the $B_c^+ \to J/\psi\,\mu^+X$ mode [93], which led to the following B_c mass and lifetime determinations:

$$M_{B_c} = (5.95^{+0.14}_{-0.13} \pm 0.34)\,\text{GeV}, \quad \tau_{B_c} = (0.448^{+0.123}_{-0.096} \pm 0.121)\,\text{ps}\,, \tag{108}$$

and CDF reported evidence for the $B_c^+ \to J/\psi\pi^+$ channel [94], implying

$$M_{B_c} = (6.2870 \pm 0.0048 \pm 0.0011)\,\text{GeV}\,. \tag{109}$$

Since Run II of the Tevatron will provide further insights into B_c physics and a huge number of B_c mesons will be produced at LHCb, the natural question of how to explore CP violation with charged B_c

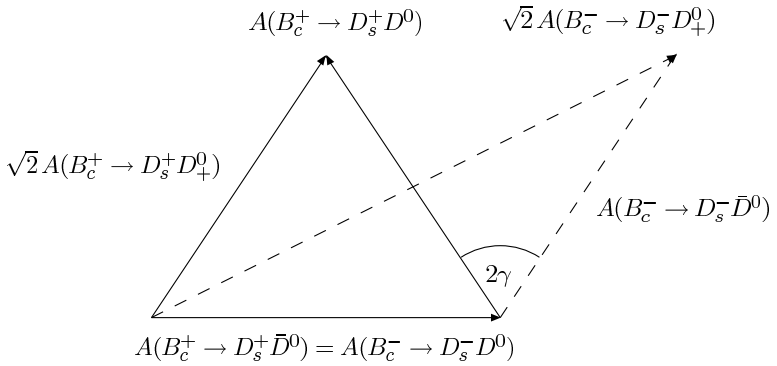

Fig. 15: The extraction of γ from $B_c^\pm \to D_s^\pm\{D^0, \bar{D}^0, D_+^0\}$ decays

decays arises, in particular whether an extraction of γ with the help of the triangle approach is possible. Such a determination is actually offered by $B_c^\pm \to D_s^\pm D$ decays, which are the B_c counterparts of the $B_u^\pm \to K^\pm D$ modes (see Fig. 14), and satisfy the following amplitude relations [95]:

$$\sqrt{2}A(B_c^+ \to D_s^+ D_+^0) = A(B_c^+ \to D_s^+ D^0) + A(B_c^+ \to D_s^+ \bar{D}^0) \tag{110}$$

$$\sqrt{2}A(B_c^- \to D_s^- D_+^0) = A(B_c^- \to D_s^- \bar{D}^0) + A(B_c^- \to D_s^- D^0)\,, \tag{111}$$

with

$$A(B_c^+ \to D_s^+ \bar{D}^0) = A(B_c^- \to D_s^- D^0) \tag{112}$$

$$A(B_c^+ \to D_s^+ D^0) = A(B_c^- \to D_s^- \bar{D}^0) \times e^{2i\gamma}\,. \tag{113}$$

At first sight, everything is completely analogous to the $B_u^\pm \to K^\pm D$ case. However, there is an important difference [86], which becomes obvious by comparing the Feynman diagrams shown in Figs. 12 and 14: in the $B_c^\pm \to D_s^\pm D$ system, the amplitude with the rather small CKM matrix element V_{ub} is not colour-suppressed, while the larger element V_{cb} comes with a colour-suppression factor. Therefore, we obtain

$$\left|\frac{A(B_c^+ \to D_s^+ D^0)}{A(B_c^+ \to D_s^+ \bar{D}^0)}\right| = \left|\frac{A(B_c^- \to D_s^- \bar{D}^0)}{A(B_c^- \to D_s^- D^0)}\right| \approx \frac{1}{\lambda}\frac{|V_{ub}|}{|V_{cb}|} \times \frac{a_1}{a_2} \approx 0.4 \times 3 = \mathcal{O}(1)\,, \tag{114}$$

and conclude that the two amplitudes are similar in size. In contrast to this favourable situation, in the decays $B_u^\pm \to K^\pm D$, the matrix element V_{ub} comes with the colour-suppression factor, resulting in a very stretched triangle. The extraction of γ from the $B_c^\pm \to D_s^\pm D$ triangles is illustrated in Fig. 15, which should be compared with the squashed $B_u^\pm \to K^\pm D$ triangles shown in Fig. 13. Another important advantage is that the interference effects arising from $D^0, \bar{D}^0 \to \pi^+ K^-$ are practically unimportant for the measurement of $\text{BR}(B_c^+ \to D_s^+ D^0)$ and $\text{BR}(B_c^+ \to D_s^+ \bar{D}^0)$ since the B_c-decay amplitudes are of the same order of magnitude. Consequently, the $B_c^\pm \to D_s^\pm D$ decays provide—from the theoretical point of view—the ideal realization of the 'triangle' approach to determine γ. On the other hand, the practical implementation still appears to be challenging, although detailed experimental feasibility studies for LHCb are strongly encouraged. The corresponding branching ratios were estimated in Ref. [96], with a pattern in accordance with (114).

5 Features of neutral B mesons

5.1 Schrödinger equation for B_q^0–$\bar{B}_q^0$ mixing

Within the SM, B_q^0–$\bar{B}_q^0$ mixing ($q \in \{d, s\}$) arises from the box diagrams shown in Fig. 16. Because of this phenomenon, an initially, i.e., at time $t = 0$, present B_q^0-meson state evolves into a time-dependent

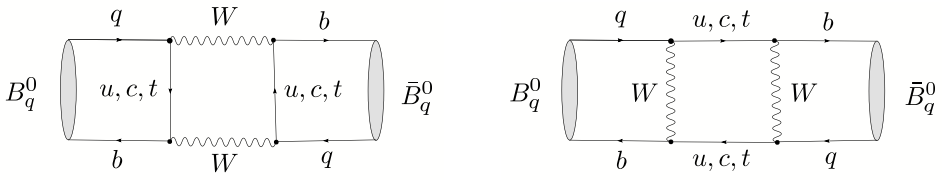

Fig. 16: Box diagrams contributing to B_q^0–$\bar{B}_q^0$ mixing in the SM ($q \in \{d, s\}$)

linear combination of B_q^0 and $\bar{B}_q^0$ states:

$$|B_q(t)\rangle = a(t)|B_q^0\rangle + b(t)|\bar{B}_q^0\rangle, \tag{115}$$

where $a(t)$ and $b(t)$ are governed by a Schrödinger equation of the following form:

$$i\,\frac{\mathrm{d}}{\mathrm{d}t}\begin{pmatrix} a(t) \\ b(t) \end{pmatrix} = H \cdot \begin{pmatrix} a(t) \\ b(t) \end{pmatrix} \equiv \Bigg[\underbrace{\begin{pmatrix} M_0^{(q)} & M_{12}^{(q)} \\ M_{12}^{(q)*} & M_0^{(q)} \end{pmatrix}}_{\text{mass matrix}} - \frac{i}{2}\underbrace{\begin{pmatrix} \Gamma_0^{(q)} & \Gamma_{12}^{(q)} \\ \Gamma_{12}^{(q)*} & \Gamma_0^{(q)} \end{pmatrix}}_{\text{decay matrix}}\Bigg] \cdot \begin{pmatrix} a(t) \\ b(t) \end{pmatrix}.$$

The special form $H_{11} = H_{22}$ of the Hamiltonian H is an implication of the CPT theorem, i.e., of the invariance under combined CP and time-reversal (T) transformations.

It is straightforward to calculate the eigenstates $|B_\pm^{(q)}\rangle$ and eigenvalues $\lambda_\pm^{(q)}$ of (116):

$$|B_\pm^{(q)}\rangle = \frac{1}{\sqrt{1+|\alpha_q|^2}}\left(|B_q^0\rangle \pm \alpha_q|\bar{B}_q^0\rangle\right) \tag{116}$$

$$\lambda_\pm^{(q)} = \left(M_0^{(q)} - \frac{i}{2}\Gamma_0^{(q)}\right) \pm \left(M_{12}^{(q)} - \frac{i}{2}\Gamma_{12}^{(q)}\right)\alpha_q\,, \tag{117}$$

where

$$\alpha_q e^{+i\left(\Theta_{\Gamma_{12}}^{(q)} + n'\pi\right)} = \sqrt{\frac{4|M_{12}^{(q)}|^2 e^{-i2\delta\Theta_{M/\Gamma}^{(q)}} + |\Gamma_{12}^{(q)}|^2}{4|M_{12}^{(q)}|^2 + |\Gamma_{12}^{(q)}|^2 - 4|M_{12}^{(q)}||\Gamma_{12}^{(q)}|\sin\delta\Theta_{M/\Gamma}^{(q)}}}\,. \tag{118}$$

Here we have written

$$M_{12}^{(q)} \equiv e^{i\Theta_{M_{12}}^{(q)}}|M_{12}^{(q)}|, \quad \Gamma_{12}^{(q)} \equiv e^{i\Theta_{\Gamma_{12}}^{(q)}}|\Gamma_{12}^{(q)}|, \quad \delta\Theta_{M/\Gamma}^{(q)} \equiv \Theta_{M_{12}}^{(q)} - \Theta_{\Gamma_{12}}^{(q)}\,, \tag{119}$$

and have introduced the quantity $n' \in \{0, 1\}$ to parametrize the sign of the square root in (118).

Evaluating the dispersive parts of the box diagrams shown in Fig. 16, which are dominated by internal top-quark exchanges, yields (for a more detailed discussion, see Ref. [17]):

$$M_{12}^{(q)} = \frac{G_\mathrm{F}^2 M_W^2}{12\pi^2}\eta_B M_{B_q} f_{B_q}^2 \hat{B}_{B_q}\left(V_{tq}^* V_{tb}\right)^2 S_0(x_t) e^{i(\pi - \phi_{\mathrm{CP}}(B_q))}\,, \tag{120}$$

where $\phi_{\mathrm{CP}}(B_q)$ is a convention-dependent phase, which is defined in analogy to (94). The short-distance physics is encoded in the 'Inami–Lim' function $S_0(x_t \equiv m_t^2/M_W^2)$ [97], which can be written—to a good approximation—in the SM as [98]

$$S_0(x_t) = 2.40 \times \left[\frac{m_t}{167\,\mathrm{GeV}}\right]^{1.52}\,, \tag{121}$$

and in the perturbative QCD correction factor $\eta_B = 0.55 \pm 0.01$ [99], which does *not* depend on $q \in \{d, s\}$, i.e., is the same for B_d and B_s mesons. On the other hand, the non-perturbative physics is

described by the quantities $f_{B_q}\hat{B}_{B_q}^{1/2}$, involving—in addition to the B_q decay constant f_{B_q}—the 'bag' parameter $\hat{B}_{B_q}$, which is related to the hadronic matrix element $\langle \bar{B}_q^0|(\bar{b}q)_{\rm V-A}(\bar{b}q)_{\rm V-A}|B_q^0\rangle$. These non-perturbative parameters can be determined through QCD sum-rule calculations [100] or lattice studies. Concerning the latter analyses, the front runners are now unquenched calculations with 2 or 3 dynamical quarks. Despite tremendous progress, the results still suffer from several uncertainties. For the analysis of the mixing parameters discussed below [101], we use two sets of parameters from the JLQCD [102] and HPQCD [103] lattice collaborations:

$$\begin{aligned} f_{B_d}\hat{B}_{B_d}^{1/2}\Big|_{\rm JLQCD} &= (0.215 \pm 0.019^{+0}_{-0.023})\,{\rm GeV} \\ f_{B_s}\hat{B}_{B_s}^{1/2}\Big|_{\rm JLQCD} &= (0.245 \pm 0.021^{+0.003}_{-0.002})\,{\rm GeV}\,, \end{aligned} \tag{122}$$

which were obtained for two flavours of dynamical light ('Wilson') quarks, and

$$\begin{aligned} f_{B_d}\hat{B}_{B_d}^{1/2}\Big|_{\rm (HP+JL)QCD} &= (0.244 \pm 0.026)\,{\rm GeV} \\ f_{B_s}\hat{B}_{B_s}^{1/2}\Big|_{\rm (HP+JL)QCD} &= (0.295 \pm 0.036)\,{\rm GeV}\,, \end{aligned} \tag{123}$$

where f_{B_q} comes from HPQCD (3 dynamical flavours) and $\hat{B}_{B_q}$ from JLQCD as no value for this parameter is available from the former collaboration [104].

If we calculate also the absorptive parts of the box diagrams in Fig 16, we obtain

$$\frac{\Gamma_{12}^{(q)}}{M_{12}^{(q)}} \approx -\frac{3\pi}{2S_0(x_t)}\left(\frac{m_b^2}{M_W^2}\right) = \mathcal{O}(m_b^2/m_t^2) \ll 1\,. \tag{124}$$

Consequently, we may expand (118) in $\Gamma_{12}^{(q)}/M_{12}^{(q)}$. Neglecting second-order terms, we arrive at

$$\alpha_q = \left[1 + \frac{1}{2}\left|\frac{\Gamma_{12}^{(q)}}{M_{12}^{(q)}}\right|\sin\delta\Theta_{M/\Gamma}^{(q)}\right] e^{-i\left(\Theta_{M_{12}}^{(q)} + n'\pi\right)}\,. \tag{125}$$

The deviation of $|\alpha_q|$ from 1 measures CP violation in B_q^0–$\bar{B}_q^0$ oscillations, and can be probed through the following 'wrong-charge' lepton asymmetries:

$$\mathcal{A}_{\rm SL}^{(q)} \equiv \frac{\Gamma(B_q^0(t) \to \ell^-\bar{\nu}X) - \Gamma(\bar{B}_q^0(t) \to \ell^+\nu X)}{\Gamma(B_q^0(t) \to \ell^-\bar{\nu}X) + \Gamma(\bar{B}_q^0(t) \to \ell^+\nu X)} = \frac{|\alpha_q|^4 - 1}{|\alpha_q|^4 + 1} \approx \left|\frac{\Gamma_{12}^{(q)}}{M_{12}^{(q)}}\right|\sin\delta\Theta_{M/\Gamma}^{(q)}\,. \tag{126}$$

Because of $|\Gamma_{12}^{(q)}|/|M_{12}^{(q)}| \propto m_b^2/m_t^2$ and $\sin\delta\Theta_{M/\Gamma}^{(q)} \propto m_c^2/m_b^2$, the asymmetry $\mathcal{A}_{\rm SL}^{(q)}$ is suppressed by a factor of $m_c^2/m_t^2 = \mathcal{O}(10^{-4})$ and is hence tiny in the SM. However, this observable may be enhanced through NP effects, thereby representing an interesing probe for physics beyond the SM [105, 106]. The current experimental average for the B_d-meson system compiled by the 'Heavy Flavour Averaging Group' [61] reads as follows:

$$\mathcal{A}_{\rm SL}^{(d)} = 0.0030 \pm 0.0078\,, \tag{127}$$

and does not indicate any non-vanishing effect.

5.2 Mixing parameters

Let us denote the masses of the eigenstates of (116) by $M_{\rm H}^{(q)}$ ('heavy') and $M_{\rm L}^{(q)}$ ('light'). It is then useful to introduce

$$M_q \equiv \frac{M_{\rm H}^{(q)} + M_{\rm L}^{(q)}}{2} = M_0^{(q)}\,, \tag{128}$$

as well as the mass difference

$$\Delta M_q \equiv M_{\rm H}^{(q)} - M_{\rm L}^{(q)} = 2|M_{12}^{(q)}| > 0 \,, \tag{129}$$

which is by definition *positive*. While B_d^0–$\bar{B}_d^0$ mixing is well established and

$$\Delta M_d = (0.507 \pm 0.004)\,{\rm ps}^{-1} \tag{130}$$

known with impressive experimental accuracy [61], only lower bounds on ΔM_s were available, for many years, from the LEP (CERN) experiments and SLD (SLAC) [107]. In the spring of 2006, ΔM_s could eventually be pinned down at the Tevatron: the D0 Collaboration reported a two-sided bound

$$17\,{\rm ps}^{-1} < \Delta M_s < 21\,{\rm ps}^{-1} \quad (90\%\ {\rm C.L.}) \,, \tag{131}$$

corresponding to a 2.5 σ signal at $\Delta M_s = 19\,{\rm ps}^{-1}$ [108], and CDF announced the following result [109]:

$$\Delta M_s = \left[17.31^{+0.33}_{-0.18}({\rm stat}) \pm 0.07({\rm syst})\right]{\rm ps}^{-1} \,. \tag{132}$$

The decay widths $\Gamma_{\rm H}^{(q)}$ and $\Gamma_{\rm L}^{(q)}$ of the mass eigenstates, which correspond to $M_{\rm H}^{(q)}$ and $M_{\rm L}^{(q)}$, respectively, satisfy

$$\Delta\Gamma_q \equiv \Gamma_{\rm H}^{(q)} - \Gamma_{\rm L}^{(q)} = \frac{4\,{\rm Re}\left[M_{12}^{(q)}\Gamma_{12}^{(q)*}\right]}{\Delta M_q} \,, \tag{133}$$

whereas

$$\Gamma_q \equiv \frac{\Gamma_{\rm H}^{(q)} + \Gamma_{\rm L}^{(q)}}{2} = \Gamma_0^{(q)} \,. \tag{134}$$

There is the following interesting relation:

$$\frac{\Delta\Gamma_q}{\Gamma_q} \approx -\frac{3\pi}{2S_0(x_t)}\left(\frac{m_b^2}{M_W^2}\right) x_q = -\mathcal{O}(10^{-2}) \times x_q \,, \tag{135}$$

where

$$x_q \equiv \frac{\Delta M_q}{\Gamma_q} = \begin{cases} 0.771 \pm 0.012 & (q = d) \\ \mathcal{O}(20) & (q = s) \end{cases} \tag{136}$$

is often referred to as *the* B_q^0–$\bar{B}_q^0$ 'mixing parameter'[2]. Consequently, we observe that $\Delta\Gamma_d/\Gamma_d \sim 10^{-2}$ is negligibly small, while $\Delta\Gamma_s/\Gamma_s \sim 10^{-1}$ may be sizeable. In fact, as was reviewed in Ref. [110], the state of the art of calculations of these quantities is given as follows:

$$\frac{|\Delta\Gamma_d|}{\Gamma_d} = (3 \pm 1.2) \times 10^{-3}, \quad \frac{|\Delta\Gamma_s|}{\Gamma_s} = 0.12 \pm 0.05 \,. \tag{137}$$

Recently, the first results for $\Delta\Gamma_s$ were reported from the Tevatron, using the $B_s^0 \to J/\psi\phi$ channel [111]:

$$\frac{|\Delta\Gamma_s|}{\Gamma_s} = \begin{cases} 0.65^{+0.25}_{-0.33} \pm 0.01 & ({\rm CDF\ [112]}) \\ 0.24^{+0.28+0.03}_{-0.38-0.04} & ({\rm D0\ [113]}) \,. \end{cases} \tag{138}$$

It will be interesting to follow the evolution of the data for this quantity.

In Sections 7.1 and 10.1, we give detailed discussions of the theoretical interpretation of the data for the B_q^0–$\bar{B}_q^0$ mixing parameters.

[2]Note that $\Delta\Gamma_q/\Gamma_q$ is negative in the SM because of the minus sign in (135).

5.3 Time-dependent decay rates

The time evolution of initially, i.e., at $t = 0$, pure B_q^0- and $\bar{B}_q^0$-meson states is given by

$$|B_q^0(t)\rangle = f_+^{(q)}(t)|B_q^0\rangle + \alpha_q f_-^{(q)}(t)|\bar{B}_q^0\rangle \tag{139}$$

and

$$|\bar{B}_q^0(t)\rangle = \frac{1}{\alpha_q} f_-^{(q)}(t)|B_q^0\rangle + f_+^{(q)}(t)|\bar{B}_q^0\rangle \,, \tag{140}$$

respectively, with

$$f_\pm^{(q)}(t) = \frac{1}{2}\left[e^{-i\lambda_+^{(q)}t} \pm e^{-i\lambda_-^{(q)}t}\right]. \tag{141}$$

These time-dependent state vectors allow the calculation of the corresponding transition rates. To this end, it is useful to introduce

$$|g_\pm^{(q)}(t)|^2 = \frac{1}{4}\left[e^{-\Gamma_{\rm L}^{(q)}t} + e^{-\Gamma_{\rm H}^{(q)}t} \pm 2\, e^{-\Gamma_q t}\cos(\Delta M_q t)\right] \tag{142}$$

$$g_-^{(q)}(t)\, g_+^{(q)}(t)^* = \frac{1}{4}\left[e^{-\Gamma_{\rm L}^{(q)}t} - e^{-\Gamma_{\rm H}^{(q)}t} + 2\, i\, e^{-\Gamma_q t}\sin(\Delta M_q t)\right], \tag{143}$$

as well as

$$\xi_f^{(q)} = e^{-i\Theta_{M_{12}}^{(q)}}\frac{A(\bar{B}_q^0 \to f)}{A(B_q^0 \to f)}, \quad \xi_{\bar{f}}^{(q)} = e^{-i\Theta_{M_{12}}^{(q)}}\frac{A(\bar{B}_q^0 \to \bar{f})}{A(B_q^0 \to \bar{f})}\,. \tag{144}$$

Looking at (120), we find

$$\Theta_{M_{12}}^{(q)} = \pi + 2{\rm arg}(V_{tq}^* V_{tb}) - \phi_{\rm CP}(B_q)\,, \tag{145}$$

and observe that this phase depends on the chosen CKM and CP phase conventions specified in (11) and (94), respectively. However, these dependences are cancelled through the amplitude ratios in (144), so that $\xi_f^{(q)}$ and $\xi_{\bar{f}}^{(q)}$ are *convention-independent* observables. Whereas n' enters the functions in (141) through (117), the dependence on this parameter is cancelled in (142) and (143) through the introduction of the *positive* mass difference ΔM_q [see (129)]. Combining the formulae listed above, we eventually arrive at the following transition rates for decays of initially, i.e., at $t = 0$, present B_q^0 or $\bar{B}_q^0$ mesons:

$$\Gamma(\overset{(-)}{B}{}_q^0(t) \to f) = \left[|g_\mp^{(q)}(t)|^2 + |\xi_f^{(q)}|^2|g_\pm^{(q)}(t)|^2 - 2\,{\rm Re}\left\{\xi_f^{(q)} g_\pm^{(q)}(t) g_\mp^{(q)}(t)^*\right\}\right]\tilde{\Gamma}_f\,, \tag{146}$$

where the time-independent rate $\tilde{\Gamma}_f$ corresponds to the 'unevolved' decay amplitude $A(B_q^0 \to f)$, and can be calculated by performing the usual phase-space integrations. The rates into the CP-conjugate final state $\bar{f}$ can straightforwardly be obtained from (146) by making the substitutions

$$\tilde{\Gamma}_f \;\to\; \tilde{\Gamma}_{\bar{f}}, \quad \xi_f^{(q)} \;\to\; \xi_{\bar{f}}^{(q)}\,. \tag{147}$$

5.4 'Untagged' rates

The expected sizeable width difference $\Delta\Gamma_s$ may provide interesting studies of CP violation through 'untagged' B_s rates (see Ref. [111] and [114]– [117]), which are defined as

$$\langle\Gamma(B_s(t) \to f)\rangle \equiv \Gamma(B_s^0(t) \to f) + \Gamma(\bar{B}_s^0(t) \to f)\,, \tag{148}$$

and are characterized by the feature that we do not distinguish between initially, i.e., at time $t = 0$, present B_s^0 or $\bar{B}_s^0$ mesons. If we consider a final state f to which both a B_s^0 and a $\bar{B}_s^0$ may decay, and use the expressions in (146), we find

$$\langle\Gamma(B_s(t) \to f)\rangle \propto \left[\cosh(\Delta\Gamma_s t/2) - \mathcal{A}_{\Delta\Gamma}(B_s \to f)\sinh(\Delta\Gamma_s t/2)\right] e^{-\Gamma_s t}\,, \tag{149}$$

with

$$\mathcal{A}_{\Delta\Gamma}(B_s \to f) \equiv \frac{2\,\mathrm{Re}\,\xi_f^{(s)}}{1+\left|\xi_f^{(s)}\right|^2}\,. \tag{150}$$

We observe that the rapidly oscillating $\Delta M_s t$ terms cancel, and that we may obtain information about the phase structure of the observable $\xi_f^{(s)}$, thereby providing valuable insights into CP violation.

Following these lines, for instance, the untagged observables offered by the angular distribution of the $B_s \to K^{*+}K^{*-}, K^{*0}\bar{K}^{*0}$ decay products allow a determination of the UT angle γ, provided $\Delta\Gamma_s$ is actually sizeable [115]. Untagged B_s-decay rates are interesting in terms of efficiency, acceptance and purity, and are already applied for the physics analyses at the Tevatron. Later on, they will help to fully exploit the physics potential of the B_s-meson system at the LHC.

5.5 CP asymmetries

A particularly simple—but also very interesting—situation arises if we restrict ourselves to decays of neutral B_q mesons into final states f that are eigenstates of the CP operator, i.e., satisfy the relation

$$(\mathcal{CP})|f\rangle = \pm|f\rangle\,. \tag{151}$$

Consequently, we have $\xi_f^{(q)} = \xi_{\bar{f}}^{(q)}$ in this case, as can be seen in (144). Using the decay rates in (146), we find that the corresponding time-dependent CP asymmetry is given by

$$\begin{aligned}\mathcal{A}_{\mathrm{CP}}(t) &\equiv \frac{\Gamma(B_q^0(t)\to f)-\Gamma(\bar{B}_q^0(t)\to f)}{\Gamma(B_q^0(t)\to f)+\Gamma(\bar{B}_q^0(t)\to f)}\\ &= \left[\frac{\mathcal{A}_{\mathrm{CP}}^{\mathrm{dir}}(B_q\to f)\,\cos(\Delta M_q t)+\mathcal{A}_{\mathrm{CP}}^{\mathrm{mix}}(B_q\to f)\,\sin(\Delta M_q t)}{\cosh(\Delta\Gamma_q t/2)-\mathcal{A}_{\Delta\Gamma}(B_q\to f)\,\sinh(\Delta\Gamma_q t/2)}\right],\end{aligned} \tag{152}$$

with

$$\mathcal{A}_{\mathrm{CP}}^{\mathrm{dir}}(B_q\to f) \equiv \frac{1-\left|\xi_f^{(q)}\right|^2}{1+\left|\xi_f^{(q)}\right|^2}, \qquad \mathcal{A}_{\mathrm{CP}}^{\mathrm{mix}}(B_q\to f) \equiv \frac{2\,\mathrm{Im}\,\xi_f^{(q)}}{1+\left|\xi_f^{(q)}\right|^2}\,. \tag{153}$$

Because of the relation

$$\mathcal{A}_{\mathrm{CP}}^{\mathrm{dir}}(B_q\to f) = \frac{|A(B_q^0\to f)|^2-|A(\bar{B}_q^0\to\bar{f})|^2}{|A(B_q^0\to f)|^2+|A(\bar{B}_q^0\to\bar{f})|^2}\,, \tag{154}$$

this observable measures the direct CP violation in the decay $B_q \to f$, which originates from the interference between different weak amplitudes, as we have seen in (97). On the other hand, the interesting *new* aspect of (152) is due to $\mathcal{A}_{\mathrm{CP}}^{\mathrm{mix}}(B_q\to f)$, which originates from interference effects between B_q^0–$\bar{B}_q^0$ mixing and decay processes, and describes 'mixing-induced' CP violation. Finally, the width difference $\Delta\Gamma_q$, which may be sizeable in the B_s-meson system, provides access to $\mathcal{A}_{\Delta\Gamma}(B_q\to f)$ introduced in (150). However, this observable is not independent from $\mathcal{A}_{\mathrm{CP}}^{\mathrm{dir}}(B_q\to f)$ and $\mathcal{A}_{\mathrm{CP}}^{\mathrm{mix}}(B_q\to f)$, satisfying

$$\left[\mathcal{A}_{\mathrm{CP}}^{\mathrm{dir}}(B_q\to f)\right]^2+\left[\mathcal{A}_{\mathrm{CP}}^{\mathrm{mix}}(B_q\to f)\right]^2+\left[\mathcal{A}_{\Delta\Gamma}(B_q\to f)\right]^2 = 1\,. \tag{155}$$

In order to calculate $\xi_f^{(q)}$, we use the general expressions (95) and (96), where $e^{-i\phi_{\mathrm{CP}}(f)} = \pm 1$ because of (151), and $\phi_{\mathrm{CP}}(B) = \phi_{\mathrm{CP}}(B_q)$. If we insert these amplitude parametrizations into (144) and take (145) into account, we observe that the phase-convention-dependent quantity $\phi_{\mathrm{CP}}(B_q)$ cancels, and finally arrive at

$$\xi_f^{(q)} = \mp\, e^{-i\phi_q}\left[\frac{e^{+i\varphi_1}|A_1|e^{i\delta_1}+e^{+i\varphi_2}|A_2|e^{i\delta_2}}{e^{-i\varphi_1}|A_1|e^{i\delta_1}+e^{-i\varphi_2}|A_2|e^{i\delta_2}}\right]\,, \tag{156}$$

where

$$\phi_q \equiv 2\arg(V_{tq}^* V_{tb}) = \begin{cases} +2\beta & (q=d) \\ -2\delta\gamma & (q=s) \end{cases} \tag{157}$$

is associated with the CP-violating weak B_q^0–$\bar{B}_q^0$ mixing phase arising in the SM; β and $\delta\gamma$ refer to the corresponding angles in the unitarity triangles shown in Fig. 3.

In analogy to (97), the caclulation of $\xi_f^{(q)}$ is—in general—also affected by large hadronic uncertainties. However, if one CKM amplitude plays the dominant role in the $B_q \to f$ transition, we obtain

$$\xi_f^{(q)} = \mp\, e^{-i\phi_q} \left[\frac{e^{+i\phi_f/2}|M_f|e^{i\delta_f}}{e^{-i\phi_f/2}|M_f|e^{i\delta_f}}\right] = \mp\, e^{-i(\phi_q-\phi_f)}\,, \tag{158}$$

and observe that the hadronic matrix element $|M_f|e^{i\delta_f}$ cancels in this expression. Since the requirements for direct CP violation discussed above are no longer satisfied, direct CP violation vanishes in this important special case, i.e., $\mathcal{A}_{\rm CP}^{\rm dir}(B_q \to f) = 0$. On the other hand, this is *not* the case for the mixing-induced CP asymmetry. In particular,

$$\mathcal{A}_{\rm CP}^{\rm mix}(B_q \to f) = \pm\sin\phi \tag{159}$$

is now governed by the CP-violating weak phase difference $\phi \equiv \phi_q - \phi_f$ and is not affected by hadronic uncertainties. The corresponding time-dependent CP asymmetry takes then the simple form

$$\left.\frac{\Gamma(B_q^0(t)\to f) - \Gamma(\bar{B}_q^0(t)\to \bar{f})}{\Gamma(B_q^0(t)\to f) + \Gamma(\bar{B}_q^0(t)\to \bar{f})}\right|_{\Delta\Gamma_q=0} = \pm\sin\phi\,\sin(\Delta M_q t)\,, \tag{160}$$

and allows an elegant determination of $\sin\phi$.

6 How could new physics enter?

Using the concept of the low-energy effective Hamiltonians introduced in Section 3.3.2, we may address this important question in a systematic manner [118]:

- NP may modify the 'strength' of the SM operators through new short-distance functions which depend on the NP parameters, such as the masses of charginos, squarks, charged Higgs particles and $\tan\bar{\beta} \equiv v_2/v_1$ in the 'minimal supersymmetric SM' (MSSM). The NP particles may enter in box and penguin topologies, and are 'integrated out' as the W boson and top quark in the SM. Consequently, the initial conditions for the renormalization-group evolution take the following form:

  $$C_k \to C_k^{\rm SM} + C_k^{\rm NP}\,. \tag{161}$$

  It should be emphasized that the NP pieces $C_k^{\rm NP}$ may also involve new CP-violating phases which are *not* related to the CKM matrix.
- NP may enhance the operator basis:

  $$\{Q_k\} \to \{Q_k^{\rm SM}, Q_l^{\rm NP}\}\,, \tag{162}$$

  so that operators which are not present (or strongly suppressed) in the SM may actually play an important role. In this case, we encounter, in general, also new sources for flavour and CP violation.

The B-meson system offers a variety of processes and strategies for the exploration of CP violation [12, 119], as we have illustrated in Fig. 17 through a collection of prominent examples. We see that there are processes with a very *different* dynamics that are—in the SM—sensitive to the *same* angles of the UT. Moreover, rare B- and K-meson decays [120], which originate from loop effects in the SM,

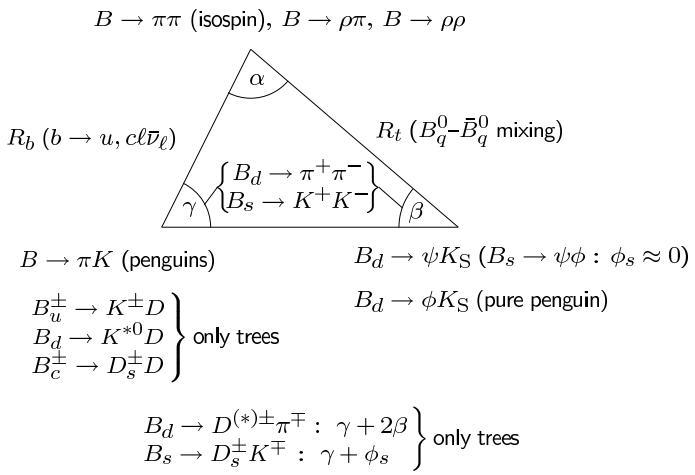

Fig. 17: A brief roadmap of B-decay strategies for the exploration of CP violation

provide complementary insights into flavour physics and interesting correlations with the CP-B sector; key examples are $B \to X_s\gamma$ and the exclusive modes $B \to K^*\gamma$, $B \to \rho\gamma$, as well as $B_{s,d} \to \mu^+\mu^-$ and $K^+ \to \pi^+\nu\bar{\nu}$, $K_{\rm L} \to \pi^0\nu\bar{\nu}$.

In the presence of NP contributions, the subtle interplay between the different processes could well be disturbed. There are two popular avenues for NP to enter the roadmap of quark-flavour physics:

– B_q^0–$\bar{B}_q^0$ *mixing:* NP could enter through the exchange of new particles in the box diagrams, or through new contributions at the tree level. In general, we may write

$$M_{12}^{(q)} = M_{12}^{q,\rm SM}\left(1 + \kappa_q e^{i\sigma_q}\right), \tag{163}$$

where the expression for $M_{12}^{q,\rm SM}$ can be found in (120). Consequently, we obtain

$$\Delta M_q = \Delta M_q^{\rm SM} + \Delta M_q^{\rm NP} = \Delta M_q^{\rm SM}\left|1 + \kappa_q e^{i\sigma_q}\right|, \tag{164}$$

$$\phi_q = \phi_q^{\rm SM} + \phi_q^{\rm NP} = \phi_q^{\rm SM} + \arg(1 + \kappa_q e^{i\sigma_q}), \tag{165}$$

with $\Delta M_q^{\rm SM}$ and $\phi_q^{\rm SM}$ given in (129) and (157), respectively. Using dimensional arguments borrowed from effective field theory [121, 122], it can be shown that $\Delta M_q^{\rm NP}/\Delta M_q^{\rm SM} \sim 1$ and $\phi_q^{\rm NP}/\phi_q^{\rm SM} \sim 1$ could—in principle—be possible for a NP scale $\Lambda_{\rm NP}$ in the TeV regime; such a pattern may also arise in specific NP scenarios. Introducing

$$\rho_q \equiv \left|\frac{\Delta M_q}{\Delta M_q^{\rm SM}}\right| = \sqrt{1 + 2\kappa_q\cos\sigma_q + \kappa_q^2}\,, \tag{166}$$

the measured values of the mass differences ΔM_q can be converted into constraints in NP parameter space through the contours shown in Fig. 18. Further constraints are implied by the NP phases $\phi_q^{\rm NP}$, which can be probed through mixing-induced CP asymmetries, through the curves in the σ_q–κ_q plane shown in Fig. 19. Interestingly, κ_q is bounded from below for any value of $\phi_q^{\rm NP} \neq 0$. For example, even a small phase $|\phi_q^{\rm NP}| = 10^\circ$ implies a clean lower bound of $\kappa_q \geq 0.17$, i.e., NP contributions of at most 17% [101].

– *Decay amplitudes:* NP has typically a small effect if SM tree processes play the dominant role. However, NP could well have a significant impact on the FCNC sector: new particles may enter in penguin or box diagrams, or new FCNC contributions may even be generated at the tree level. In fact, sizeable contributions arise generically in field-theoretical estimates with $\Lambda_{\rm NP} \sim$ TeV [123], as well as in specific NP models.

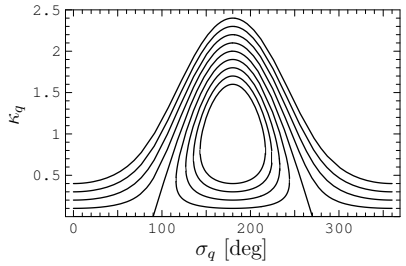

Fig. 18: The dependence of κ_q on σ_q for values of ρ_q varied between 1.4 (most upper curve) and 0.6 (most inner curve), in steps of 0.1

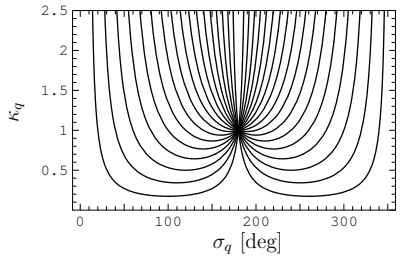

Fig. 19: The dependence of κ_q on σ_q for values of $\phi_q^{\rm NP}$ varied between $\pm 10^\circ$ (lower curves) and $\pm 170^\circ$ in steps of 10°: the curves for $0^\circ < \sigma_q < 180^\circ$ and $180^\circ < \sigma_q < 360^\circ$ correspond to positive and negative values of $\phi_q^{\rm NP}$, respectively.

Concerning model-dependent NP analyses, SUSY scenarios in particular have received a lot of attention; for a selection of recent studies, see Refs. [124]– [129]. Examples of other fashionable NP scenarios are left–right-symmetric models [130], scenarios with extra dimensions [131], models with an extra Z' [132], 'little Higgs' scenarios [133], and models with a fourth generation [134].

The simplest extension of the SM is given by models with 'minimal flavour violation' (MFV). Following the characterization given in Ref. [135], the flavour-changing processes are here still governed by the CKM matrix—in particular there are no new sources for CP violation—and the only relevant operators are those present in the SM (for an alternative definition, see Ref. [136]). Specific examples are the Two-Higgs Doublet Model II, the MSSM without new sources of flavour violation and $\tan\bar{\beta}$ not too large, models with one extra universal dimension and the simplest little Higgs models. Because of their simplicity, the extensions of the SM with MFV show several correlations between various observables, thereby allowing for powerful tests of this scenario [137]. A systematic discussion of models with 'next-to-minimal flavour violation' was recently given in Ref. [138].

There are other fascinating probes for the search of NP. Important examples are the D-meson system [139], electric dipole moments [140], or flavour-violating charged lepton decays [141]. Since a discussion of these topics is beyond the scope of these lectures, the interested reader should consult the corresponding references. Let us next have a closer look at prominent B decays, with a particular emphasis of the impact of NP.

7 Status of important B-factory benchmark modes

7.1 $B_d^0 \to J/\psi K_{\rm S}$

7.1.1 Basic formulae

This decay has a CP-odd final state, and originates from $\bar{b} \to \bar{c}c\bar{s}$ quark-level transitions. Consequently, as we discussed in Section 3.3.1, it receives contributions both from tree and from penguin topologies,

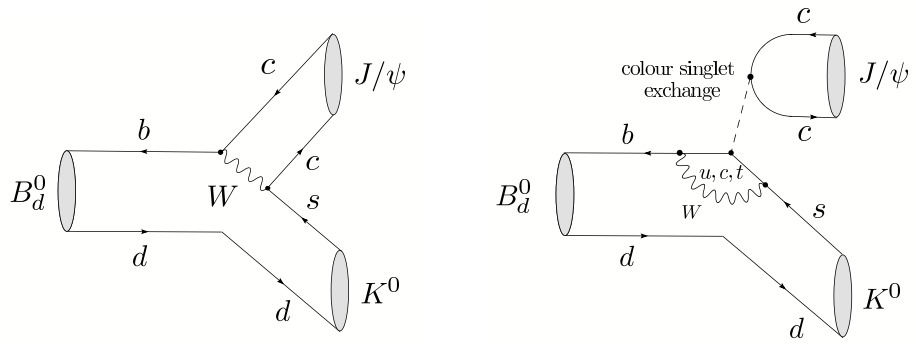

Fig. 20: Feynman diagrams contributing to $B_d^0 \to J/\psi K^0$ decays

as can be seen in Fig. 20. In the SM, the decay amplitude can hence be written as follows [142]:

$$A(B_d^0 \to J/\psi K_{\rm S}) = \lambda_c^{(s)} \left(A_{\rm T}^{c'} + A_{\rm P}^{c'} \right) + \lambda_u^{(s)} A_{\rm P}^{u'} + \lambda_t^{(s)} A_{\rm P}^{t'} \,. \tag{167}$$

Here the

$$\lambda_q^{(s)} \equiv V_{qs} V_{qb}^* \tag{168}$$

are CKM factors, $A_{\rm T}^{c'}$ is the CP-conserving strong tree amplitude, while the $A_{\rm P}^{q'}$ describe the penguin topologies with internal q quarks ($q \in \{u, c, t\}$), including QCD and EW penguins; the primes remind us that we are dealing with a $\bar{b} \to \bar{s}$ transition. If we eliminate now $\lambda_t^{(s)}$ through (79) and apply the Wolfenstein parametrization, we obtain

$$A(B_d^0 \to J/\psi K_{\rm S}) \propto \left[1 + \lambda^2 a e^{i\theta} e^{i\gamma} \right] \,, \tag{169}$$

where

$$a e^{i\vartheta} \equiv \left(\frac{R_b}{1-\lambda^2} \right) \left[\frac{A_{\rm P}^{u'} - A_{\rm P}^{t'}}{A_{\rm T}^{c'} + A_{\rm P}^{c'} - A_{\rm P}^{t'}} \right] \tag{170}$$

is a hadronic parameter. Using now the formalism of Section 5.5 yields

$$\xi_{\psi K_{\rm S}}^{(d)} = +e^{-i\phi_d} \left[\frac{1 + \lambda^2 a e^{i\vartheta} e^{-i\gamma}}{1 + \lambda^2 a e^{i\vartheta} e^{+i\gamma}} \right] . \tag{171}$$

Unfortunately, $a e^{i\vartheta}$, which is a measure for the ratio of the $B_d^0 \to J/\psi K_{\rm S}$ penguin to tree contributions, can only be estimated with large hadronic uncertainties. However, since this parameter enters (171) in a doubly Cabibbo-suppressed way, its impact on the CP-violating observables is practically negligible. We can put this important statement on a more quantitative basis by making the plausible assumption that $a = \mathcal{O}(\bar{\lambda}) = \mathcal{O}(0.2) = \mathcal{O}(\lambda)$, where $\bar{\lambda}$ is a 'generic' expansion parameter:

$$\mathcal{A}_{\rm CP}^{\rm dir}(B_d \to J/\psi K_{\rm S}) \;=\; 0 + \mathcal{O}(\overline{\lambda}^3) \tag{172}$$

$$\mathcal{A}_{\rm CP}^{\rm mix}(B_d \to J/\psi K_{\rm S}) \;=\; -\sin\phi_d + \mathcal{O}(\overline{\lambda}^3) \stackrel{\rm SM}{=} -\sin 2\beta + \mathcal{O}(\overline{\lambda}^3) \,. \tag{173}$$

Consequently, (173) allows an essentially *clean* determination of $\sin 2\beta$ [88].

7.1.2 Experimental status

Since the CKM fits performed within the SM pointed to a large value of $\sin 2\beta$, $B_d^0 \to J/\psi K_{\rm S}$ offered the exciting perspective of exhibiting *large* mixing-induced CP violation. In 2001, the measurement of $\mathcal{A}_{\rm CP}^{\rm mix}(B_d \to J/\psi K_{\rm S})$ allowed indeed the first observation of CP violation *outside* the K-meson

system [5]. The most recent data are still not showing any signal for *direct* CP violation in $B_d^0 \to J/\psi K_{\rm S}$ within the current uncertainties, as is expected from (172). The current world average reads [61]

$$\mathcal{A}_{\rm CP}^{\rm dir}(B_d \to J/\psi K_{\rm S}) = 0.026 \pm 0.041. \tag{174}$$

As far as (173) is concerned, we have

$$(\sin 2\beta)_{\psi K_{\rm S}} \equiv -\mathcal{A}_{\rm CP}^{\rm mix}(B_d \to J/\psi K_{\rm S}) = \left\{ \begin{array}{ll} 0.722 \pm 0.040 \pm 0.023 & \text{(BaBar [143])} \\ 0.652 \pm 0.039 \pm 0.020 & \text{(Belle [144])}\,, \end{array} \right. \tag{175}$$

which gives the following world average [61]:

$$(\sin 2\beta)_{\psi K_{\rm S}} = 0.687 \pm 0.032\,. \tag{176}$$

In the SM, the theoretical uncertainties are generically expected to be below the 0.01 level; significantly smaller effects are found in Ref. [145], whereas a fit performed in Ref. [146] yields a theoretical penguin uncertainty comparable to the present experimental systematic error. A possibility to control these uncertainties is provided by the $B_s^0 \to J/\psi K_{\rm S}$ channel [142], which can be explored at the LHC [147].

In Ref. [121], a set of observables to search for NP contributions to the $B \to J/\psi K$ decay amplitudes was introduced. It uses also the charged $B^\pm \to J/\psi K^\pm$ decay, and is given by

$$\mathcal{B}_{\psi K} \equiv \frac{1 - \mathcal{A}_{\psi K}}{1 + \mathcal{A}_{\psi K}}\,, \tag{177}$$

with

$$\mathcal{A}_{\psi K} \equiv \left[\frac{\mathrm{BR}(B^+ \to J/\psi K^+) + \mathrm{BR}(B^- \to J/\psi K^-)}{\mathrm{BR}(B_d^0 \to J/\psi K^0) + \mathrm{BR}(\bar{B}_d^0 \to J/\psi \bar{K}^0)}\right] \left[\frac{\tau_{B_d^0}}{\tau_{B^+}}\right], \tag{178}$$

and

$$\mathcal{D}_{\psi K}^{\pm} \equiv \frac{1}{2}\left[\mathcal{A}_{\rm CP}^{\rm dir}(B_d \to J/\psi K_{\rm S}) \pm \mathcal{A}_{\rm CP}^{\rm dir}(B^\pm \to J/\psi K^\pm)\right]. \tag{179}$$

As discussed in detail in Refs. [119, 121], the observables $\mathcal{B}_{\psi K}$ and $\mathcal{D}_{\psi K}^-$ are sensitive to NP in the $I = 1$ isospin sector, whereas a non-vanishing value of $\mathcal{D}_{\psi K}^+$ would signal NP in the $I = 0$ isospin sector. Moreover, the NP contributions with $I = 1$ are expected to be dynamically suppressed with respect to the $I = 0$ case because of their flavour structure. The most recent B-factory results yield

$$\mathcal{B}_{\psi K} = -0.035 \pm 0.037, \quad \mathcal{D}_{\psi K}^- = 0.010 \pm 0.023, \quad \mathcal{D}_{\psi K}^+ = 0.017 \pm 0.023\,. \tag{180}$$

Consequently, NP effects of $\mathcal{O}(10\%)$ in the $I = 1$ sector of the $B \to J/\psi K$ decay amplitudes are already disfavoured by the data for $\mathcal{B}_{\psi K}$ and $\mathcal{D}_{\psi K}^-$. However, since a non-vanishing value of $\mathcal{D}_{\psi K}^+$ requires also a large CP-conserving strong phase, this observable still leaves room for sizeable $I = 0$ NP contributions.

7.1.3 A closer look at new-physics effects

Thanks to the new Belle result listed in (175), the average for $(\sin 2\beta)_{\psi K_{\rm S}}$ went down by about 1σ, which was a somewhat surprising development of the summer of 2005. Consequently, the comparison of (176) with the CKM fits in the $\bar{\rho}$–$\bar{\eta}$ plane no longer looks 'perfect', as we saw in Fig. 4. Let us have a closer look at this feature. If we use γ determined from non-leptonic $B \to D^{(*)}K^{(*)}$ tree modes and R_b from semileptonic decays, we may calculate the 'true' value of β with the help of the relations

$$\sin\beta = \frac{R_b \sin\gamma}{\sqrt{1 - 2R_b\cos\gamma + R_b^2}}\,, \quad \cos\beta = \frac{1 - R_b\cos\gamma}{\sqrt{1 - 2R_b\cos\gamma + R_b^2}}\,, \tag{181}$$

which follow from the unitarity of the CKM matrix; the UTfit value

$$\gamma = (65 \pm 20)^\circ \tag{182}$$

in (106) and the inclusive and exclusive values of R_b in (72) yield

$$\beta_{\rm incl} = (26.7 \pm 1.9)^\circ\,, \quad \beta_{\rm excl} = (22.9 \pm 3.8)^\circ\,, \tag{183}$$

which can be converted into

$$\sin 2\beta|_{\rm incl} = 0.80 \pm 0.04, \quad \sin 2\beta|_{\rm excl} = 0.71 \pm 0.09\,. \tag{184}$$

Consequently, we find

$$\mathcal{S}_{\psi K} \equiv (\sin 2\beta)_{\psi K_{\rm S}} - \sin 2\beta = \left\{ \begin{array}{ll} -0.11 \pm 0.05 & \text{(incl)} \\ -0.02 \pm 0.10 & \text{(excl)}\,, \end{array} \right. \tag{185}$$

and see nicely the discrepancy arising for the inclusive determination of $|V_{ub}|$. As discussed in detail in Ref. [101], R_b is actually the key parameter for this possible discrepancy with the SM, whereas the situation is remarkably stable with respect to γ. There are two limiting cases of this possible discrepancy with the KM mechanism of CP violation:

- NP contributions to the $B \to J/\psi K$ decay amplitudes;
- NP effects entering through B^0_d–$\bar{B}^0_d$ mixing.

Let us first illustrate the former case. As the NP effects in the $I = 1$ sector are expected to be dynamically suppressed, we consider only NP in the $I = 0$ isospin sector, which implies $\mathcal{B}_{\psi K} = \mathcal{D}^-_{\psi K} = 0$, in accordance with (180). To simplify the discussion, we assume that there is effectively only a single NP contribution of this kind, so that we may write

$$A(B^0_d \to J/\psi K^0) = A_0 \left[1 + v_0 e^{i(\Delta_0 + \phi_0)}\right] = A(B^+ \to J/\psi K^+)\,. \tag{186}$$

Here v_0 and the CP-conserving strong phase Δ_0 are hadronic parameters, whereas ϕ_0 denotes a CP-violating phase originating beyond the SM. An interesting specific scenario falling into this category arises if the NP effects enter through EW penguins. This kind of NP has recently received a lot of attention in the context of the $B \to \pi K$ puzzle, which we shall discuss in Section 8. Also within the SM, where ϕ_0 vanishes, EW penguins have a sizeable impact on the $B \to J/\psi K$ system [148]. Using factorization, the following estimate can be obtained [83]:

$$v_0 e^{i\Delta_0}\big|^{\rm SM}_{\rm fact} \approx -0.03\,. \tag{187}$$

In Figs. 21 (a) and (b), we consider the inclusive value of (185), and show the situation in the $\mathcal{S}_{\psi K}$–$\mathcal{D}^+_{\psi K}$ plane for $\phi_0 = -90^\circ$ and $\phi_0 = +90^\circ$, respectively. The contours correspond to different values of v_0, and are obtained by varying Δ_0 between 0° and 360°; the experimental data are represented by the diamonds with the error bars. Since factorization gives $\Delta_0 = 180^\circ$, as can be seen in (187), the case of $\phi_0 = -90^\circ$ is disfavoured. On the other hand, in the case of $\phi_0 = +90^\circ$, the experimental region can straightforwardly be reached for Δ_0 not differing too much from the factorization result, although an enhancement of v_0 by a factor of $\mathcal{O}(3)$ with respect to the SM estimate in (187), which suffers from large uncertainties, would simultaneously be required in order to reach the central experimental value. Consequently, NP contributions to the EW penguin sector could, in principle, be at the origin of the possible discrepancy indicated by the inclusive value of (185). This scenario should be carefully monitored in the future.

Another explanation of (185) is provided by CP-violating NP contributions to B^0_d–$\bar{B}^0_d$ mixing, which affect the corresponding mixing phase as in (165), so that

$$\phi_d = 2\beta + \phi_d^{\rm NP}\,. \tag{188}$$

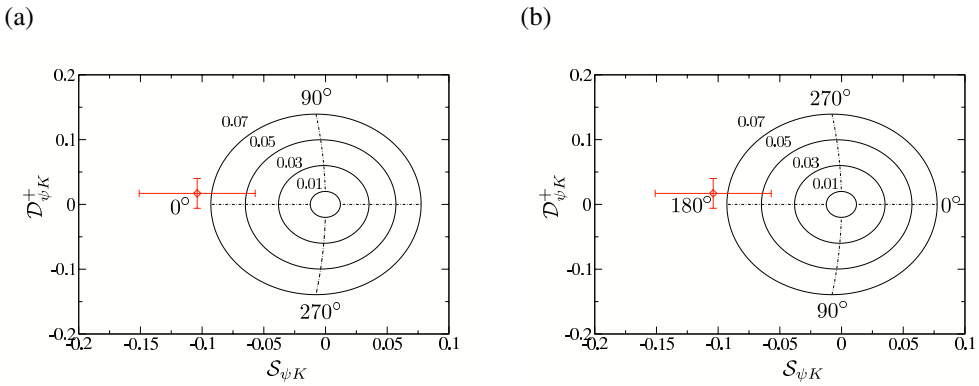

Fig. 21: The situation in the $\mathcal{S}_{\psi K}$–$\mathcal{D}^+_{\psi K}$ plane for NP contributions to the $B \to J/\psi K$ decay amplitudes in the $I = 0$ isospin sector for NP phases $\phi_0 = -90^\circ$ (a) and $\phi_0 = +90^\circ$ (b). The diamonds with the error bars represent the averages of the current data [for the inclusive value of (185)], whereas the numbers correspond to the values of Δ_0 and v_0.

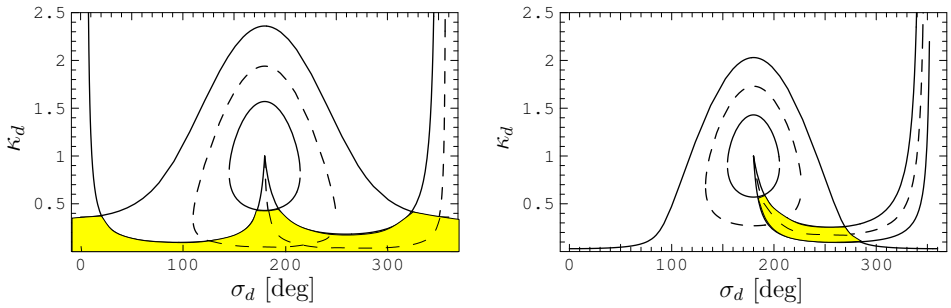

Fig. 22: Left panel: allowed region (yellow/grey) in the σ_d–κ_d plane in a scenario with the JLQCD lattice results (122) and $\phi_d^{\rm NP}\big|_{\rm excl}$. Dashed lines: central values of ρ_d and $\phi_d^{\rm NP}$, solid lines: $\pm 1\,\sigma$. Right panel: ditto for the scenario with the (HP+JL)QCD lattice results (123) and $\phi_d^{\rm NP}\big|_{\rm incl}$.

Assuming that the NP contributions to the $B \to J/\psi K$ amplitudes are negligible, (176) implies

$$\phi_d = (43.4 \pm 2.5)^\circ \quad \vee \quad (136.6 \pm 2.5)^\circ \,. \tag{189}$$

Here the latter solution would be in dramatic conflict with the CKM fits, and would require a large NP contribution to B^0_d–$\bar{B}^0_d$ mixing [122, 149]. Both solutions can be distinguished through the measurement of the sign of $\cos\phi_d$, where a positive value would select the SM-like branch. Using an angular analysis of the $B_d \to J/\psi[\to \ell^+\ell^-]K^*[\to \pi^0 K_{\rm S}]$ decay products, the BaBar Collaboration finds [150]

$$\cos\phi_d = 2.72^{+0.50}_{-0.79} \pm 0.27 \,, \tag{190}$$

thereby favouring the solution around $\phi_d = 43^\circ$. Interestingly, this picture emerges also from the first data for CP-violating effects in $B_d \to D^{(*)\pm}\pi^\mp$ modes [90], and an analysis of the $B \to \pi\pi, \pi K$ system [83], although in an indirect manner. Recently, a new method has been proposed, which makes use of the interference pattern in $D \to K_{\rm S}\pi^+\pi^-$ decays emerging from $B_d \to D\pi^0$ and similar decays [151]. The results of this method are also consistent with the SM, so that a negative value of $\cos\phi_d$ is now ruled out with greater than 95% confidence [89].

Using the 'true' values of β in (183), the value of $\phi_d = (43.4 \pm 2.5)^\circ$ implies

$$\phi_d^{\rm NP}\big|_{\rm incl} = -(10.1 \pm 4.6)^\circ \,, \qquad \phi_d^{\rm NP}\big|_{\rm excl} = -(2.5 \pm 8.0)^\circ \,; \tag{191}$$

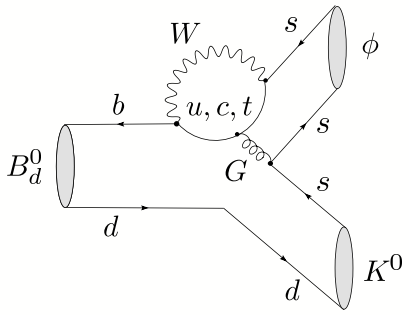

Fig. 23: Feynman diagrams contributing to $B_d^0 \to \phi K^0$ decays

results of $\phi_d^{\rm NP} \approx -10^\circ$ were also recently obtained in Refs. [91, 152]. The contours in Fig. 19 allow us now to convert these numbers into constraints in the σ_d–κ_d plane. Further constraints can be obtained through the experimental value of ΔM_d in (130) with the help of the contours in Fig. 18, where ρ_d is introduced in (166). In addition to hadronic parameters, the SM prediction of ΔM_d involves also the CKM factor $|V_{td}^* V_{tb}|$, which can—if we use the unitarity of the CKM matrix—be expressed as

$$|V_{td}^* V_{tb}| = |V_{cb}| \lambda \sqrt{1 - 2R_b \cos\gamma + R_b^2}\,. \tag{192}$$

The values in (72) and (182), as well as the relevant lattice parameters in (122) and (123) yield then

$$\rho_d|_{\rm JLQCD} = 0.97 \pm 0.33^{-0.17}_{+0.26} \tag{193}$$

$$\rho_d|_{\rm (HP+JL)QCD} = 0.75 \pm 0.25 \pm 0.16\,, \tag{194}$$

where the first and second errors are due to γ (and a small extent to R_b) and $f_{B_d}\hat{B}_{B_d}^{1/2}$, respectively [101]. These results are compatible with the SM value $\rho_d = 1$, but suffer from considerable uncertainties. In Fig. 22, we finally show the situation in the σ_d–κ_d plane. We see that the information about the CP-violating phase ϕ_d has a dramatic impact, reducing the allowed NP parameter space significantly.

The possibility of having a non-zero value of (185) could of course just be due to a statistical fluctuation. However, should it be confirmed, it could be due to CP-violating NP contributions to the $B_d^0 \to J/\psi K_{\rm S}$ decay amplitude or to B_d^0–$\bar{B}_d^0$ mixing, as we just saw. A tool to distinguish between these avenues is provided by decays of the kind $B_d \to D\pi^0, D\rho^0, ...$, which are pure 'tree' decays, i.e., they do *not* receive any penguin contributions. If the neutral D mesons are observed through their decays into CP eigenstates $D_\pm$, these decays allow extremely clean determinations of the 'true' value of $\sin\phi_d$ [153], as we shall discuss in more detail in Section 10.3. In view of (185), this would be very interesting, so that detailed feasibility studies for the exploration of the $B_d \to D\pi^0, D\rho^0, ...$ modes at a super-B factory are strongly encouraged.

7.2 $B_d^0 \to \phi K_{\rm S}$

Another important probe for the testing of the KM mechanism is offered by $B_d^0 \to \phi K_{\rm S}$, which is a decay into a CP-odd final state. As can be seen in Fig. 23, it originates from $\bar{b} \to \bar{s}s\bar{s}$ transitions and is, therefore, a pure penguin mode. This decay is described by the low-energy effective Hamiltonian in (80) with $r = s$, where the current–current operators may only contribute through penguin-like contractions, which describe the penguin topologies with internal up- and charm-quark exchanges. The dominant role is played by the QCD penguin operators [154]. However, thanks to the large top-quark mass, EW penguins have a sizeable impact as well [72, 155]. In the SM, we may write

$$A(B_d^0 \to \phi K_{\rm S}) = \lambda_u^{(s)} \tilde{A}_{\rm P}^{u'} + \lambda_c^{(s)} \tilde{A}_{\rm P}^{c'} + \lambda_t^{(s)} \tilde{A}_{\rm P}^{t'}\,, \tag{195}$$

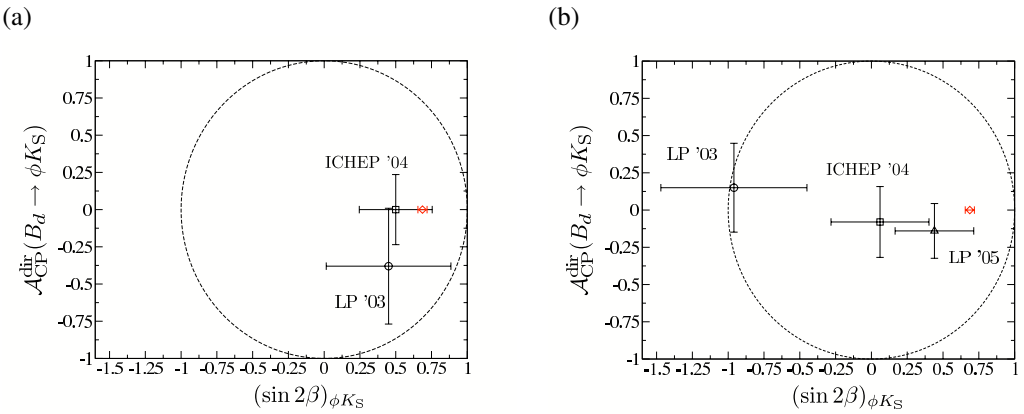

Fig. 24: The time evolution of the BaBar (a) and Belle (b) data for the CP violation in $B_d \to \phi K_{\rm S}$. The diamonds represent the SM relations (199)–(201) with (176).

where we have applied the same notation as in Section 7.1. Eliminating the CKM factor $\lambda_t^{(s)}$ with the help of (79) yields

$$A(B_d^0 \to \phi K_{\rm S}) \propto \left[1 + \lambda^2 b e^{i\Theta} e^{i\gamma}\right], \tag{196}$$

where

$$b e^{i\Theta} \equiv \left(\frac{R_b}{1-\lambda^2}\right)\left[\frac{\tilde{A}_{\rm P}^{u'} - \tilde{A}_{\rm P}^{t'}}{\tilde{A}_{\rm P}^{c'} - \tilde{A}_{\rm P}^{t'}}\right]. \tag{197}$$

Consequently, we obtain

$$\xi_{\phi K_{\rm S}}^{(d)} = +e^{-i\phi_d}\left[\frac{1 + \lambda^2 b e^{i\Theta} e^{-i\gamma}}{1 + \lambda^2 b e^{i\Theta} e^{+i\gamma}}\right]. \tag{198}$$

The theoretical estimates of $be^{i\Theta}$ suffer from large hadronic uncertainties. However, since this parameter enters (198) in a doubly Cabibbo-suppressed way, we obtain the following expressions [148]:

$$\mathcal{A}_{\rm CP}^{\rm dir}(B_d \to \phi K_{\rm S}) = 0 + \mathcal{O}(\lambda^2) \tag{199}$$

$$\mathcal{A}_{\rm CP}^{\rm mix}(B_d \to \phi K_{\rm S}) = -\sin\phi_d + \mathcal{O}(\lambda^2)\,, \tag{200}$$

where we made the plausible assumption that $b = \mathcal{O}(1)$. On the other hand, the mixing-induced CP asymmetry of $B_d \to J/\psi K_{\rm S}$ measures also $-\sin\phi_d$, as we saw in (173). We arrive therefore at the following relation [148, 156]:

$$-(\sin 2\beta)_{\phi K_{\rm S}} \equiv \mathcal{A}_{\rm CP}^{\rm mix}(B_d \to \phi K_{\rm S}) = \mathcal{A}_{\rm CP}^{\rm mix}(B_d \to J/\psi K_{\rm S}) + \mathcal{O}(\lambda^2)\,, \tag{201}$$

which offers an interesting test of the SM. Since $B_d \to \phi K_{\rm S}$ is governed by penguin processes in the SM, this decay may well be affected by NP. In fact, if we assume that NP arises generically in the TeV regime, it can be shown through field-theoretical estimates that the NP contributions to $b \to s\bar{s}s$ transitions may well lead to sizeable violations of (199) and (201) [119, 123]. Moreover, this is also the case for several specific NP scenarios; for examples, see Refs. [126, 128, 129, 157].

In Fig. 24, we show the time evolution of the B-factory data for the measurements of CP violation in $B_d \to \phi K_{\rm S}$, using the results reported at the LP '03 [158], ICHEP '04 [159] and LP '05 [160] conferences. Because of (155), the corresponding observables have to lie inside a circle with radius one around the origin, which is represented by the dashed lines. The result announced by the Belle Collaboration in 2003 led to quite some excitement in the community. Meanwhile, the Babar [161] and Belle [162] results are in good agreement with each other, yielding the following averages [61]:

$$\mathcal{A}_{\rm CP}^{\rm dir}(B_d \to \phi K_{\rm S}) = -0.09 \pm 0.14, \quad (\sin 2\beta)_{\phi K_{\rm S}} = 0.47 \pm 0.19\,. \tag{202}$$

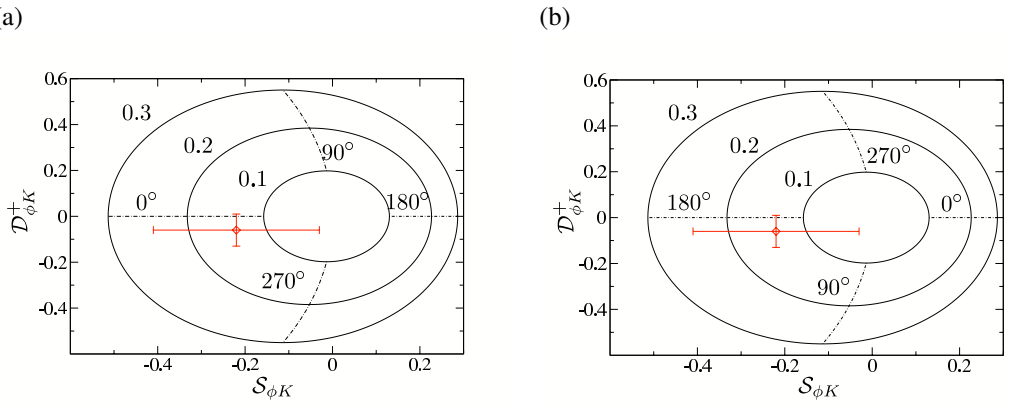

Fig. 25: The situation in the $\mathcal{S}_{\phi K}$–$\mathcal{D}^+_{\phi K}$ plane for NP contributions to the $B \to \phi K$ decay amplitudes in the $I = 0$ isospin sector for NP phases $\phi_0 = -90°$ (a) and $\phi_0 = +90°$ (b). The diamonds with the error bars represent the averages of the current data, whereas the numbers correspond to the values of $\tilde{\Delta}_0$ and $\tilde{v}_0$.

If we take (176) into account, we obtain the following result for the counterpart of (185):

$$\mathcal{S}_{\phi K} \equiv (\sin 2\beta)_{\phi K_S} - (\sin 2\beta)_{\psi K_S} = -0.22 \pm 0.19 \,. \tag{203}$$

This number still appears to be somewhat on the lower side, thereby indicating potential NP contributions to $b \to s\bar{s}s$ processes.

Further insights into the origin and the isospin structure of NP contributions can be obtained through a combined analysis of the neutral and charged $B \to \phi K$ modes with the help of observables $\mathcal{B}_{\phi K}$ and $\mathcal{D}^{\pm}_{\phi K}$ [123], which are defined in analogy to (177) and (179), respectively. The current experimental results read as follows:

$$\mathcal{B}_{\phi K} = 0.00 \pm 0.08 \,, \quad \mathcal{D}^-_{\phi K} = -0.03 \pm 0.07 \,, \quad \mathcal{D}^+_{\phi K} = -0.06 \pm 0.07 \,. \tag{204}$$

As in the $B \to J/\psi K$ case, $\mathcal{B}_{\phi K}$ and $\mathcal{D}^-_{\phi K}$ probe NP effects in the $I = 1$ sector, which are expected to be dynamically suppressed, whereas $\mathcal{D}^+_{\phi K}$ is sensitive to NP in the $I = 0$ sector. The latter kind of NP could also manifest itself as a non-vanishing value of (203).

In order to illustrate these effects, let us consider again the case where NP enters only in the $I = 0$ isospin sector. An important example is given by EW penguins, which have a significant impact on $B \to \phi K$ decays [72]. In analogy to the discussion in Section 7.1, we may then write

$$A(B^0_d \to \phi K^0) = \tilde{A}_0 \left[1 + \tilde{v}_0 e^{i(\tilde{\Delta}_0 + \phi_0)}\right] = A(B^+ \to \phi K^+) \,, \tag{205}$$

which implies $\mathcal{B}_{\phi K} = \mathcal{D}^-_{\phi K} = 0$, in accordance with (204). The notation corresponds to that of (186). Using the factorization approach to deal with the QCD and EW penguin contributions, we obtain the following estimate in the SM, where the CP-violating NP phase ϕ_0 vanishes [83]:

$$\tilde{v}_0 e^{i\tilde{\Delta}_0}\Big|^{\rm SM}_{\rm fact} \approx -0.2 \,. \tag{206}$$

In Figs. 25 (a) and (b), we show the situation in the $\mathcal{S}_{\phi K}$–$\mathcal{D}^+_{\phi K}$ plane for NP phases $\phi_0 = -90°$ and $\phi_0 = +90°$, respectively, and various values of $\tilde{v}_0$; each point of the contours is parametrized by $\tilde{\Delta}_0 \in [0°, 360°]$. We observe that the central values of the current experimental data, which are represented by the diamonds with the error bars, can straightforwardly be accommodated in this scenario in the case of $\phi_0 = +90°$ for strong phases satisfying $\cos\tilde{\Delta}_0 < 0$, as in factorization. Moreover, as can also be seen

in Fig. 25 (b), the EW penguin contributions would then have to be suppressed with respect to the SM estimate, which would be an interesting feature in view of the discussion of the $B \to \pi K$ puzzle and the rare decay constraints in Section 8.

It will be interesting to follow the evolution of the B-factory data, and to monitor also similar modes, such as $B_d^0 \to \pi^0 K_{\rm S}$ [163] and $B_d^0 \to \eta' K_{\rm S}$ [164]. For a compilation of the corresponding experimental results, see Ref. [61]; recent theoretical papers dealing with these channels can be found in Refs. [82, 83, 91, 165, 166]. We shall return to the CP asymmetries of the $B_d^0 \to \pi^0 K_{\rm S}$ channel in Section 8.

7.3 $B_d^0 \to \pi^+\pi^-$

This decay is a transition into a CP eigenstate with eigenvalue $+1$, and originates from $\bar{b} \to \bar{u}u\bar{d}$ processes, as can be seen in Fig. 26. In analogy to (167) and (195), its decay amplitude can be written as follows [167]:

$$A(B_d^0 \to \pi^+\pi^-) = \lambda_u^{(d)} \left(A_{\rm T}^u + A_{\rm P}^u\right) + \lambda_c^{(d)} A_{\rm P}^c + \lambda_t^{(d)} A_{\rm P}^t \,. \tag{207}$$

Using again (79) to eliminate the CKM factor $\lambda_t^{(d)} = V_{td}V_{tb}^*$ and applying once more the Wolfenstein parametrization yields

$$A(B_d^0 \to \pi^+\pi^-) = \mathcal{C}\left[e^{i\gamma} - de^{i\theta}\right], \tag{208}$$

where the overall normalization $\mathcal{C}$ and

$$de^{i\theta} \equiv \frac{1}{R_b}\left[\frac{A_{\rm P}^c - A_{\rm P}^t}{A_{\rm T}^u + A_{\rm P}^u - A_{\rm P}^t}\right] \tag{209}$$

are hadronic parameters. The formalism discussed in Section 5.5 then implies

$$\xi_{\pi^+\pi^-}^{(d)} = -e^{-i\phi_d}\left[\frac{e^{-i\gamma} - de^{i\theta}}{e^{+i\gamma} - de^{i\theta}}\right]. \tag{210}$$

In contrast to the expressions (171) and (198) for the $B_d^0 \to J/\psi K_{\rm S}$ and $B_d^0 \to \phi K_{\rm S}$ counterparts, respectively, the hadronic parameter $de^{i\theta}$, which suffers from large theoretical uncertainties, does *not* enter (210) in a doubly Cabibbo-suppressed way. This feature is at the basis of the famous 'penguin problem' in $B_d^0 \to \pi^+\pi^-$, which was addressed in many papers (see, for instance, [168]– [173]). If the penguin contributions to this channel were negligible, i.e., $d = 0$, its CP asymmetries were simply given by

$$\mathcal{A}_{\rm CP}^{\rm dir}(B_d \to \pi^+\pi^-) = 0 \tag{211}$$

$$\mathcal{A}_{\rm CP}^{\rm mix}(B_d \to \pi^+\pi^-) = \sin(\phi_d + 2\gamma) \stackrel{\rm SM}{=} \sin(\underbrace{2\beta + 2\gamma}_{2\pi - 2\alpha}) = -\sin 2\alpha \,. \tag{212}$$

Consequently, $\mathcal{A}_{\rm CP}^{\rm mix}(B_d \to \pi^+\pi^-)$ would then allow us to determine α. However, in the general case, we obtain expressions with the help of (153) and (210) of the form

$$\mathcal{A}_{\rm CP}^{\rm dir}(B_d \to \pi^+\pi^-) = G_1(d, \theta; \gamma) \tag{213}$$

$$\mathcal{A}_{\rm CP}^{\rm mix}(B_d \to \pi^+\pi^-) = G_2(d, \theta; \gamma, \phi_d) \,; \tag{214}$$

for explicit formulae, see Ref. [167]. We observe that actually the phases ϕ_d and γ enter directly in the $B_d \to \pi^+\pi^-$ observables, and not α. Consequently, since ϕ_d can be fixed through the mixing-induced CP violation in the 'golden' mode $B_d \to J/\psi K_{\rm S}$, as we have seen in Subsection 7.1, we may use $B_d \to \pi^+\pi^-$ to probe γ.

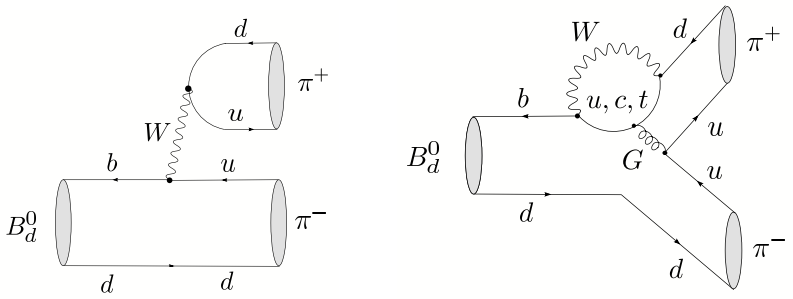

Fig. 26: Feynman diagrams contributing to $B_d^0 \to \pi^+\pi^-$ decays

The current measurements of the $B_d \to \pi^+\pi^-$ CP asymmetries are given as follows:

$$\mathcal{A}_{\rm CP}^{\rm dir}(B_d \to \pi^+\pi^-) = \begin{cases} -0.09 \pm 0.15 \pm 0.04 & \text{(BaBar [174])} \\ -0.56 \pm 0.12 \pm 0.06 & \text{(Belle [175])} \end{cases} \tag{215}$$

$$\mathcal{A}_{\rm CP}^{\rm mix}(B_d \to \pi^+\pi^-) = \begin{cases} +0.30 \pm 0.17 \pm 0.03 & \text{(BaBar [174])} \\ +0.67 \pm 0.16 \pm 0.06 & \text{(Belle [175])} \,. \end{cases} \tag{216}$$

The BaBar and Belle results are still not fully consistent with each other, although the experiments are now in better agreement. In Ref. [61], the following averages were obtained:

$$\mathcal{A}_{\rm CP}^{\rm dir}(B_d \to \pi^+\pi^-) = -0.37 \pm 0.10 \tag{217}$$

$$\mathcal{A}_{\rm CP}^{\rm mix}(B_d \to \pi^+\pi^-) = +0.50 \pm 0.12 \,. \tag{218}$$

The central values of these averages are remarkably stable in time. Direct CP violation at this level would require large penguin contributions with large CP-conserving strong phases, thereby indicating large non-factorizable effects.

This picture is in fact supported by the direct CP violation in $B_d^0 \to \pi^- K^+$ modes that could be established by the B factories in the summer of 2004 [6]. Here the BaBar and Belle results agree nicely with each other, yielding the following average [61]:

$$\mathcal{A}_{\rm CP}^{\rm dir}(B_d \to \pi^\mp K^\pm) = 0.115 \pm 0.018 \,. \tag{219}$$

The diagrams contributing to $B_d^0 \to \pi^- K^+$ can straightforwardly be obtained from those in Fig. 26 by just replacing the anti-down quark emerging from the W boson through an anti-strange quark. Consequently, the hadronic matrix elements entering $B_d^0 \to \pi^+\pi^-$ and $B_d^0 \to \pi^- K^+$ can be related to one another through the $SU(3)$ flavour symmetry of strong interactions and the additional assumption that the penguin annihilation and exchange topologies contributing to $B_d^0 \to \pi^+\pi^-$, which have no counterpart in $B_d^0 \to \pi^- K^+$ and involve the 'spectator" down quark in Fig. 26, play actually a negligible role [176]. Following these lines, we obtain the following relation in the SM:

$$H_{\rm BR} \equiv \underbrace{\frac{1}{\epsilon}\left(\frac{f_K}{f_\pi}\right)^2 \left[\frac{\rm BR}(B_d \to \pi^+\pi^-)}{\rm BR}(B_d \to \pi^\mp K^\pm)\right]}_{7.5 \pm 0.7} = \underbrace{-\frac{1}{\epsilon}\left[\frac{\mathcal{A}_{\rm CP}^{\rm dir}(B_d \to \pi^\mp K^\pm)}{\mathcal{A}_{\rm CP}^{\rm dir}(B_d \to \pi^+\pi^-)}\right]}_{6.7 \pm 2.0} \equiv H_{\mathcal{A}_{\rm CP}^{\rm dir}} \,, \tag{220}$$

where

$$\epsilon \equiv \frac{\lambda^2}{1-\lambda^2} = 0.053 \,, \tag{221}$$

and the ratio $f_K/f_\pi = 160/131$ of the kaon and pion decay constants defined through

$$\langle 0|\bar{s}\gamma_\alpha\gamma_5 u|K^+(k)\rangle = i f_K k_\alpha \,, \quad \langle 0|\bar{d}\gamma_\alpha\gamma_5 u|\pi^+(k)\rangle = i f_\pi k_\alpha \tag{222}$$

describes factorizable $SU(3)$-breaking corrections. As usual, the CP-averaged branching ratios are defined as

$$\text{BR} \equiv \frac{1}{2}\left[\text{BR}(B \to f) + \text{BR}(\bar{B} \to \bar{f})\right] . \tag{223}$$

In (220), we have also given the numerical values following from the data. Consequently, this relation is well satisfied within the experimental uncertainties, and does not show any anomalous behaviour. It supports therefore the SM description of the $B^0_d \to \pi^- K^+$, $B^0_d \to \pi^+\pi^-$ decay amplitudes, and our working assumptions listed before (220).

The quantities $H_{\rm BR}$ and $H_{\mathcal{A}_{\rm CP}^{\rm dir}}$ introduced in this relation can be written as follows:

$$H_{\rm BR} = G_3(d, \theta; \gamma) = H_{\mathcal{A}_{\rm CP}^{\rm dir}} . \tag{224}$$

If we complement this expression with (213) and (214), and use [see (189)]

$$\phi_d = (43.4 \pm 2.5)^\circ , \tag{225}$$

we have sufficient information to determine γ, as well as (d, θ) [167,176,177]. In using (225), we assume that the possible discrepancy with the SM described by (185) is only due to NP in B^0_d–$\bar{B}^0_d$ mixing and not to effects entering through the $B^0_d \to J/\psi K_{\rm S}$ decay amplitude. As was recently shown in Ref. [91], the results following from $H_{\rm BR}$ and $H_{\mathcal{A}_{\rm CP}^{\rm dir}}$ give results that are in good agreement with one another. Since the avenue offered by $H_{\mathcal{A}_{\rm CP}^{\rm dir}}$ is cleaner than the one provided by $H_{\rm BR}$, it is preferable to use the former quantity to determine γ, yielding the following result [91]:

$$\gamma = (73.9^{+5.8}_{-6.5})^\circ . \tag{226}$$

Here a second solution around 42° was discarded, which can be excluded through an analysis of the whole $B \to \pi\pi, \pi K$ system [83]. As was recently discussed [91] (see also Refs. [176, 177]), even large non-factorizable $SU(3)$-breaking corrections have a remarkably small impact on the numerical result in (226). The value of γ in (226) is somewhat higher than the central values in (106), but fully consistent within the large errors. An even larger value in the ballpark of 80° was recently extracted from the $B \to \pi\pi$ data with the help of SCET [178, 179].

8 The $B \to \pi K$ puzzle and its relation to rare B and K decays

8.1 Preliminaries

We already made first contact with a $B \to \pi K$ decay in Section 7.3, the $B^0_d \to \pi^- K^+$ channel. It receives contributions both from tree and from penguin topologies. Since this decay originates from a $\bar{b} \to \bar{s}$ transition, the tree amplitude is suppressed by a CKM factor $\lambda^2 R_b \sim 0.02$ with respect to the penguin amplitude. Consequently, $B^0_d \to \pi^- K^+$ is governed by QCD penguins; the tree topologies contribute only at the 20% level to the decay amplitude. The feature of the dominance of QCD penguins applies to all $B \to \pi K$ modes, which can be classified with respect to their EW penguin contributions as follows (see Fig. 27):

(a) In the $B^0_d \to \pi^- K^+$ and $B^+ \to \pi^+ K^0$ decays, EW penguins contribute in colour-suppressed form and are hence expected to play a minor role.

(b) In the $B^0_d \to \pi^0 K^0$ and $B^+ \to \pi^0 K^+$ decays, EW penguins contribute in colour-allowed form and have therefore a significant impact on the decay amplitude, entering at the same order of magnitude as the tree contributions.

As we noted above, EW penguins offer an attractive avenue for NP to enter non-leptonic B decays, which is also the case for the $B \to \pi K$ system [180, 181]. Indeed, the decays of class (b) show a puzzling pattern, which may point towards such a NP scenario. This feature emerged already in 2000 [182],

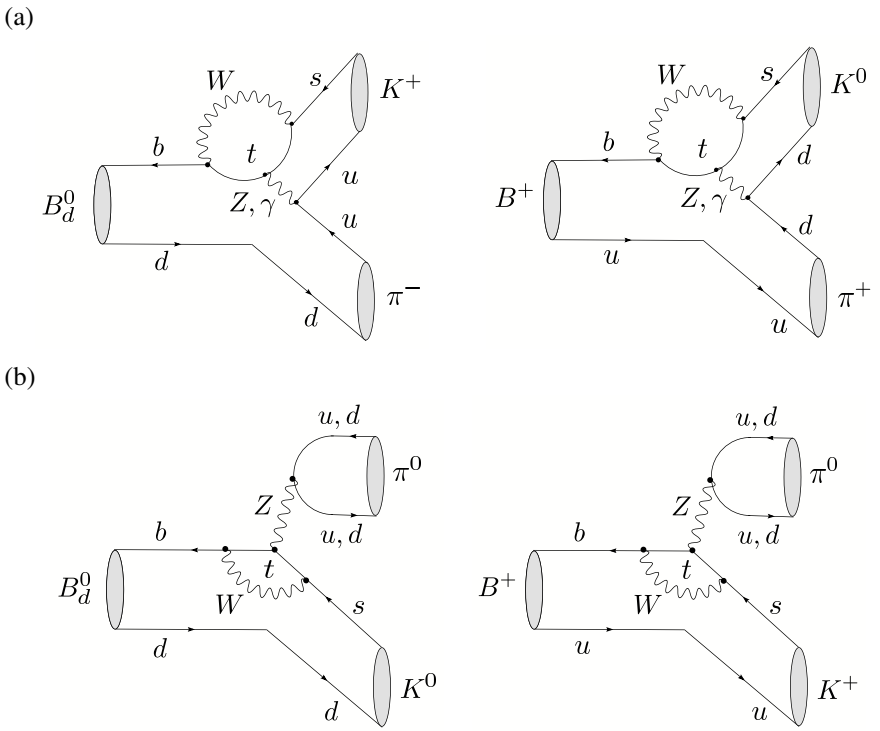

Fig. 27: Examples of the colour-suppressed (a) and colour-allowed (b) EW penguin contributions to the $B \to \pi K$ system

when the CLEO Collaboration reported the observation of the $B_d^0 \to \pi^0 K^0$ channel with a surprisingly prominent rate [183], and is still present in the most recent BaBar and Belle data, thereby receiving a lot of attention in the literature (see, for instance, Refs. [157] and [184]– [188]).

In the following discussion, we focus on the systematic strategy to explore the '$B \to \pi K$ puzzle' developed in Refs. [82, 83]; all numerical results refer to the most recent analysis presented in Ref. [91]. The logical structure is very simple: the starting point is given by the values of ϕ_d and γ in (225) and (226), respectively, and by the $B \to \pi\pi$ system, which allows us to extract a set of hadronic parameters from the data with the help of the isospin symmetry of strong interactions. Then we make, in analogy to the determination of γ in Section 7.3, the following working hypotheses:

(i) $SU(3)$ flavour symmetry of strong interactions (but taking factorizable $SU(3)$-breaking corrections into account),

(ii) neglect of penguin annihilation and exchange topologies,

which allow us to fix the hadronic $B \to \pi K$ parameters through their $B \to \pi\pi$ counterparts. Interestingly, we may gain confidence in these assumptions through internal consistency checks [an example is relation (220)], which work nicely within the experimental uncertainties. Having the hadronic $B \to \pi K$ parameters at hand, we can predict the $B \to \pi K$ observables in the SM. The comparison of the corresponding picture with the B-factory data will then guide us to NP in the EW penguin sector, involving in particular a large CP-violating NP phase. In the final step, we explore the interplay of this NP scenario with rare K and B decays.

8.2 Extracting hadronic parameters from the $B \to \pi\pi$ system

In order to fully exploit the information that is provided by the whole $B \to \pi\pi$ system, we use—in addition to the two CP-violating $B_d^0 \to \pi^+\pi^-$ observables—the following ratios of CP-averaged

branching ratios:

$$R_{+-}^{\pi\pi} \equiv 2\left[\frac{\mathrm{BR}(B^+\to\pi^+\pi^0)+\mathrm{BR}(B^-\to\pi^-\pi^0)}{\mathrm{BR}(B_d^0\to\pi^+\pi^-)+\mathrm{BR}(\bar{B}_d^0\to\pi^+\pi^-)}\right] = 2.04\pm0.28 \tag{227}$$

$$R_{00}^{\pi\pi} \equiv 2\left[\frac{\mathrm{BR}(B_d^0\to\pi^0\pi^0)+\mathrm{BR}(\bar{B}_d^0\to\pi^0\pi^0)}{\mathrm{BR}(B_d^0\to\pi^+\pi^-)+\mathrm{BR}(\bar{B}_d^0\to\pi^+\pi^-)}\right] = 0.58\pm0.13\,. \tag{228}$$

The pattern of the experimental numbers in these expressions came as quite a surprise, as the central values calculated in QCDF gave $R_{+-}^{\pi\pi}=1.24$ and $R_{00}^{\pi\pi}=0.07$ [184]. As discussed in detail in Ref. [83], this '$B\to\pi\pi$ puzzle' can straightforwardly be accommodated in the SM through large non-factorizable hadronic interference effects, i.e., does not point towards NP. For recent SCET analyses, see Refs. [179, 189, 190].

Using the isospin symmetry of strong interactions, we can write

$$R_{+-}^{\pi\pi} = F_1(d,\theta,x,\Delta;\gamma)\,, \quad R_{00}^{\pi\pi} = F_2(d,\theta,x,\Delta;\gamma)\,, \tag{229}$$

where $xe^{i\Delta}$ is another hadronic parameter, which was introduced in Refs. [82, 83]. Using now, in addition, the CP-violating observables in (213) and (214), we arrive at the following set of haronic parameters:

$$d=0.52^{+0.09}_{-0.09},\quad \theta=(146^{+7.0}_{-7.2})^\circ,\quad x=0.96^{+0.13}_{-0.14},\quad \Delta=-(53^{+18}_{-26})^\circ\,. \tag{230}$$

In the extraction of these quantities, also the EW penguin effects in the $B\to\pi\pi$ system are included [191, 192], although these topologies have a tiny impact [163]. Let us emphasize that the results for the hadronic parameters listed above, which are consistent with the picture emerging in the analyses of other authors (see, for example, Refs. [193, 194]), are essentially clean and serve as a testing ground for calculations within QCD-related approaches. For instance, in recent QCDF [195] and PQCD [196] analyses, the following numbers were obtained:

$$d|_{\mathrm{QCDF}} = 0.29\pm0.09\,, \quad \theta|_{\mathrm{QCDF}} = -\,(171.4\pm14.3)^\circ\,, \tag{231}$$

$$d|_{\mathrm{PQCD}} = 0.23^{+0.07}_{-0.05}\,, \quad +139^\circ < \theta|_{\mathrm{PQCD}} < +148^\circ\,, \tag{232}$$

which depart significantly from the pattern in (230) that is implied by the data.

Finally, we can predict the CP asymmetries of the decay $B_d\to\pi^0\pi^0$:

$$\mathcal{A}_{\mathrm{CP}}^{\mathrm{dir}}(B_d\to\pi^0\pi^0) = -0.30^{+0.48}_{-0.26}\,, \quad \mathcal{A}_{\mathrm{CP}}^{\mathrm{mix}}(B_d\to\pi^0\pi^0) = -0.87^{+0.29}_{-0.19}\,. \tag{233}$$

The current experimental value for the direct CP asymmetry is given as follows [61]:

$$\mathcal{A}_{\mathrm{CP}}^{\mathrm{dir}}(B_d\to\pi^0\pi^0) = -0.28^{+0.40}_{-0.39}\,. \tag{234}$$

Consequently, no stringent test of the corresponding prediction in (233) is provided at this stage, although the indicated agreement is encouraging.

8.3 Analysis of the $B\to\pi K$ system

Let us begin the analysis of the $B\to\pi K$ system by having a closer look at the modes of class (a) introduced above, $B_d\to\pi^\mp K^\pm$ and $B^\pm\to\pi^\pm K$, which are only marginally affected by EW penguin contributions. We already used the branching ratio and direct CP asymmetry of the former channel in the $SU(3)$ relation (220), which is nicely satisfied by the current data, and in the extraction of γ with the help of the CP-violating $B_d\to\pi^+\pi^-$ observables, yielding the value in (226). The $B_d\to\pi^\mp K^\pm$ modes provide the CP-violating asymmetry

$$\mathcal{A}_{\mathrm{CP}}^{\mathrm{dir}}(B^\pm\to\pi^\pm K) \equiv \frac{\mathrm{BR}(B^+\to\pi^+K^0)-\mathrm{BR}(B^-\to\pi^-\bar{K}^0)}{\mathrm{BR}(B^+\to\pi^+K^0)+\mathrm{BR}(B^-\to\pi^-\bar{K}^0)} = 0.02\pm0.04\,, \tag{235}$$

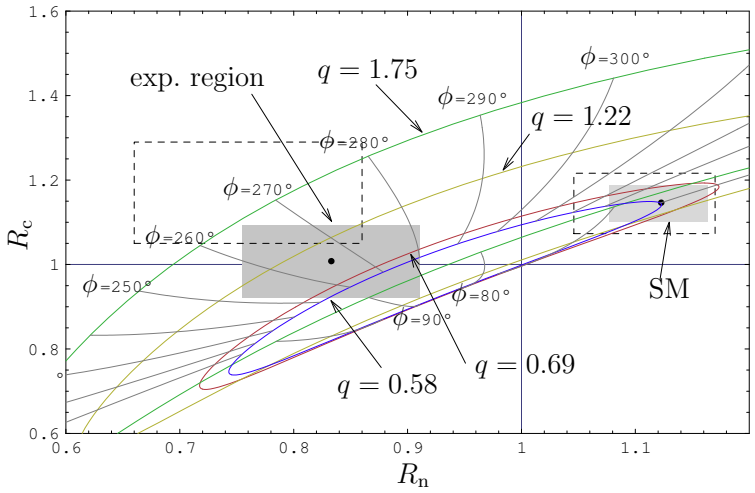

Fig. 28: The current situation in the R_n–R_c plane: the shaded areas indicate the experimental and SM 1σ ranges, while the lines show the theory predictions for the central values of the hadronic parameters and various values of q with $\phi \in [0°, 360°]$

and enter in the following ratio [197]:

$$R \equiv \left[\frac{\text{BR}(B_d^0 \to \pi^- K^+) + \text{BR}(\bar{B}_d^0 \to \pi^+ K^-)}{\text{BR}(B^+ \to \pi^+ K^0) + \text{BR}(B^- \to \pi^- \bar{K}^0)}\right] \frac{\tau_{B^+}}{\tau_{B_d^0}} = 0.86 \pm 0.06 \; ; \tag{236}$$

the numerical values refer again to the most recent compilation in [61]. The $B^+ \to \pi^+ K^0$ channel involves another hadronic parameter $\rho_c e^{i\theta_c}$ which cannot be determined through the $B \to \pi\pi$ data [191, 198, 199]:

$$A(B^+ \to \pi^+ K^0) = -P' \left[1 + \rho_c e^{i\theta_c} e^{i\gamma}\right] ; \tag{237}$$

the overall normalization P' cancels in (235) and (236). Usually, it is assumed that the parameter $\rho_c e^{i\theta_c}$ can be neglected. In this case, the direct CP asymmetry in (235) vanishes, and R can be calculated through the $B \to \pi\pi$ data with the help of the assumptions specified in Section 8.1:

$$R|_{\text{SM}} = 0.963^{+0.019}_{-0.022} \; . \tag{238}$$

This numerical result is 1.6σ larger than the experimental value in (236). As was discussed in detail in Ref. [200], the experimental range for the direct CP asymmetry in (235) and the first direct signals for the $B^\pm \to K^\pm K$ decays favour a value of θ_c around $0°$. This feature allows us to essentially resolve the small discrepancy concerning R for values of ρ_c around 0.05. The remaining small numerical difference between the calculated value of R and the experimental result, if confirmed by future data, could be due to (small) colour-suppressed EW penguins, which enter R as well [83]. As was recently discussed in Ref. [91], even large non-factorizable $SU(3)$-breaking effects would have a small impact on the predicted value of R. In view of these results, it would not be a surprise to see an increase of the experimental value of R in the future.

Let us now turn to the $B^+ \to \pi^0 K^+$ and $B_d^0 \to \pi^0 K^0$ channels, which are the $B \to \pi K$ modes with significant contributions from EW penguin topologies. The key observables for the exploration of these modes are the following ratios of their CP-averaged branching ratios [182, 191]:

$$R_c \equiv 2\left[\frac{\text{BR}(B^+ \to \pi^0 K^+) + \text{BR}(B^- \to \pi^0 K^-)}{\text{BR}(B^+ \to \pi^+ K^0) + \text{BR}(B^- \to \pi^- \bar{K}^0)}\right] = 1.01 \pm 0.09 \tag{239}$$

$$R_{\rm n} \equiv \frac{1}{2}\left[\frac{{\rm BR}(B_d^0 \to \pi^- K^+) + {\rm BR}(\bar{B}_d^0 \to \pi^+ K^-)}{{\rm BR}(B_d^0 \to \pi^0 K^0) + {\rm BR}(\bar{B}_d^0 \to \pi^0 \bar{K}^0)}\right] = 0.83 \pm 0.08 \,, \tag{240}$$

where the overall normalization factors of the decay amplitudes cancel, as in (236). In order to describe the EW penguin effects, both a parameter q, which measures the strength of the EW penguins with respect to tree-like topologies, and a CP-violating phase ϕ are introduced. In the SM, this phase vanishes, and q can be calculated with the help of the $SU(3)$ flavour symmetry, yielding a value of $0.69 \times 0.086/|V_{ub}/V_{cb}| = 0.58$ [201]. Following the strategy described above yields the following SM predictions:

$$R_{\rm c}|_{\rm SM} = 1.15 \pm 0.05 \,, \quad R_{\rm n}|_{\rm SM} = 1.12 \pm 0.05 \,, \tag{241}$$

where in particular the value of $R_{\rm n}$ does not agree with the experimental number, which is a manifestation of the $B \to \pi K$ puzzle. As was recently discussed in Ref. [91], the internal consistency checks of the working assumptions listed in Subsection 8.1 are currently satisfied at the level of 25%, and can be systematically improved through better data. A detailed study of the numerical predictions in (241) (and those given below) shows that their sensitivity on non-factorizable $SU(3)$-breaking effects of this order of magnitude is surprisingly small. Consequently, it is very exciting to speculate that NP effects in the EW penguin sector, which are described effectively through (q, ϕ), are at the origin of the $B \to \pi K$ puzzle. Following Refs. [82, 83], we show the situation in the $R_{\rm n}$–$R_{\rm c}$ plane in Fig. 28, where—for the convenience of the reader—also the experimental range and the SM predictions at the time of the original analysis of Refs. [82, 83] are indicated through the dashed rectangles. We observe that although the central values of $R_{\rm n}$ and $R_{\rm c}$ have slightly moved towards each other, the puzzle is as prominent as ever. The experimental region can now be reached without an enhancement of q, but a large CP-violating phase ϕ of the order of -90° is still required:

$$q = 0.99\,^{+0.66}_{-0.70} \,, \quad \phi = -(94\,^{+16}_{-17})^\circ \,. \tag{242}$$

Interestingly, ϕ of the order of $+90^\circ$ can now also bring us rather close to the experimental range of $R_{\rm n}$ and $R_{\rm c}$.

An interesting probe of the NP phase ϕ is also provided by the CP violation in $B_d^0 \to \pi^0 K_{\rm S}$. Within the SM, the corresponding observables are expected to satisfy the following relations [163]:

$$\mathcal{A}_{\rm CP}^{\rm dir}(B_d \to \pi^0 K_{\rm S}) \approx 0 \,, \quad \mathcal{A}_{\rm CP}^{\rm mix}(B_d \to \pi^0 K_{\rm S}) \approx \mathcal{A}_{\rm CP}^{\rm mix}(B_d \to \psi K_{\rm S}) \,. \tag{243}$$

The most recent Belle [162] and BaBar [202] measurements of these quantities are in agreement with each other, and lead to the following averages [61]:

$$\mathcal{A}_{\rm CP}^{\rm dir}(B_d \to \pi^0 K_{\rm S}) = -0.02 \pm 0.13 \tag{244}$$

$$\mathcal{A}_{\rm CP}^{\rm mix}(B_d \to \pi^0 K_{\rm S}) = -0.31 \pm 0.26 \equiv -(\sin 2\beta)_{\pi^0 K_{\rm S}} \,. \tag{245}$$

Taking (176) into account yields

$$\Delta S \equiv (\sin 2\beta)_{\pi^0 K_{\rm S}} - (\sin 2\beta)_{\psi K_{\rm S}} = -0.38 \pm 0.26 \,, \tag{246}$$

which may indicate a sizeable deviation of the experimentally measured value of $(\sin 2\beta)_{\pi^0 K_{\rm S}}$ from $(\sin 2\beta)_{\psi K_{\rm S}}$, and is therefore one of the recent hot topics. Since the strategy developed in Refs. [82, 83] allows us also to predict the CP-violating observables of the $B_d^0 \to \pi^0 K_{\rm S}$ channel both within the SM and within our scenario of NP, it allows us to address this issue, yielding

$$\mathcal{A}_{\rm CP}^{\rm dir}(B_d \to \pi^0 K_{\rm S})|_{\rm SM} = 0.06^{+0.09}_{-0.10} \,, \qquad \Delta S|_{\rm SM} = 0.13 \pm 0.05 \,, \tag{247}$$

$$\mathcal{A}_{\rm CP}^{\rm dir}(B_d \to \pi^0 K_{\rm S})|_{\rm NP} = 0.01\,^{+0.14}_{-0.18} \,, \qquad \Delta S|_{\rm NP} = 0.27\,^{+0.05}_{-0.09} \,, \tag{248}$$

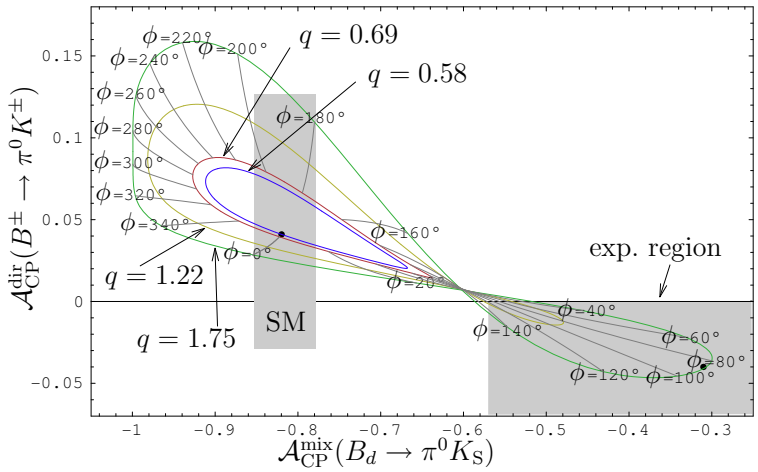

Fig. 29: The situation in the $\mathcal{A}_{\rm CP}^{\rm mix}(B_d \to \pi^0 K_{\rm S})$–$\mathcal{A}_{\rm CP}^{\rm dir}(B^\pm \to \pi^0 K^\pm)$ plane: the shaded regions represent the experimental and SM 1σ ranges, while the lines show the theory predictions for the central values of the hadronic parameters and various values of q with $\phi \in [0°, 360°]$.

where the NP results refer to the EW penguin parameters in (242). Consequently, ΔS is found to be *positive* in the SM. In the literature, values of $\Delta S|_{\rm SM} \sim 0.04$–$0.08$ can be found, which were obtained—in contrast to (247)—with the help of dynamical approaches such as QCDF [166] and SCET [179]. Moreover, bounds were derived with the help of the $SU(3)$ flavour symmetry [203]. Looking at (248), we see that the modified parameters (q, ϕ) in (242) imply an enhancement of ΔS with respect to the SM case. Consequently, the best values of (q, ϕ) that are favoured by the measurements of $R_{\rm n,c}$ make the potential $\mathcal{A}_{\rm CP}^{\rm mix}(B_d \to \pi^0 K_{\rm S})$ discrepancy even larger than in the SM.

There is one CP asymmetry of the $B \to \pi K$ system left, which is measured as

$$\mathcal{A}_{\rm CP}^{\rm dir}(B^\pm \to \pi^0 K^\pm) = -0.04 \pm 0.04 \,. \tag{249}$$

In the limit of vanishing colour-suppressed tree and EW penguin topologies, it is expected to be equal to the direct CP asymmetry of the $B_d \to \pi^\mp K^\pm$ modes. Since the experimental value of the latter asymmetry in (219) does not agree with (249), the direct CP violation in $B^\pm \to \pi^0 K^\pm$ has also received a lot of attention. The lifted colour suppression described by the large value of x in (230) could, in principle, be responsible for a non-vanishing difference between (219) and (249),

$$\Delta A \equiv \mathcal{A}_{\rm CP}^{\rm dir}(B^\pm \to \pi^0 K^\pm) - \mathcal{A}_{\rm CP}^{\rm dir}(B_d \to \pi^\mp K^\pm) \stackrel{\rm exp}{=} -0.16 \pm 0.04 \,. \tag{250}$$

However, applying once again the strategy described above yields

$$\mathcal{A}_{\rm CP}^{\rm dir}(B^\pm \to \pi^0 K^\pm)|_{\rm SM} = 0.04\,^{+0.09}_{-0.07} \,, \tag{251}$$

so that the SM still prefers a positive value of this CP asymmetry; the NP scenario characterized by (242) corresponds to

$$\mathcal{A}_{\rm CP}^{\rm dir}(B^\pm \to \pi^0 K^\pm)|_{\rm NP} = 0.09\,^{+0.20}_{-0.16} \,. \tag{252}$$

In view of the large uncertainties, no stringent test is provided at this point. Nevertheless, it is tempting to play a bit with the CP asymmetries of the $B^\pm \to \pi^0 K^\pm$ and $B_d \to \pi^0 K_{\rm S}$ decays. In Fig. 29, we show the situation in the $\mathcal{A}_{\rm CP}^{\rm mix}(B_d \to \pi^0 K_{\rm S})$–$\mathcal{A}_{\rm CP}^{\rm dir}(B^\pm \to \pi^0 K^\pm)$ plane for various values of q with $\phi \in [0°, 360°]$. We see that these observables seem to show a preference for positive values of ϕ around $+90°$. As we noted above, in this case, we can also get rather close to the experimental region in the $R_{\rm n}$–$R_{\rm c}$ plane. It is now interesting to return to the discussion of the NP effects in the $B \to \phi K$ system given

in Section 7.2. In our scenario of NP in the EW penguin sector, we have just to identify the CP-violating phase ϕ_0 in (205) with the NP phase ϕ [83]. Unfortunately, we cannot determine the hadronic $B \to \phi K$ parameters $\tilde{v}_0$ and $\tilde{\Delta}_0$ through the $B \to \pi\pi$ data as in the case of the $B \to \pi K$ system. However, if we take into account that $\tilde{\Delta}_0 = 180^\circ$ in factorization and look at Fig. 25, we see again that the case of $\phi \sim +90^\circ$ would be favoured by the data for $\mathcal{S}_{\phi K}$. Alternatively, in the case of $\phi \sim -90^\circ$, $\tilde{\Delta}_0 \sim 0^\circ$ would be required to accommodate a negative value of $\mathcal{S}_{\phi K}$, which appears unlikely. Interestingly, a similar comment applies to the $B \to J/\psi K$ observables shown in Fig. 21, although here a dramatic enhancement of the EW penguin parameter v_0 relative to the SM estimate would be simultaneously needed to reach the central experimental values, in contract to the reduction of $\tilde{v}_0$ in the $B \to \phi K$ case. In view of rare decay constraints, the behaviour of the $B \to \phi K$ parameter $\tilde{v}_0$ appears much more likely, thereby supporting the assumption after (225).

8.4 The interplay with rare K and B decays and future scenarios

In order to explore the implications of the $B \to \pi K$ puzzle for rare K and B decays, we assume that the NP enters the EW penguin sector through Z^0 penguins with a new CP-violating phase. This scenario was already considered in the literature, where model-independent analyses and studies within SUSY can be found [204, 205]. In the strategy discussed here, the short-distance function C characterizing the Z^0 penguins is determined through the $B \to \pi K$ data [206]. Performing a renormalization-group analysis yields

$$C(\bar{q}) = 2.35\, \bar{q} e^{i\phi} - 0.82 \quad \text{with} \quad \bar{q} = q \left[\frac{|V_{ub}/V_{cb}|}{0.086}\right]. \tag{253}$$

Evaluating then the relevant box-diagram contributions in the SM and using (253), the short-distance functions

$$X = 2.35\, \bar{q} e^{i\phi} - 0.09 \quad \text{and} \quad Y = 2.35\, \bar{q} e^{i\phi} - 0.64 \tag{254}$$

can also be calculated, which govern the rare K, B decays with $\nu\bar{\nu}$ and $\ell^+\ell^-$ in the final states, respectively. In the SM, we have $C = 0.79$, $X = 1.53$ and $Y = 0.98$, with *vanishing* CP-violating phases. An analysis along these lines shows that the value of (q, ϕ) in (242), which is preferred by the $B \to \pi K$ observables $R_{\rm n,c}$, requires the following lower bounds for X and Y [91]:

$$|X|_{\rm min} \approx |Y|_{\rm min} \approx 2.2\,, \tag{255}$$

which appear to violate the 95% probability upper bounds

$$X \leq 1.95, \quad Y \leq 1.43 \tag{256}$$

that were recently obtained within the context of MFV [207]. Although we have to deal with CP-violating NP phases in our scenario, which goes therefore beyond the MFV framework, a closer look at $B \to X_s \ell^+ \ell^-$ shows that the upper bound on $|Y|$ in (256) is difficult to avoid if NP enters only through EW penguins and the operator basis is the same as in the SM. A possible solution to the clash between (255) and (256) would be given by more complicated NP scenarios [91]. However, unless a specific model is chosen, the predictive power is then significantly reduced. For the exploration of the NP effects in rare decays, we shall therefore not follow this avenue.

Using an only slightly more generous bound on $|Y|$ by imposing $|Y| \leq 1.5$ and taking only those values of (242) that satisfy the constraint $|Y| = 1.5$ yields

$$q = 0.48 \pm 0.07\,, \quad \phi = -(93 \pm 17)^\circ\,, \tag{257}$$

corresponding to a modest *suppression* of q relative to its updated SM value of 0.58. It is interesting to investigate the impact of various modifications of (q, ϕ), which allow us to satisfy the bounds in (256), for the $B \to \pi K$ observables and rare decays. To this end, three scenarios for the possible future evolution of the measurements of $R_{\rm n}$ and $R_{\rm c}$ were introduced in Ref. [91]:

Table 1: The $B \to \pi K$ observables for the three scenarios introduced in the text

Quantity	SM	Scen. A	Scen. B	Scen. C	Experiment
$R_{\rm n}$	1.12	0.88	1.03	1	0.83 ± 0.08
$R_{\rm c}$	1.15	0.96	1.13	1	1.01 ± 0.09
$\mathcal{A}_{\rm CP}^{\rm dir}(B^\pm \to \pi^0 K^\pm)$	0.04	0.07	0.06	0.02	-0.04 ± 0.04
$\mathcal{A}_{\rm CP}^{\rm dir}(B_d \to \pi^0 K_{\rm S})$	0.06	0.04	0.03	0.09	-0.02 ± 0.13
$\mathcal{A}_{\rm CP}^{\rm mix}(B_d \to \pi^0 K_{\rm S})$	-0.82	-0.89	-0.91	-0.70	-0.31 ± 0.26
ΔS	0.13	0.21	0.22	0.01	-0.38 ± 0.26
ΔA	-0.07	-0.04	-0.05	-0.09	-0.16 ± 0.04

Table 2: Rare decay branching ratios for the three scenarios introduced in the text. The $B_s \to \mu^+\mu^-$ channel will be discussed in more detail in Section 10.5.

Decay	SM	Scen. A	Scen. B	Scen. C	Exp. bound (90% C.L.)
$\text{BR}(K^+ \to \pi^+ \nu\bar{\nu})/10^{-11}$	9.3	2.7	8.3	8.4	$(14.7^{+13.0}_{-8.9})$
$\text{BR}(K_{\rm L} \to \pi^0 \nu\bar{\nu})/10^{-11}$	4.4	11.6	27.9	7.2	$< 2.9 \times 10^4$
$\text{BR}(K_{\rm L} \to \pi^0 e^+ e^-)/10^{-11}$	3.6	4.6	7.1	4.9	< 28
$\text{BR}(B \to X_s \nu\bar{\nu})/10^{-5}$	3.6	2.8	4.8	3.3	< 64
$\text{BR}(B_s \to \mu^+\mu^-)/10^{-9}$	3.9	9.2	9.1	7.0	$< 1.5 \times 10^2$
$\text{BR}(K_{\rm L} \to \mu^+\mu^-)_{\rm SD}/10^{-9}$	0.9	0.9	0.001	0.6	< 2.5

- *Scenario A:* $q = 0.48$, $\phi = -93^\circ$, which is in accordance with the currrent rare decay bounds and the $B \to \pi K$ data [see (257)].
- *Scenario B:* $q = 0.66$, $\phi = -50^\circ$, which yields an increase of $R_{\rm n}$ to 1.03, and some interesting effects in rare decays. This could, for example, happen if radiative corrections to the $B_d^0 \to \pi^- K^+$ branching ratio enhance $R_{\rm n}$ [208], though this alone would probably account for only about 5%.
- *Scenario C:* here it is assumed that $R_{\rm n} = R_{\rm c} = 1$, which corresponds to $q = 0.54$ and $\phi = 61^\circ$. The *positive* sign of ϕ distinguishes this scenario strongly from the others.

The patterns of the observables of the $B \to \pi K$ and rare decays corresponding to these scenarios are collected in Tables 1 and 2, respectively. We observe that the $K \to \pi\nu\bar{\nu}$ modes, which are theoretically very clean (for a recent review, see Ref. [209]), offer a particularly interesting probe for the different scenarios. Concerning the observables of the $B \to \pi K$ system, $\mathcal{A}_{\rm CP}^{\rm mix}(B_d \to \pi^0 K_{\rm S})$ is very interesting: this CP asymmetry is found to be very large in Scenarios A and B, where the NP phase ϕ is negative. On the other hand, the positive sign of ϕ in Scenario C brings $\mathcal{A}_{\rm CP}^{\rm mix}(B_d \to \pi^0 K_{\rm S})$ closer to the data, in agreement with the features discussed in Section 8.3. A similar comment applies to the direct CP asymmetry of $B^\pm \to \pi^0 K^\pm$.

In view of the large uncertainties, unfortunately no definite conclusions on the presence of NP can be drawn at this stage. However, the possible anomalies in the $B \to \pi K$ system complemented with the one in $B \to \phi K$ may actually indicate the effects of a modified EW penguin sector with a large CP-violating NP phase. As we just saw, rare K and B decays have an impressive power to reveal such a kind of NP. Finally, let us stress that the analysis of the $B \to \pi\pi$ modes, which signals large non-factorizable effects, and the determination of the UT angle γ described above are not affected by such NP effects. It will be interesting to monitor the evolution of the corresponding data with the help of the strategy discussed above.

9 Entering a new territory: $b \to d$ penguins

9.1 Preliminaries

Another hot topic which emerged recently is the exploration of $b \to d$ penguin processes. The non-leptonic decays belonging to this category, which are mediated by $b \to d\bar{s}s$ quark transitions (see the classification in Section 3.3.1), are now coming within experimental reach at the B factories. A similar comment applies to the radiative decays originating from $b \to d\gamma$ processes, whereas $b \to d\ell^+\ell^-$ modes are still far from being accessible. The B factories are therefore just entering a new territory, which is still essentially unexplored. Let us now have a closer look at the corresponding processes.

9.2 A prominent example: $B_d^0 \to K^0\bar{K}^0$

The Feynman diagrams contributing to this decay can be obtained from those for $B_d^0 \to \phi K^0$ shown in Fig. 23 by replacing the anti-strange quark emerging from the W boson through an anti-down quark. The $B_d^0 \to K^0\bar{K}^0$ decay is described by the low-energy effective Hamiltonian in (80) with $r = d$, where the current–current operators may only contribute through penguin-like contractions, corresponding to the penguin topologies with internal up- and charm-quark exchanges. The dominant role is played by QCD penguins; since EW penguins contribute only in colour-suppressed form, they have a minor impact on $B_d^0 \to K^0\bar{K}^0$, in contrast to the case of $B_d^0 \to \phi K^0$, where they may also contribute in colour-allowed form.

If we apply the notation introduced in Section 7, again make use of the unitarity of the CKM matrix and apply the Wolfenstein parametrization, we may write the $B_d^0 \to K^0\bar{K}^0$ amplitude as follows:

$$A(B_d^0 \to K^0\bar{K}^0) = \lambda^3 A(\tilde{A}_{\rm P}^t - \tilde{A}_{\rm P}^c)\left[1 - \rho_{KK}e^{i\theta_{KK}}e^{i\gamma}\right], \tag{258}$$

where

$$\rho_{KK}e^{i\theta_{KK}} \equiv R_b\left[\frac{\tilde{A}_{\rm P}^t - \tilde{A}_{\rm P}^u}{\tilde{A}_{\rm P}^t - \tilde{A}_{\rm P}^c}\right]. \tag{259}$$

This expression allows us to calculate the CP-violating asymmetries with the help of the formulae given in Section 5.5, taking the following form:

$$\mathcal{A}_{\rm CP}^{\rm dir}(B_d \to K^0\bar{K}^0) = D_1(\rho_{KK}, \theta_{KK}; \gamma) \tag{260}$$

$$\mathcal{A}_{\rm CP}^{\rm mix}(B_d \to K^0\bar{K}^0) = D_2(\rho_{KK}, \theta_{KK}; \gamma, \phi_d)\,. \tag{261}$$

Let us assume, for a moment, that the penguin contributions are dominated by top-quark exchanges. In this case, (259) simplifies as

$$\rho_{KK}e^{i\theta_{KK}} \to R_b\,. \tag{262}$$

Since the CP-conserving strong phase θ_{KK} vanishes in this limit, the direct CP violation in $B_d^0 \to K^0\bar{K}^0$ vanishes, too. Moreover, if we take into account that $\phi_d = 2\beta$ in the SM and use trigonometrical relations which can be derived for the UT, we find that the mixing-induced CP asymmetry also would be zero. These features suggest an interesting test of the $b \to d$ flavour sector of the SM (see, for instance, Ref. [210]). However, contributions from penguins with internal up- and charm-quark exchanges are expected to yield sizeable CP asymmetries in $B_d^0 \to K^0\bar{K}^0$ even within the SM, so that the interpretation of these effects is much more complicated [211]; these contributions contain also possible long-distance rescattering effects [212], which are often referred to as 'GIM' and 'charming' penguins and recently received a lot of attention [213].

Despite this problem, interesting insights can be obtained through the $B_d^0 \to K^0\bar{K}^0$ observables [214]. By the time the CP-violating asymmetries in (260) and (261) can be measured, the angle

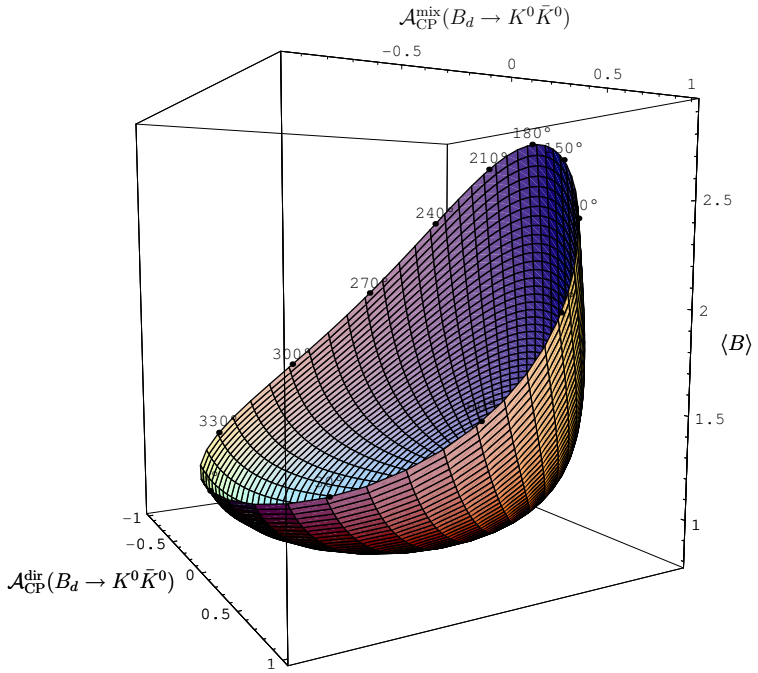

Fig. 30: Illustration of the surface in the $\mathcal{A}_{\rm CP}^{\rm dir}$–$\mathcal{A}_{\rm CP}^{\rm mix}$–$\langle B \rangle$ observable space characterizing the $B_d^0 \to K^0\bar{K}^0$ decay in the SM. The intersecting lines on the surface correspond to constant values of ρ_{KK} and θ_{KK}; the numbers on the fringe indicate the value of θ_{KK}, while the fringe itself is defined by $\rho_{KK} = 1$.

γ of the UT will also be reliably known, in addition to the B_d^0–$\bar{B}_d^0$ mixing phase ϕ_d. The experimental values of the CP asymmetries can then be converted into ρ_{KK} and θ_{KK}, in analogy to the $B \to \pi\pi$ discussion in Section 8.2. Although these quantities are interesting to obtain insights into the $B \to \pi K$ parameter $\rho_{\rm c} e^{i\theta_{\rm c}}$ [see (237)] through $SU(3)$ arguments, and can be compared with theoretical predictions, for instance, those of QCDF, PQCD or SCET, they do not provide—by themselves—a test of the SM description of the FCNC processes mediating the decay $B_d^0 \to K^0\bar{K}^0$. However, so far, we have not yet used the information offered by the CP-averaged branching ratio of this channel. It takes the following form:

$$\text{BR}(B_d \to K^0\bar{K}^0) = \frac{\tau_{B_d}}{16\pi M_{B_d}} \times \Phi_{KK} \times |\lambda^3 A\, \tilde{A}_{\rm P}^{tc}|^2 \langle B \rangle \,, \tag{263}$$

where Φ_{KK} denotes a two-body phase-space factor, $\tilde{A}_{\rm P}^{tc} \equiv \tilde{A}_{\rm P}^{t} - \tilde{A}_{\rm P}^{c}$, and

$$\langle B \rangle \equiv 1 - 2\rho_{KK} \cos\theta_{KK} \cos\gamma + \rho_{KK}^2 \,. \tag{264}$$

If we now use ϕ_d and the SM value of γ, we may characterize the decay $B_d^0 \to K^0\bar{K}^0$—within the SM—through a surface in the observable space of $\mathcal{A}_{\rm CP}^{\rm dir}$, $\mathcal{A}_{\rm CP}^{\rm mix}$ and $\langle B \rangle$. In Fig. 30, we show this surface, where each point corresponds to a given value of ρ_{KK} and θ_{KK}. It should be emphasized that this surface is *theoretically clean* since it relies only on the general SM parametrization of $B_d^0 \to K^0\bar{K}^0$. Consequently, should future measurements give a value in observable space that should *not* lie on the SM surface, we would have immediate evidence for NP contributions to $\bar{b} \to \bar{d}s\bar{s}$ processes.

Looking at Fig. 30, we see that $\langle B \rangle$ takes an absolute minimum. Indeed, if we keep ρ_{KK} and θ_{KK} as free parameters in (264), we find

$$\langle B \rangle \geq \sin^2\gamma \,, \tag{265}$$

which yields a strong lower bound because of the favourably large value of γ. Whereas the direct and mixing-induced CP asymmetries can be extracted from a time-dependent rate asymmetry [see (152)], the determination of $\langle B \rangle$ requires further information to fix the overall normalization factor involving

the penguin amplitude $\tilde{A}_{\rm P}^{tc}$. The strategy developed in Refs. [82, 83] offers the following two avenues, using data for

i) $B \to \pi\pi$ decays, i.e., $b \to d$ transitions, implying the following lower bound:

$$\mathrm{BR}(B_d \to K^0\bar{K}^0)_{\rm min} = \Xi_\pi^K \times \left(1.39\,^{+1.54}_{-0.95}\right) \times 10^{-6}\,, \tag{266}$$

ii) $B \to \pi K$ decays, i.e., $b \to s$ transitions, which are complemented by the $B \to \pi\pi$ system to determine a small correction, implying the following lower bound:

$$\mathrm{BR}(B_d \to K^0\bar{K}^0)_{\rm min} = \Xi_\pi^K \times \left(1.36\,^{+0.18}_{-0.21}\right) \times 10^{-6}\,. \tag{267}$$

Here factorizable $SU(3)$-breaking corrections are included, as is made explicit through

$$\Xi_\pi^K = \left[\frac{f_0^K}{0.331}\frac{0.258}{f_0^\pi}\right]^2\,, \tag{268}$$

where the numerical values for the $B \to K, \pi$ form factors $f_0^{K,\pi}$ refer to a recent light-cone sum-rule analysis [215]. At the time of the derivation of these bounds, the B factories reported an experimental *upper* bound of $\mathrm{BR}(B_d \to K^0\bar{K}^0) < 1.5\times 10^{-6}$ (90% C.L.). Consequently, the theoretical *lower* bounds given above suggested that the observation of this channel should just be ahead of us. Subsequently, the first signals were indeed announced, in accordance with (266) and (267):

$$\mathrm{BR}(B_d \to K^0\bar{K}^0) = \begin{cases} (1.19^{+0.40}_{-0.35} \pm 0.13) \times 10^{-6} & \text{(BaBar [216])}\,, \\ (0.8 \pm 0.3 \pm 0.1) \times 10^{-6} & \text{(Belle [217])}\,. \end{cases} \tag{269}$$

The SM description of $B_d^0 \to K^0\bar{K}^0$ has thus successfully passed its first test. However, the experimental errors are still very large, and the next crucial step—a measurement of the CP asymmetries—is still missing. Using QCDF, an analysis of NP effects in this channel was recently performed in the minimal supersymmetric standard model [218]. For further aspects of $B_d^0 \to K^0\bar{K}^0$, the reader is referred to Ref. [214].

9.3 Radiative $b \to d$ penguin decays: $\bar{B} \to \rho\gamma$

Another important tool to explore $b \to d$ penguins is provided by $\bar{B} \to \rho\gamma$ modes. In the SM, these decays are described by a Hamiltonian with the following structure [67]:

$$\mathcal{H}_{\rm eff}^{b\to d\gamma} = \frac{G_{\rm F}}{\sqrt{2}} \sum_{j=u,c} V_{jd}^* V_{jb} \left[\sum_{k=1}^{2} C_k Q_k^{jd} + \sum_{k=3}^{8} C_k Q_k^d\right]. \tag{270}$$

Here the $Q_{1,2}^{jd}$ denote the current–current operators, whereas the $Q_{3\ldots6}^d$ are the QCD penguin operators, which govern the decay $\bar{B}_d^0 \to K^0\bar{K}^0$ together with the penguin-like contractions of $Q_{1,2}^{cd}$ and $Q_{1,2}^{ud}$. In contrast to these four-quark operators,

$$Q_{7,8}^d = \frac{1}{8\pi^2} m_b \bar{d}_i \sigma^{\mu\nu}(1+\gamma_5)\left\{e b_i F_{\mu\nu},\, g_{\rm s} T_{ij}^a b_j G_{\mu\nu}^a\right\} \tag{271}$$

are electro- and chromomagnetic penguin operators. The most important contributions to $\bar{B} \to \rho\gamma$ originate from $Q_{1,2}^{jd}$ and $Q_{7,8}^d$, whereas the QCD penguin operators play only a minor role, in contrast to $\bar{B}_d^0 \to K^0\bar{K}^0$. If we use again the unitarity of the CKM matrix and apply the Wolfenstein parametrization, we may write

$$A(\bar{B} \to \rho\gamma) = c_\rho \lambda^3 A \mathcal{P}_{tc}^{\rho\gamma}\left[1 - \rho_{\rho\gamma} e^{i\theta_{\rho\gamma}} e^{-i\gamma}\right], \tag{272}$$

where $c_\rho = 1/\sqrt{2}$ and 1 for $\rho = \rho^0$ and $\rho^\pm$, respectively, $\mathcal{P}^{\rho\gamma}_{tc} \equiv \mathcal{P}^{\rho\gamma}_t - \mathcal{P}^{\rho\gamma}_c$, and

$$\rho_{\rho\gamma} e^{i\theta_{\rho\gamma}} \equiv R_b \left[\frac{\mathcal{P}^{\rho\gamma}_t - \mathcal{P}^{\rho\gamma}_u}{\mathcal{P}^{\rho\gamma}_t - \mathcal{P}^{\rho\gamma}_c}\right]. \tag{273}$$

Here we follow our previous notation, i.e., the $\mathcal{P}^{\rho\gamma}_j$ are strong amplitudes with the following interpretation: $\mathcal{P}^{\rho\gamma}_u$ and $\mathcal{P}^{\rho\gamma}_c$ refer to the matrix elements of $\sum_{k=1}^2 C_k Q_k^{ud}$ and $\sum_{k=1}^2 C_k Q_k^{cd}$, respectively, whereas $\mathcal{P}^{\rho\gamma}_t$ corresponds to $-\sum_{k=3}^8 C_k Q_k^d$. Consequently, $\mathcal{P}^{\rho\gamma}_u$ and $\mathcal{P}^{\rho\gamma}_c$ describe the penguin topologies with internal up- and charm-quark exchanges, respectively, whereas $\mathcal{P}^{\rho\gamma}_t$ corresponds to the penguins with the top quark running in the loop. Let us note that (272) refers to a given photon helicity. However, the b quarks couple predominantly to left-handed photons in the SM, so that the right-handed amplitude is usually neglected [219]; we shall return to this point below. Comparing (272) with (258), we observe that the structure of both amplitudes is the same. In analogy to $\rho_{KK} e^{i\theta_{KK}}$, $\rho_{\rho\gamma} e^{i\theta_{\rho\gamma}}$ may also be affected by long-distance effects, which represent a key uncertainty of $\bar{B} \to \rho\gamma$ decays [147, 219].

If we replace all down quarks in (270) by strange quarks, we obtain the Hamiltonian for $b \to s\gamma$ processes, which are already well established experimentally [61]:

$$\text{BR}(B^\pm \to K^{*\pm}\gamma) = (40.3 \pm 2.6) \times 10^{-6} \tag{274}$$

$$\text{BR}(B^0_d \to K^{*0}\gamma) = (40.1 \pm 2.0) \times 10^{-6}\,. \tag{275}$$

In analogy to (272), we may write

$$A(\bar{B} \to K^*\gamma) = -\frac{\lambda^3 A \mathcal{P}^{K^*\gamma}_{tc}}{\sqrt{\epsilon}} \Big[1 + \epsilon \rho_{K^*\gamma} e^{i\theta_{K^*\gamma}} e^{-i\gamma}\Big], \tag{276}$$

where ϵ was introduced in (221). Thanks to the smallness of ϵ, the parameter $\rho_{K^*\gamma} e^{i\theta_{K^*\gamma}}$ plays an essentially negligible role for the $\bar{B} \to K^*\gamma$ transitions.

Let us have a look at the charged decays $B^\pm \to \rho^\pm\gamma$ and $B^\pm \to K^{*\pm}\gamma$ first. If we consider their CP-averaged branching ratios, we obtain

$$\frac{\text{BR}(B^\pm \to \rho^\pm\gamma)}{\text{BR}(B^\pm \to K^{*\pm}\gamma)} = \epsilon \left[\frac{\Phi_{\rho\gamma}}{\Phi_{K^*\gamma}}\right] \left|\frac{\mathcal{P}^{\rho\gamma}_{tc}}{\mathcal{P}^{K^*\gamma}_{tc}}\right|^2 H^{\rho\gamma}_{K^*\gamma}\,, \tag{277}$$

where $\Phi_{\rho\gamma}$ and $\Phi_{K^*\gamma}$ denote phase-space factors, and

$$H^{\rho\gamma}_{K^*\gamma} \equiv \frac{1 - 2\rho_{\rho\gamma}\cos\theta_{\rho\gamma}\cos\gamma + \rho^2_{\rho\gamma}}{1 + 2\epsilon\rho_{K^*\gamma}\cos\theta_{K^*\gamma}\cos\gamma + \epsilon^2\rho^2_{K^*\gamma}}\,. \tag{278}$$

Since $B^\pm \to \rho^\pm\gamma$ and $B^\pm \to K^{*\pm}\gamma$ are related through the interchange of all down and strange quarks, the U-spin flavour symmetry of strong interactions allows us to relate the corresponding hadronic amplitudes to each other; the U-spin symmetry is an $SU(2)$ subgroup of the full $SU(3)_{\rm F}$ flavour-symmetry group, which relates down and strange quarks in the same manner as the conventional strong isospin symmetry relates down and up quarks. Following these lines, we obtain

$$|\mathcal{P}^{\rho\gamma}_{tc}| = |\mathcal{P}^{K^*\gamma}_{tc}| \tag{279}$$

$$\rho_{\rho\gamma} e^{i\theta_{\rho\gamma}} = \rho_{K^*\gamma} e^{i\theta_{K^*\gamma}} \equiv \rho e^{i\theta}\,. \tag{280}$$

Although we may determine the ratio of the penguin amplitudes $|\mathcal{P}_{tc}|$ in (277) with the help of (279)—up to $SU(3)$-breaking effects to be discussed below—we are still left with the dependence on ρ and θ. However, keeping ρ and θ as free parameters, it can be shown that $H^{\rho\gamma}_{K^*\gamma}$ satisfies the following relation [220]:

$$H^{\rho\gamma}_{K^*\gamma} \geq \left[1 - 2\epsilon\cos^2\gamma + \mathcal{O}(\epsilon^2)\right]\sin^2\gamma\,, \tag{281}$$

where the term linear in ϵ gives a shift of about 1.9%.

Concerning possible $SU(3)$-breaking effects to (280), they may only enter this tiny correction and are negligible for our analysis. On the other hand, the $SU(3)$-breaking corrections to (279) have a sizeable impact. Following Refs. [221, 222], we write

$$\left[\frac{\Phi_{\rho\gamma}}{\Phi_{K^*\gamma}}\right]\left|\frac{\mathcal{P}_{tc}^{\rho\gamma}}{\mathcal{P}_{tc}^{K^*\gamma}}\right|^2 = \left[\frac{M_B^2-M_\rho^2}{M_B^2-M_{K^*}^2}\right]^3\zeta^2\,, \tag{282}$$

where $\zeta = F_\rho/F_{K^*}$ is the $SU(3)$-breaking ratio of the $B^\pm\to\rho^\pm\gamma$ and $B^\pm\to K^{*\pm}\gamma$ form factors; a light-cone sum-rule analysis gives $\zeta^{-1} = 1.31\pm0.13$ [223]. Consequently, (281) and (282) allow us to convert the measured $B^\pm\to K^{*\pm}\gamma$ branching ratio (274) into a *lower* SM bound for $\mathrm{BR}(B^\pm\to\rho^\pm\gamma)$ with the help of (277) [220]:

$$\mathrm{BR}(B^\pm\to\rho^\pm\gamma)_{\rm min} = \left(1.02\,^{+0.27}_{-0.23}\right)\times10^{-6}\,. \tag{283}$$

A similar kind of reasoning holds also for the U-spin pairs $B^\pm\to K^\pm K,\pi^\pm K$ and $B^\pm\to K^\pm K^*,\pi^\pm K^*$, where the following lower bounds can be derived [220]:

$$\mathrm{BR}(B^\pm\to K^\pm K)_{\rm min} = \Xi_\pi^K\times\left(1.69\,^{+0.21}_{-0.24}\right)\times10^{-6} \tag{284}$$

$$\mathrm{BR}(B^\pm\to K^\pm K^*)_{\rm min} = \Xi_\pi^K\times\left(0.68\,^{+0.11}_{-0.13}\right)\times10^{-6}\,, \tag{285}$$

with Ξ_π^K given in (268). Thanks to the most recent B-factory data, we now also have evidence for $B^\pm\to K^\pm K$ decays:

$$\mathrm{BR}(B^\pm\to K^\pm K) = \begin{cases} (1.5\pm0.5\pm0.1)\times10^{-6} & \text{(BaBar [216])}\\ (1.0\pm0.4\pm0.1)\times10^{-6} & \text{(Belle [217])}\,,\end{cases} \tag{286}$$

whereas the upper limit of 5.3×10^{-6} for $B^\pm\to K^\pm K^*$ still leaves a lot of space. Obviously, we may also consider the $B^\pm\to K^{*\pm}K,\rho^\pm K$ system [220]. However, since currently only the upper bound $\mathrm{BR}(B^\pm\to\rho^\pm K)<48\times10^{-6}$ is available, we cannot yet give a number for the lower bound on $\mathrm{BR}(B^\pm\to K^{*\pm}K)$. Experimental analyses of these modes are strongly encouraged.

Let us now turn to $\bar{B}_d^0\to\rho^0\gamma$, which receives contributions from exchange and penguin annihilation topologies that are not present in $\bar{B}_d^0\to\bar{K}^{*0}\gamma$; in the case of $B^\pm\to\rho^\pm\gamma$ and $B^\pm\to K^{*\pm}\gamma$, which are related by the U-spin symmetry, there is a one-to-one correspondence of topologies. Making the plausible assumption that the topologies involving the spectator quarks play a minor role, and taking the factor of $c_{\rho^0}=1/\sqrt{2}$ in (272) into account, the counterpart of (283) is given by

$$\mathrm{BR}(B_d\to\rho^0\gamma)_{\rm min} = \left(0.51\,^{+0.13}_{-0.11}\right)\times10^{-6}\,. \tag{287}$$

At the time of the derivation of the *lower* bounds for the $B\to\rho\gamma$ branching ratios given above, the following experimental *upper* bounds (90% C.L.) were available:

$$\mathrm{BR}(B^\pm\to\rho^\pm\gamma) < \begin{cases} 1.8\times10^{-6} & \text{(BaBar [224])}\\ 2.2\times10^{-6} & \text{(Belle [225])}\end{cases} \tag{288}$$

$$\mathrm{BR}(B_d\to\rho^0\gamma) < \begin{cases} 0.4\times10^{-6} & \text{(BaBar [224])}\\ 0.8\times10^{-6} & \text{(Belle [225])}\,.\end{cases} \tag{289}$$

Consequently, it was expected that the $\bar{B}\to\rho\gamma$ modes should soon be discovered at the B factories [220]. Indeed, the Belle Collaboration recently reported the first observation of $b\to d\gamma$ processes [226]:

$$\mathrm{BR}(B^\pm\to\rho^\pm\gamma) = \left(0.55^{+0.43+0.12}_{-0.37-0.11}\right)\times10^{-6} \tag{290}$$

$$\text{BR}(B_d \to \rho^0\gamma) = \left(1.17^{+0.35+0.09}_{-0.31-0.08}\right) \times 10^{-6} \quad (291)$$

$$\text{BR}(B \to (\rho,\omega)\gamma) = \left(1.34^{+0.34+0.14}_{-0.31-0.10}\right) \times 10^{-6}\,, \quad (292)$$

which was one of the hot topics of the 2005 summer conferences [227]. These measurements still suffer from large uncertainties, and the pattern of the central values of (290) and (291) would be in conflict with the expectation following from the isospin symmetry. It will be interesting to follow the evolution of the data. The next important conceptual step would be the measurement of the corresponding CP-violating observables, though this is still in the distant future.

An alternative avenue to confront the data for the $B \to \rho\gamma$ branching ratios with the SM is provided by converting them into information on the side R_t of the UT. To this end, the authors of Refs. [221, 222] also use (282), and calculate the CP-conserving (complex) parameter δa entering $\rho_{\rho\gamma}e^{i\theta_{\rho\gamma}} = R_b\,[1+\delta a]$ in the QCDF approach. The corresponding result, which favours a small impact of δa, takes leading and next-to-leading order QCD corrections into account and holds to leading order in the heavy-quark limit [222]. In view of the remarks about possible long-distance effects made above and the B-factory data for the $B \to \pi\pi$ system, which indicate large corrections to the QCDF picture for non-leptonic B decays into two light pseudoscalar mesons (see Section 8.2), it is, however, not obvious that the impact of δa is actually small. The advantage of the bound following from (281) is that it is—by construction—*not* affected by $\rho_{\rho\gamma}e^{i\theta_{\rho\gamma}}$ at all.

9.4 General lower bounds for $b \to d$ penguin processes

Interestingly, the bounds discussed above are actually realizations of a general, model-independent bound that can be derived in the SM for $b \to d$ penguin processes [220]. If we consider such a decay, $\bar{B} \to \bar{f}_d$, we may—in analogy to (258) and (272)—write

$$A(\bar{B} \to \bar{f}_d) = A_d^{(0)}\left[1 - \varrho_d e^{i\theta_d}e^{-i\gamma}\right], \quad (293)$$

so that the CP-averaged amplitude square is given as follows:

$$\langle |A(B \to f_d)|^2\rangle = |A_d^{(0)}|^2\left[1 - 2\varrho_d\cos\theta_d\cos\gamma + \varrho_d^2\right]. \quad (294)$$

In general, ϱ_d and θ_d depend on the point in phase space considered. Consequently, the expression

$$\text{BR}(B \to f_d) = \tau_B\left[\sum_{\text{Pol}}\int d\,\text{PS}\,\langle |A(B \to f_d)|^2\rangle\right] \quad (295)$$

for the CP-averaged branching ratio, where the sum runs over possible polarization configurations of f_d, does *not* factorize into $|A_d^{(0)}|^2$ and $[1 - 2\varrho_d\cos\theta_d\cos\gamma + \varrho_d^2]$ as in the case of the two-body decays considered above. However, if we keep ϱ_d and θ_d as free, 'unknown' parameters at any given point in phase space, we obtain

$$\langle |A(B \to f_d)|^2\rangle \geq |A_d^{(0)}|^2\sin^2\gamma\,, \quad (296)$$

which implies

$$\text{BR}(B \to f_d) \geq \tau_B\left[\sum_{\text{Pol}}\int d\,\text{PS}\,|A_d^{(0)}|^2\right]\sin^2\gamma\,. \quad (297)$$

In order to deal with the term in square brackets, we use a $b \to s$ penguin decay $\bar{B} \to \bar{f}_s$, which is the counterpart of $\bar{B} \to \bar{f}_d$ in that the corresponding CP-conserving strong amplitudes can be related to one another through the $SU(3)$ flavour symmetry. In analogy to (276), we may then write

$$A(\bar{B} \to \bar{f}_s) = -\frac{A_s^{(0)}}{\sqrt{\epsilon}}\left[1 + \epsilon\varrho_s e^{i\theta_s}e^{-i\gamma}\right]. \quad (298)$$

If we neglect the term proportional to ϵ in the square bracket, we arrive at

$$\frac{\mathrm{BR}(B \to f_d)}{\mathrm{BR}(B \to f_s)} \geq \epsilon \left[\frac{\sum_{\mathrm{Pol}} \int d\,\mathrm{PS}\, |A_d^{(0)}|^2}{\sum_{\mathrm{Pol}} \int d\,\mathrm{PS}\, |A_s^{(0)}|^2}\right] \sin^2\gamma\,. \tag{299}$$

Apart from the tiny ϵ correction, which gave a shift of about 1.9% in (281), (299) is valid exactly in the SM. If we now apply the $SU(3)$ flavour symmetry, we obtain

$$\frac{\sum_{\mathrm{Pol}} \int d\,\mathrm{PS}\, |A_d^{(0)}|^2}{\sum_{\mathrm{Pol}} \int d\,\mathrm{PS}\, |A_s^{(0)}|^2} \stackrel{SU(3)_{\mathrm{F}}}{\longrightarrow} 1\,. \tag{300}$$

Since $\sin^2\gamma$ is favourably large in the SM and the decay $\bar{B} \to \bar{f}_s$ will be measured before its $b \to d$ counterpart—simply because of the CKM enhancement—(299) provides strong lower bounds for $\mathrm{BR}(B \to f_d)$.

It is instructive to return briefly to $B \to \rho\gamma$. If we look at (299), we observe immediately that the assumption that these modes are governed by a single photon helicity is no longer required. Consequently, (283) and (287) are actually very robust with respect to this issue, which may only affect the $SU(3)$-breaking corrections to a small extent. This feature is interesting in view of the recent discussion in Ref. [228], where the photon polarization in $B \to \rho\gamma$ and $B \to K^*\gamma$ decays was critically analysed.

We can now also derive a bound for the $B^\pm \to K^{*\pm}K^*, \rho^\pm K^*$ system, where we have to sum in (299) over three polarization configurations of the vector mesons. The analysis of the $SU(3)$-breaking corrections is more involved than in the case of the decays considered above, and the emerging lower bound of $\mathrm{BR}(B^\pm \to K^{*\pm}K^*)_{\min} \sim 0.6 \times 10^{-6}$ is still very far from the experimental upper bound of 71×10^{-6}. Interestingly, the theoretical lower bound would be reduced by ~ 0.6 in the strict $SU(3)$ limit, i.e., would be more conservative [220]. A similar comment applies to (266), (267) and (284), (285). On the other hand, the $B \to \rho\gamma$ bounds in (283) and (287) would be enhanced by ~ 1.7 in this case. However, here the theoretical situation is more favourable since we have not to rely on the factorization hypothesis to deal with the $SU(3)$-breaking effects as in the case of the non-leptonic decays.

Let us finally come to another application of (299), which is offered by decays of the kind $\bar{B} \to \pi\ell^+\ell^-$ and $\bar{B} \to \rho\ell^+\ell^-$. It is well known that the ρ_d terms complicate the interpretation of the corresponding data considerably [147]; the bound offers SM tests that are not affected by these contributions. The structure of the $b \to d\ell^+\ell^-$ Hamiltonian is similar to (270), but involves the additional operators

$$Q_{9,10} = \frac{\alpha}{2\pi}(\bar{\ell}\ell)_{\mathrm{V,\,A}}(\bar{d}_i b_i)_{\mathrm{V-A}}\,. \tag{301}$$

The $b \to s\ell^+\ell^-$ modes $\bar{B} \to K\ell^+\ell^-$ and $\bar{B} \to K^*\ell^+\ell^-$ were already observed at the B factories, with branching ratios at the 0.6×10^{-6} and 1.4×10^{-6} levels [61], respectively, and received considerable theoretical attention (see, for example, Ref. [229]). For the application of (299), the charged decay combinations $B^\pm \to \pi^\pm\ell^+\ell^-, K^\pm\ell^+\ell^-$ and $B^\pm \to \rho^\pm\ell^+\ell^-, K^{*\pm}\ell^+\ell^-$ are suited best since the corresponding decay pairs are related to each other through the U-spin symmetry [230]. The numbers given above suggest

$$\mathrm{BR}(B^\pm \to \pi^\pm\ell^+\ell^-), \quad \mathrm{BR}(B^\pm \to \rho^\pm\ell^+\ell^-) \gtrsim 10^{-8}\,, \tag{302}$$

thereby leaving the exploration of these $b \to d$ penguin decays for the more distant future. Detailed studies of the associated $SU(3)$-breaking corrections are encouraged. It is hoped that by the time the $B^\pm \to \pi^\pm\ell^+\ell^-, \rho^\pm\ell^+\ell^-$ modes can be measured, we shall have a good picture of these effects.

It will be interesting to confront all of these bounds with experimental data. In the case of the non-leptonic $B_d \to K^0\bar{K}^0, B^\pm \to K^\pm K$ modes and their radiative $B \to \rho\gamma$ counterparts, they have already provided a first successful test of the SM description of the corresponding FCNC processes, although the uncertainties are still very large in view of the fact that we are just at the beginning of the experimental

exploration of these channels. A couple of other non-leptonic decays of this kind may just be around the corner. It would be exciting if some bounds were significantly violated through destructive interference between SM and NP contributions. Since the different decay classes are governed by different operators, we could actually encounter surprises!

10 B-decay studies in the LHC era: fully exploiting the B_s system

10.1 In pursuit of new physics with ΔM_s

Concerning experimental information about this mass difference, only lower bounds were available for many years from the LEP experiments at CERN and SLD at SLAC [107]. Since the currently operating e^+e^- B factories run at the $\Upsilon(4S)$ resonance, which decays into $B_{u,d}$, but not into B_s mesons, the B_s system cannot be explored by the BaBar and Belle experiments[3]. However, plenty of B_s mesons are produced at the Tevatron (and will be later on at the LHC [232]), which—very recently—allowed the measurement of ΔM_s, as summarized in (131) and (132). These new results were one of the hot topics of spring 2006, and have already triggered several phenomenological papers (see, for example, Refs. [233]– [241]).

As in Section 6 and Section 7.1, we shall follow the analysis of Ref. [101]. In order to describe possible NP effects, we parametrize them through (164) and (165). The relevant CKM factor is $|V_{ts}^* V_{tb}|$. Using once again the unitarity of the CKM matrix and including next-to-leading order terms in the Wolfenstein expansion as given in Ref. [36], we have

$$\left|\frac{V_{ts}}{V_{cb}}\right| = 1 - \frac{1}{2}\left(1 - 2R_b\cos\gamma\right)\lambda^2 + \mathcal{O}(\lambda^4)\,. \tag{303}$$

Consequently, apart from the tiny correction in λ^2, the CKM factor for ΔM_s is independent of γ and R_b, which is an important advantage in comparison with the B_d-meson system. The accuracy of the SM prediction of ΔM_s is hence limited by the hadronic mixing parameter $f_{B_s}\hat{B}_{B_s}^{1/2}$. If we consider the ratio ρ_s introduced in (166) and use the CDF measurement in (132), we obtain

$$\rho_s|_{\rm JLQCD} = 1.08^{+0.03}_{-0.01}({\rm exp}) \pm 0.19({\rm th}) \tag{304}$$

$$\rho_s|_{\rm (HP+JL)QCD} = 0.74^{+0.02}_{-0.01}({\rm exp}) \pm 0.18({\rm th})\,, \tag{305}$$

where we made the experimental and theoretical errors explicit. These numbers are consistent with the SM case $\rho_s = 1$, but suffer from significant theoretical uncertainties, which are much larger than the experimental errors. Nevertheless, it is interesting to note that the (HP+JL)QCD result is $1.5\,\sigma$ below the SM; a similar pattern arises in (193) and (194), though at the $1\,\sigma$ level. Any more precise statement about the presence or absence of NP requires the reduction of theoretical uncertainties.

In Fig. 31, we show the constraints in the σ_s–κ_s plane, which can be obtained from ρ_s with the help of the contours shown in Fig. 18. We see that upper bounds of $\kappa_s \lesssim 2.5$ arise from the measurement of ΔM_s. In the case of (305), σ_s would be constrainted to lie within the range $110^\circ \leq \sigma_s \leq 250^\circ$. Consequently, the CDF measurement of ΔM_s leaves ample space for the NP parameters σ_s and κ_s. As in the case of the B_d-meson system discussed in Section 7.1, this situation will change significantly as soon as information about CP violation in the B_s-meson system becomes available. We shall return to this topic in Section 10.2.

It is interesting to consider the ratio of ΔM_s and ΔM_d, which can be written as follows:

$$\frac{\Delta M_s}{\Delta M_d} = \frac{\rho_s}{\rho_d}\left|\frac{V_{ts}}{V_{td}}\right|^2 \frac{M_{B_s}}{M_{B_d}}\,\xi^2\,, \tag{306}$$

[3]The asymmetric e^+e^- KEKB collider was recently also operated at the $\Upsilon(5S)$ resonance in an engineering run, allowing the Belle experiment to take first B_s data [231].

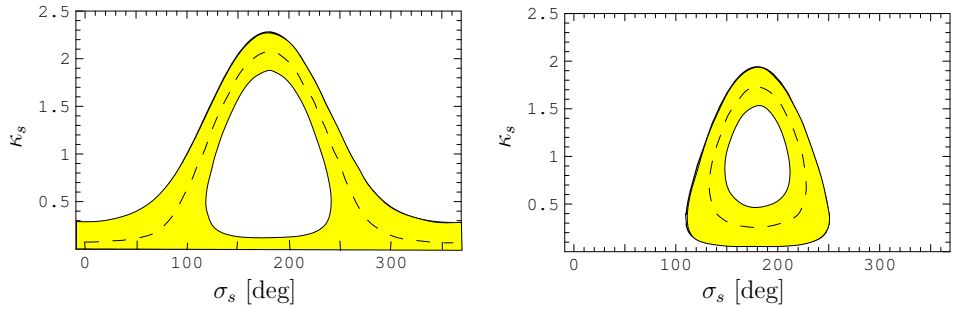

Fig. 31: The allowed regions (yellow/grey) in the σ_s–κ_s plane. Left panel: JLQCD lattice results (122). Right panel: (HP+JL)QCD lattice results (123).

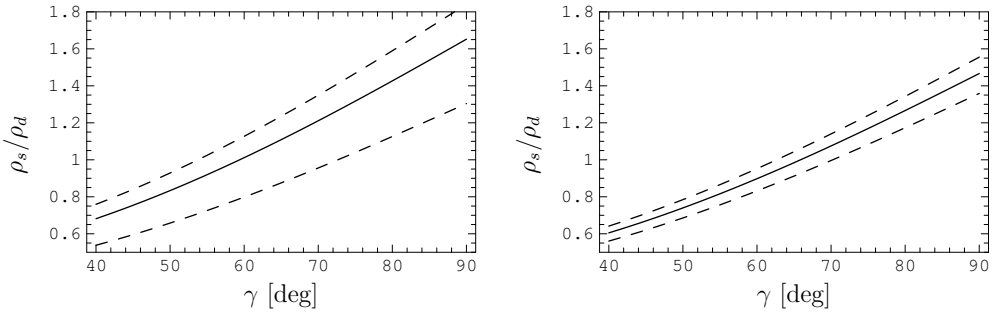

Fig. 32: The dependence of ρ_s/ρ_d on γ for the central values of $\Delta M_{d,s}$ in (130) and (132). Left panel: JLQCD results (308). Right panel: (HP+JL)QCD results (309). The plots are nearly independent of R_b.

where the hadronic $SU(3)$-breaking parameter ξ is defined through

$$\xi \equiv \frac{f_{B_s}\hat{B}_{B_s}^{1/2}}{f_{B_d}\hat{B}_{B_d}^{1/2}} \,. \tag{307}$$

In the class of NP models with 'minimal flavour violation' (see Section 6, and Ref. [237] for a recent analysis addressing also the ΔM_s measurement), we have $\rho_s/\rho_d = 1$, so that (306) allows the extraction of the CKM factor $|V_{ts}/V_{td}|$, and hence $|V_{td}|$, as $|V_{ts}|$ is known—to excellent accuracy—from (303). The advantage of this determination lies in the reduced theoretical uncertainty of ξ as compared to $f_{B_d}\hat{B}_{B_d}^{1/2}$. For the sets of lattice results in (122) and (123), we have

$$\xi_{\rm JLQCD} = 1.14 \pm 0.06^{+0.13}_{-0} \tag{308}$$

$$\xi_{\rm (HP+JL)QCD} = 1.210^{+0.047}_{-0.035} \,. \tag{309}$$

Using the expression

$$R_t \equiv \frac{1}{\lambda}\left|\frac{V_{td}}{V_{cb}}\right| = \frac{1}{\lambda}\left|\frac{V_{td}}{V_{ts}}\right|\left[1 - \frac{1}{2}\left(1 - 2R_b\cos\gamma\right)\lambda^2 + \mathcal{O}(\lambda^4)\right], \tag{310}$$

we may convert the extracted value of $|V_{ts}/V_{td}|$ into a measurement of the UT side R_t. As we noted in Subsection 9.3, another determination of R_t can, in principle, be obtained from radiative decays, in particular the ratio of branching ratios $\mathcal{B}(B \to (\rho,\omega)\gamma)/\mathcal{B}(B \to K^*\gamma)$, but is presently limited by experimental statistics; see Ref. [242] for a recent analysis.

Alternatively, following Ref. [101], we may constrain the ratio ρ_s/ρ_d through the measured value of $\Delta M_s/\Delta M_d$. To this end, we express—in analogy to (192)—the UT side R_t in terms of R_b and γ:

$$R_t = \sqrt{1 - 2R_b\cos\gamma + R_b^2}\,, \tag{311}$$

allowing the determination of R_t through processes that are essentially unaffected by NP. The resulting value of R_t depends rather strongly on γ, which is the main source of uncertainty. Combining then (306) and (310), we obtain the following expression for ρ_s/ρ_d:

$$\frac{\rho_s}{\rho_d} = \lambda^2\left[1 - 2R_b\cos\gamma + R_b^2\right]\left[1 + (1 - 2R_b\cos\gamma)\lambda^2 + \mathcal{O}(\lambda^4)\right]\frac{1}{\xi^2}\frac{M_{B_d}}{M_{B_s}}\frac{\Delta M_s}{\Delta M_d}\,. \tag{312}$$

In Fig. 32, we plot this ratio for the central values of ΔM_d and ΔM_s in (130) and (132), respectively, as a function of the UT angle γ for the values of ξ given in (122) and (123). We find that the corresponding curves are nearly independent of R_b and that γ is actually the key CKM parameter for the determination of ρ_s/ρ_d. The corresponding numerical values are given by:

$$\left.\frac{\rho_s}{\rho_d}\right|_{\rm JLQCD} = 1.11^{+0.02}_{-0.01}(\text{exp}) \pm 0.35(\gamma, R_b)^{+0.12}_{-0.28}(\xi) \tag{313}$$

$$\left.\frac{\rho_s}{\rho_d}\right|_{\rm (HP+JL)QCD} = 0.99^{+0.02}_{-0.01}(\text{exp}) \pm 0.31(\gamma, R_b)^{+0.06}_{-0.08}(\xi)\,. \tag{314}$$

Because of the large range of allowed values of γ in (182), this ratio is currently not stringently constrained. This situation should, however, improve significantly in the LHC era thanks to the impressive determination of γ to be obtained at the LHCb experiment. In fact, a statistical accuracy of $\sigma_{\rm stat}(\gamma) \approx 2.5^\circ$ is expected at LHCb after five years of data taking [232].

Let us introduce a scenario for the year 2010 that is characterized by $\gamma = (70 \pm 5)^\circ$ and the (HP+JL)QCD parameters in (123). We then find

$$\left.\frac{\rho_s}{\rho_d}\right|_{2010} = 1.07 \pm 0.09(\gamma, R_b)^{+0.06}_{-0.08}(\xi) = 1.07 \pm 0.12\,, \tag{315}$$

where we made the errors arising from the uncertainties of γ and ξ explicit, and, in the last step, added them in quadrature. Consequently, the hadronic uncertainties and those induced by γ would now be of the same size, which should provide additional motivation for the lattice community to reduce the error of ξ even further. Despite the impressive reduction of uncertainty compared to the 2006 values in (313) and (314), the numerical value in (315) would still not allow a stringent test of whether ρ_s/ρ_d equals one: to establish a $3\,\sigma$ deviation from 1, central values of $\rho_s/\rho_d = 1.4$ or 0.7 would be needed. The assumed uncertainty of γ of 5° could also turn out to be too pessimistic, in which case even more progress would be needed from the lattice side to match the experimental accuracy.

The result in (315) would not necessarily suggest that there is no physics beyond the SM. In fact, the central values of $\rho_d = 0.69 \pm 0.16$ and $\rho_s = 0.74 \pm 0.18$ would both be smaller than 1, i.e., would both deviate from the SM picture, although the hadronic uncertainties would again not allow us to draw definite conclusions. In order to shed further light on these possible NP contributions, the exploration of CP-violating effects in the B_s-meson system is essential, which can be performed with the help of the 'golden' decay $B_s^0 \to J/\psi\phi$.

10.2 $B_s^0 \to J/\psi\phi$

As can be seen in Fig. 20, the decay $B_s^0 \to J/\psi\phi$ is simply related to $B_d^0 \to J/\psi K_{\rm S}$ through a replacement of the down spectator quark by a strange quark. Consequently, the structure of the $B_s^0 \to J/\psi\phi$ decay amplitude is completely analogous to that of (169). On the other hand, the final state of $B_s^0 \to J/\psi\phi$

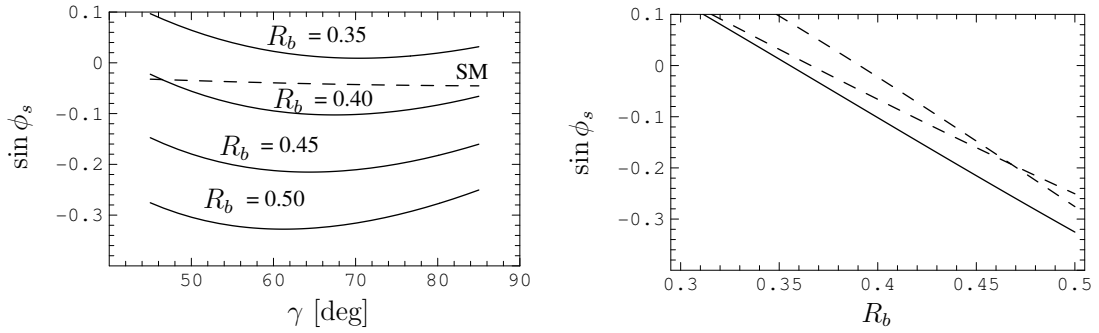

Fig. 33: $\sin\phi_s$ for a scenario with flavour-universal NP, i.e., $\phi_s^{\rm NP} = \phi_d^{\rm NP}$, as specified in Eq. (318), and $\phi_d = 43.4^\circ$. Left panel: $\sin\phi_s$ as a function of γ for various values of R_b. Right panel: $\sin\phi_s$ as a function of R_b for various values of γ [solid line: $\gamma = 65^\circ$, dashed lines: $\gamma = (45^\circ, 85^\circ)$].

consists of two vector mesons, and is hence an admixture of different CP eigenstates, which can, however, be disentangled through an angular analysis of the $B_s^0 \to J/\psi[\to \ell^+\ell^-]\phi[\to K^+K^-]$ decay products [111, 243]. The corresponding angular distribution exhibits tiny direct CP violation, and allows the extraction of

$$\sin\phi_s + \mathcal{O}(\overline{\lambda}^3) = \sin\phi_s + \mathcal{O}(10^{-3}) \tag{316}$$

through mixing-induced CP violation. Since we have $\phi_s = -2\delta\gamma = -2\lambda^2\eta \sim -2^\circ$ in the SM, the determination of this phase from (316) is affected by hadronic uncertainties of $\mathcal{O}(10\%)$, which may become an issue for the LHC era. These uncertainties can be controlled with the help of flavour-symmetry arguments through the $B_d^0 \to J/\psi\rho^0$ decay [244].

Needless to say, the big hope is that large CP violation will be found in this channel. Since the CP-violating effects in $B_s^0 \to J/\psi\phi$ are tiny in the SM, such an observation would give us an unambiguous signal for NP [117, 245, 246]. As the situation for NP entering through the decay amplitude is similar to $B \to J/\psi K$, we would get evidence for CP-violating NP contributions to B_s^0–$\bar{B}_s^0$ mixing, and could extract the corresponding sizeable value of ϕ_s [117]. Such a scenario may generically arise in the presence of NP with $\Lambda_{\rm NP} \sim$ TeV [119], as well as in specific models, including supersymmetric frameworks and models with extra Z' bosons (see Ref. [101] and references therein).

Thanks to its nice experimental signature, $B_s^0 \to J/\psi\phi$ is very accessible at hadron colliders, and can be fully exploited at the LHC. After one year of data taking (which corresponds to 2 fb^{-1}), LHCb expects a measurement with the statistical accuracy $\sigma_{\rm stat}(\sin\phi_s) \approx 0.031$; adding modes such as $B_s \to J/\psi\eta, J/\psi\eta'$ and $\eta_c\phi$, $\sigma_{\rm stat}(\sin\phi_s) \approx 0.013$ is expected after five years [232]. Also ATLAS and CMS will contribute to the measurement of $\sin\phi_s$, expecting uncertainties at the 0.1 level after one year of data taking, which corresponds to 10 fb^{-1} [247, 248]. In order to illustrate the impact of NP effects on the quantity

$$\sin\phi_s = \sin(-2\lambda^2 R_b \sin\gamma + \phi_s^{\rm NP}) \,, \tag{317}$$

let us assume that the NP parameters satisfy the simple relation

$$\sigma_d = \sigma_s, \quad \kappa_d = \kappa_s \,, \tag{318}$$

i.e., that in particular $\phi_d^{\rm NP} = \phi_s^{\rm NP}$. This scenario would be supported by (315), although it would *not* belong to the class of models with MFV, as new sources of CP violation would be required. As we have seen in Section 7.1, the analysis of the B_d^0 data for $R_b^{\rm incl} = 0.45$ indicates a small NP phase around

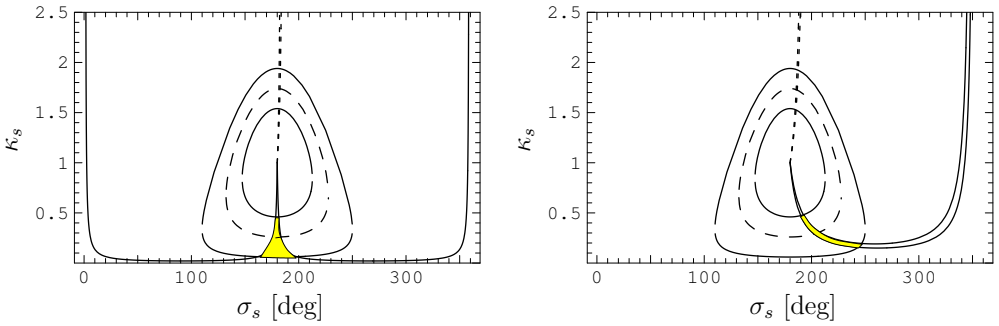

Fig. 34: Combined constraints for the allowed region (yellow/grey) in the σ_s–κ_s plane through ΔM_s in (132) for the (HP+JL)QCD results (123) and CP violation measurements. Left panel: the SM scenario $(\sin\phi_s)_{\rm exp} = -0.04 \pm 0.02$. Right panel: a NP scenario with $(\sin\phi_s)_{\rm exp} = -0.20 \pm 0.02$. The solid lines correspond to $\cos\phi_s > 0$, the dotted lines to $\cos\phi_s < 0$.

-10° in the B_d system. In the above scenario, that would imply the presence of the same phase in the B_s system, which would interfere constructively with the small SM phase and result in CP asymmetries at the level of -20%. CP-violating effects of that size can easily be detected at the LHC. This exercise demonstrates again the great power of the B_s-meson system to reveal CP-violating NP contributions to B_q^0–$\bar{B}_q^0$ mixing. The presence of a small NP phase could actually be considerably magnified, as illustrated in Fig. 33.

Let us finally also discuss the impact of CP violation measurements on the allowed region in the σ_s–κ_s plane in our 2010 scenario. To this end, we consider two cases:

i) $(\sin\phi_s)_{\rm exp} = -0.04 \pm 0.02$, in accordance with the SM;
ii) $(\sin\phi_s)_{\rm exp} = -0.20 \pm 0.02$, in accordance with the NP scenario of Fig. 33.

The measurement of $\sin\phi_s$ implies a twofold solution for ϕ_s and, therefore, also for $\phi_s^{\rm NP}$. However, this ambiguity can be resolved through the determination of the sign of $\cos\phi_s$, which can be fixed through the strategies proposed in Ref. [117]. In Fig. 34, we show the situation in the σ_s–κ_s plane[4]. The dotted lines refer to negative values of $\cos\phi_s$. Assuming that these are experimentally excluded, we are left with strongly restricted regions, although κ_s could still take sizeable ranges, with upper bounds $\kappa_s \approx 0.5$. In the SM-like scenario, values of σ_s around 180° would arise, i.e., a NP contribution with a sign opposite to the SM. However, due to the absence of new CP-violating effects, the accuracy of lattice results would have to be considerably improved in order to allow the extraction of a value of κ_s incompatible with 0. On the other hand, a measurement of $(\sin\phi_s)_{\rm exp} = -0.20 \pm 0.02$ would give a NP signal at the $10\,\sigma$ level, with $\kappa_s \gtrsim 0.2$. A determination of κ_s with 10% uncertainty requires $f_{B_s}\hat{B}_{B_s}^{1/2}$ with 5% accuracy, i.e., the corresponding error in (123) has to be reduced by a factor of 2.

Since our discussion does not refer to a specific model of NP, the question arises whether there are actually extensions of the SM that still allow large CP-violating NP phases in B_s^0–$\bar{B}_s^0$ mixing. This is in fact the case, also after the measurement of ΔM_s. In Ref. [101], where also a comprehensive guide to the relevant literature can be found, this exciting feature was illustrated by considering models with an extra Z' boson and SUSY scenarios with an approximate alignment of quark and squark masses.

Let us now continue our discussion of the B_s-meson system by having a closer look at other benchmark processes.

[4]The closed lines agree with those shown in the right panel of Fig. 31, as our 2010 scenario is based on the (HP+JL)QCD lattice results.

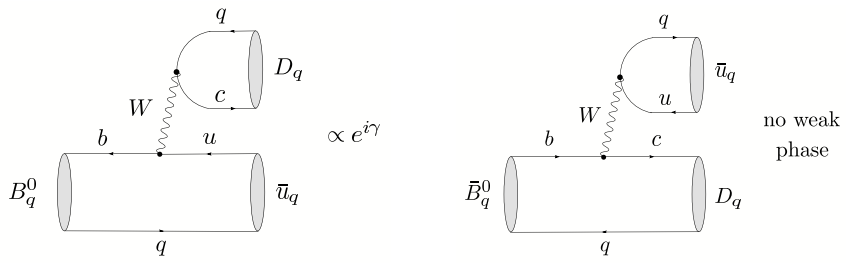

Fig. 35: Feynman diagrams contributing to $B_q^0 \to D_q\bar{u}_q$ and $\bar{B}_q^0 \to D_q\bar{u}_q$ decays

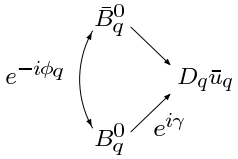

Fig. 36: Interference effects between $B_q^0 \to D_q\bar{u}_q$ and $\bar{B}_q^0 \to D_q\bar{u}_q$ decays

10.3 $B_s \to D_s^{\pm}K^{\mp}$ and $B_d \to D^{\pm}\pi^{\mp}$

The decays $B_s \to D_s^{\pm}K^{\mp}$ [249] and $B_d \to D^{\pm}\pi^{\mp}$ [250] can be treated on the same theoretical basis, and provide new strategies to determine γ [90]. Following this paper, we write these modes, which are pure 'tree' decays according to the classification of Section 3.3.1, generically as $B_q \to D_q\bar{u}_q$. As can be seen from the Feynman diagrams in Fig. 35, their characteristic feature is that both a B_q^0 and a $\bar{B}_q^0$ meson may decay into the same final state $D_q\bar{u}_q$. Consequently, as illustrated in Fig. 36, interference effects between B_q^0–$\bar{B}_q^0$ mixing and decay processes arise, which allow us to probe the weak phase $\phi_q+\gamma$ through measurements of the corresponding time-dependent decay rates.

In the case of $q = s$, i.e., $D_s \in \{D_s^+, D_s^{*+}, ...\}$ and $u_s \in \{K^+, K^{*+}, ...\}$, these interference effects are governed by a hadronic parameter $X_s e^{i\delta_s} \propto R_b \approx 0.4$, where $R_b \propto |V_{ub}/V_{cb}|$ is the usual UT side, and hence are large. On the other hand, for $q = d$, i.e., $D_d \in \{D^+, D^{*+}, ...\}$ and $u_d \in \{\pi^+, \rho^+, ...\}$, the interference effects are described by $X_d e^{i\delta_d} \propto -\lambda^2 R_b \approx -0.02$, and hence are tiny. In the following, we shall only consider $B_q \to D_q\overline{u}_q$ modes, where at least one of the D_q, $\bar{u}_q$ states is a pseudoscalar meson; otherwise a complicated angular analysis has to be performed.

The time-dependent rate asymmetries of these decays take the same form as (152). It is well known that they allow a *theoretically clean* determination of $\phi_q + \gamma$, where the 'conventional' approach works as follows [249, 250]: if we measure the observables $C(B_q \to D_q\bar{u}_q) \equiv C_q$ and $C(B_q \to \bar{D}_q u_q) \equiv \overline{C}_q$ provided by the $\cos(\Delta M_q t)$ pieces, we may determine the following quantities:

$$\langle C_q\rangle_+ \equiv \frac{1}{2}\left[\overline{C}_q + C_q\right] = 0, \quad \langle C_q\rangle_- \equiv \frac{1}{2}\left[\overline{C}_q - C_q\right] = \frac{1-X_q^2}{1+X_q^2}\,, \tag{319}$$

where $\langle C_q\rangle_-$ allows us to extract X_q. However, to this end we have to resolve terms entering at the X_q^2 level. In the case of $q = s$, we have $X_s = \mathcal{O}(R_b)$, implying $X_s^2 = \mathcal{O}(0.16)$, so that this should actually be possible, though challenging. On the other hand, $X_d = \mathcal{O}(-\lambda^2 R_b)$ is doubly Cabibbo-suppressed. Although it should be possible to resolve terms of $\mathcal{O}(X_d)$, this will be impossible for the vanishingly small $X_d^2 = \mathcal{O}(0.0004)$ terms, so that other approaches to fix X_d are required [250]. For the extraction of $\phi_q+\gamma$, the mixing-induced observables $S(B_q \to D_q\bar{u}_q) \equiv S_q$ and $S(B_q \to \bar{D}_q u_q) \equiv \overline{S}_q$ associated with the $\sin(\Delta M_q t)$ terms of the time-dependent rate asymmetry must be measured. In analogy to (319), it is convenient to introduce observable combinations $\langle S_q\rangle_\pm$. Assuming that X_q is known, we may consider the quantities

$$s_+ \equiv (-1)^L \left[\frac{1+X_q^2}{2X_q}\right] \langle S_q\rangle_+ = +\cos\delta_q \sin(\phi_q+\gamma) \tag{320}$$

$$s_- \equiv (-1)^L \left[\frac{1+X_q^2}{2X_q}\right] \langle S_q\rangle_- = -\sin\delta_q \cos(\phi_q+\gamma)\,, \tag{321}$$

which yield

$$\sin^2(\phi_q+\gamma) = \frac{1}{2}\left[(1+s_+^2-s_-^2) \pm \sqrt{(1+s_+^2-s_-^2)^2-4s_+^2}\right], \tag{322}$$

implying an eightfold solution for $\phi_q+\gamma$. If we fix the sign of $\cos\delta_q$ through factorization, still a fourfold discrete ambiguity is left, which is limiting the power for the search of NP significantly. Note that this assumption allows us also to fix the sign of $\sin(\phi_q+\gamma)$ through $\langle S_q\rangle_+$. To this end, the factor $(-1)^L$, where L is the $D_q\bar{u}_q$ angular momentum, has to be properly taken into account. This is a crucial issue for the extraction of the sign of $\sin(\phi_d+\gamma)$ from $B_d \to D^{*\pm}\pi^{\mp}$ decays.

Let us now discuss new strategies to explore CP violation through $B_q \to D_q\bar{u}_q$ modes, following Ref. [90]. If $\Delta\Gamma_s$ is sizeable, the 'untagged' rates introduced in (149) allow us to measure $\mathcal{A}_{\Delta\Gamma}(B_s \to D_s\bar{u}_s) \equiv \mathcal{A}_{\Delta\Gamma_s}$ and $\mathcal{A}_{\Delta\Gamma}(B_s \to \bar{D}_s u_s) \equiv \overline{\mathcal{A}}_{\Delta\Gamma_s}$. Introducing, in analogy to (319), observable combinations $\langle\mathcal{A}_{\Delta\Gamma_s}\rangle_\pm$, we may derive the relations

$$\tan(\phi_s+\gamma) = -\left[\frac{\langle S_s\rangle_+}{\langle\mathcal{A}_{\Delta\Gamma_s}\rangle_+}\right] = +\left[\frac{\langle\mathcal{A}_{\Delta\Gamma_s}\rangle_-}{\langle S_s\rangle_-}\right], \tag{323}$$

which allow an *unambiguous* extraction of $\phi_s+\gamma$ if we fix the sign of $\cos\delta_q$ through factorization. Another important advantage of (323) is that we do *not* have to rely on $\mathcal{O}(X_s^2)$ terms, as $\langle S_s\rangle_\pm$ and $\langle\mathcal{A}_{\Delta\Gamma_s}\rangle_\pm$ are proportional to X_s. On the other hand, a sizeable value of $\Delta\Gamma_s$ is of course needed.

If we keep the hadronic quantities X_q and δ_q as 'unknown', free parameters in the expressions for the $\langle S_q\rangle_\pm$, we may obtain bounds on $\phi_q+\gamma$ from

$$|\sin(\phi_q+\gamma)| \geq |\langle S_q\rangle_+|\,, \quad |\cos(\phi_q+\gamma)| \geq |\langle S_q\rangle_-|\,. \tag{324}$$

If X_q is known, stronger constraints are implied by

$$|\sin(\phi_q+\gamma)| \geq |s_+|\,, \quad |\cos(\phi_q+\gamma)| \geq |s_-|\,. \tag{325}$$

Once s_+ and s_- are known, we may of course determine $\phi_q+\gamma$ through the 'conventional' approach, using (322). However, the bounds following from (325) provide essentially the same information and are much simpler to implement. Moreover, as discussed in detail in Ref. [90] for several examples within the SM, the bounds following from the B_s and B_d modes may be highly complementary, thereby providing particularly narrow, theoretically clean ranges for γ.

Let us now further exploit the complementarity between the $B_s^0 \to D_s^{(*)+}K^-$ and $B_d^0 \to D^{(*)+}\pi^-$ processes. Looking at the corresponding decay topologies, we see that these channels are related to each other through an interchange of all down and strange quarks. Consequently, applying again the U-spin symmetry implies $a_s = a_d$ and $\delta_s = \delta_d$, where $a_s \equiv X_s/R_b$ and $a_d \equiv -X_d/(\lambda^2 R_b)$ are the ratios of the hadronic matrix elements entering X_s and X_d, respectively. There are various possibilities to implement these relations [90]. A particularly simple picture arises if we assume that $a_s = a_d$ *and* $\delta_s = \delta_d$, which yields

$$\tan\gamma = -\left[\frac{\sin\phi_d - S\sin\phi_s}{\cos\phi_d - S\cos\phi_s}\right] \stackrel{\phi_s=0^\circ}{=} -\left[\frac{\sin\phi_d}{\cos\phi_d - S}\right]. \tag{326}$$

Here we have introduced

$$S \equiv -R \left[\frac{\langle S_d\rangle_+}{\langle S_s\rangle_+}\right] \tag{327}$$

with

$$R \equiv \left(\frac{1-\lambda^2}{\lambda^2}\right)\left[\frac{1}{1+X_s^2}\right] , \tag{328}$$

where R can be fixed with the help of untagged B_s rates through

$$R = \left(\frac{f_K}{f_\pi}\right)^2 \left[\frac{\Gamma(\bar{B}_s^0 \to D_s^{(*)+}\pi^-) + \Gamma(B_s^0 \to D_s^{(*)-}\pi^+)}{\langle\Gamma(B_s \to D_s^{(*)+}K^-)\rangle + \langle\Gamma(B_s \to D_s^{(*)-}K^+)\rangle}\right] . \tag{329}$$

Alternatively, we can *only* assume that $\delta_s = \delta_d$ *or* that $a_s = a_d$ [90]. An important feature of this strategy is that it allows us to extract an *unambiguous* value of γ, which is crucial for the search of NP; first studies for LHCb are very promising in this respect [251]. Another advantage with respect to the 'conventional' approach is that X_q^2 terms have not to be resolved experimentally. In particular, X_d does *not* have to be fixed, and X_s may only enter through a $1+X_s^2$ correction, which can straightforwardly be determined through untagged B_s rate measurements. In the most refined implementation of this strategy, the measurement of X_d/X_s would only be interesting for the inclusion of U-spin-breaking corrections in a_d/a_s. Moreover, we may obtain interesting insights into hadron dynamics and U-spin breaking.

The colour-suppressed counterparts of the $B_q \to D_q\bar{u}_q$ modes are also interesting for the exploration of CP violation. In the case of the $B_d \to DK_{\rm S(L)}$, $B_s \to D\eta^{(\prime)}, D\phi$, ... modes, the interference effects between B_q^0–$\bar{B}_q^0$ mixing and decay processes are governed by $x_{f_s}e^{i\delta_{f_s}} \propto R_b$. If we consider the CP eigenstates $D_\pm$ of the neutral D-meson system, we obtain additional interference effects at the amplitude level, which involve γ, and may introduce the following 'untagged' rate asymmetry [153]:

$$\Gamma_{+-}^{f_s} \equiv \frac{\langle\Gamma(B_q \to D_+f_s)\rangle - \langle\Gamma(B_q \to D_-f_s)\rangle}{\langle\Gamma(B_q \to D_+f_s)\rangle + \langle\Gamma(B_q \to D_-f_s)\rangle} , \tag{330}$$

which allows us to constrain γ through the relation

$$|\cos\gamma| \geq |\Gamma_{+-}^{f_s}| . \tag{331}$$

Moreover, if we complement $\Gamma_{+-}^{f_s}$ with

$$\langle S_{f_s}\rangle_\pm \equiv \frac{1}{2}\left[S_+^{f_s} \pm S_-^{f_s}\right] , \tag{332}$$

where $S_\pm^{f_s} \equiv \mathcal{A}_{\rm CP}^{\rm mix}(B_q \to D_\pm f_s)$, we may derive the following simple but *exact* relation:

$$\tan\gamma\cos\phi_q = \left[\frac{\eta_{f_s}\langle S_{f_s}\rangle_+}{\Gamma_{+-}^{f_s}}\right] + \left[\eta_{f_s}\langle S_{f_s}\rangle_- - \sin\phi_q\right] , \tag{333}$$

with $\eta_{f_s} \equiv (-1)^L\eta_{\rm CP}^{f_s}$. This expression allows a conceptually simple, theoretically clean and essentially unambiguous determination of γ [153]. Since the interference effects are governed by the tiny parameter $x_{f_d}e^{i\delta_{f_d}} \propto -\lambda^2R_b$ in the case of $B_s \to D_\pm K_{\rm S(L)}$, $B_d \to D_\pm\pi^0, D_\pm\rho^0, ...$, these modes are not as interesting for the extraction of γ. However, they provide the relation

$$\eta_{f_d}\langle S_{f_d}\rangle_- = \sin\phi_q + \mathcal{O}(x_{f_d}^2) = \sin\phi_q + \mathcal{O}(4\times10^{-4}) , \tag{334}$$

allowing very interesting determinations of ϕ_q with theoretical accuracies one order of magnitude higher than those of the conventional $B_d^0 \to J/\psi K_{\rm S}$ and $B_s^0 \to J/\psi\phi$ approaches [153]. As we pointed out in Section 7.1, these measurements would be very interesting in view of the new world average of $(\sin 2\beta)_{\psi K_{\rm S}}$.

10.4 $B_s^0 \to K^+K^-$ and $B_d^0 \to \pi^+\pi^-$

The decay $B_s^0 \to K^+K^-$ is a $\bar{b} \to \bar{s}$ transition, and involves tree and penguin amplitudes, as the $B_d^0 \to \pi^+\pi^-$ mode [167]. However, because of the different CKM structure, the latter topologies actually play the dominant role in the $B_s^0 \to K^+K^-$ channel. In analogy to (208), we may write

$$A(B_s^0 \to K^+K^-) = \sqrt{\epsilon}\, \mathcal{C}' \left[e^{i\gamma} + \frac{1}{\epsilon}\, d' e^{i\theta'} \right] , \tag{335}$$

where ϵ was introduced in (221), and the CP-conserving hadronic parameters $\mathcal{C}'$ and $d'e^{i\theta'}$ correspond to $\mathcal{C}$ and $de^{i\theta}$, respectively. The corresponding observables then take the following generic form:

$$\mathcal{A}_{\rm CP}^{\rm dir}(B_s \to K^+K^-) = G_1'(d', \theta'; \gamma) \tag{336}$$

$$\mathcal{A}_{\rm CP}^{\rm mix}(B_s \to K^+K^-) = G_2'(d', \theta'; \gamma, \phi_s) , \tag{337}$$

in analogy to the expressions for the CP-violating $B_d^0 \to \pi^+\pi^-$ asymmetries in (213) and (214). Since $\phi_d = (43.4 \pm 2.5)^\circ$ is already known (see Section 7.1) and ϕ_s is negligibly small in the SM—or can be determined through $B_s^0 \to J/\psi\phi$ should CP-violating NP contributions to B_s^0–$\bar{B}_s^0$ mixing make it sizeable—we may convert the measured values of $\mathcal{A}_{\rm CP}^{\rm dir}(B_d \to \pi^+\pi^-)$, $\mathcal{A}_{\rm CP}^{\rm mix}(B_d \to \pi^+\pi^-)$ and $\mathcal{A}_{\rm CP}^{\rm dir}(B_s \to K^+K^-)$, $\mathcal{A}_{\rm CP}^{\rm mix}(B_s \to K^+K^-)$ into *theoretically clean* contours in the γ–d and γ–d' planes, respectively. In Fig. 37, we show these contours for an example, which corresponds to the central values of (217) and (218) with the hadronic parameters (d, θ) in (230).

As can be seen in Fig. 26, the decay $B_d^0 \to \pi^+\pi^-$ is actually related to $B_s^0 \to K^+K^-$ through the interchange of *all* down and strange quarks. Consequently, each decay topology contributing to $B_d^0 \to \pi^+\pi^-$ has a counterpart in $B_s^0 \to K^+K^-$, and the corresponding hadronic parameters can be related to each other with the help of the U-spin flavour symmetry of strong interactions, implying the following relations [167]:

$$d' = d\,, \quad \theta' = \theta\,. \tag{338}$$

Applying the former, we may extract γ and d through the intersections of the theoretically clean γ–d and γ–d' contours. As discussed in Ref. [167], it is also possible to resolve straightforwardly the twofold ambiguity for (γ, d) arising in Fig. 37, thereby leaving us with the 'true' solution of $\gamma = 74^\circ$ in this example. Moreover, we may determine θ and θ', which allow an interesting internal consistency check of the second U-spin relation in (338). An alternative avenue is provided if we eliminate d and d' through the CP-violating $B_d \to \pi^+\pi^-$ and $B_s \to K^+K^-$ observables, respectively, and then extract these parameters and γ through the U-spin relation $\theta' = \theta$.

As illustrated in Fig. 38, this strategy is very promising from an experimental point of view for the LHCb experiment, where an accuracy for γ of a few degrees can be achieved [147, 232, 252]. As far as possible U-spin-breaking corrections to $d' = d$ are concerned, they enter the determination of γ through a relative shift of the γ–d and γ–d' contours; their impact on the extracted value of γ therefore depends on the form of these curves, which is fixed through the measured observables. In the examples discussed in Refs. [119, 167], as well as in the one shown in Fig. 37, the extracted value of γ would be very stable under such effects. Let us also note that the U-spin relations in (338) are particularly robust since they involve only ratios of hadronic amplitudes, where all $SU(3)$-breaking decay constants and form factors cancel in factorization and also chirally enhanced terms would not lead to U-spin-breaking corrections [167]. On the other hand, the ratio $|\mathcal{C}'/\mathcal{C}|$, which equals 1 in the strict U-spin limit and enters the U-spin relation

$$\frac{\mathcal{A}_{\rm CP}^{\rm mix}(B_s \to K^+K^-)}{\mathcal{A}_{\rm CP}^{\rm dir}(B_d \to \pi^+\pi^-)} = -\left|\frac{\mathcal{C}'}{\mathcal{C}}\right|^2 \left[\frac{\rm BR(B_d \to \pi^+\pi^-)}{\rm BR(B_s \to K^+K^-)}\right] \frac{\tau_{B_s}}{\tau_{B_d}} , \tag{339}$$

is affected by U-spin-breaking effects within factorization. An estimate of the corresponding form factors was recently performed in Ref. [253] with the help of QCD sum rules, which is an important ingredient

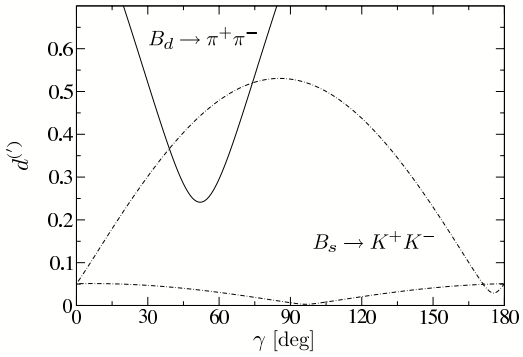

Fig. 37: The contours in the γ–$d^{(\prime)}$ plane for an example with $d = d' = 0.52$, $\theta = \theta' = 146°$, $\phi_d = 43.4°$, $\phi_s = -2°$, $\gamma = 74°$, which corresponds to the CP asymmetries $\mathcal{A}_{\rm CP}^{\rm dir}(B_d \to \pi^+\pi^-) = -0.37$ and $\mathcal{A}_{\rm CP}^{\rm mix}(B_d \to \pi^+\pi^-) = +0.50$ (see Sections 7.3 and 8.2), as well as $\mathcal{A}_{\rm CP}^{\rm dir}(B_s \to K^+K^-) = +0.12$ and $\mathcal{A}_{\rm CP}^{\rm mix}(B_s \to K^+K^-) = -0.19$.

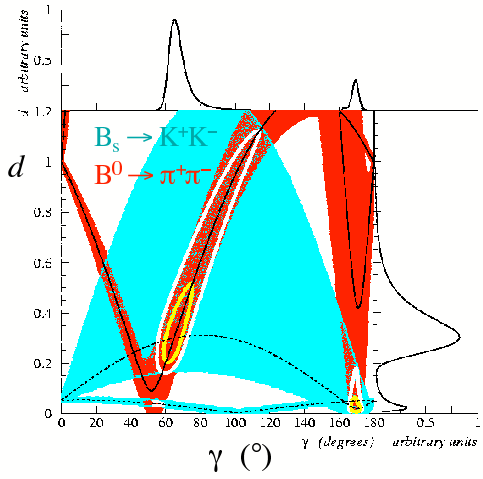

Fig. 38: Experimental LHCb feasibility study for the contours in the γ–$d^{(\prime)}$ plane, as discussed in Ref. [252]

for a SM prediction of the CP-averaged $B_s \to K^+K^-$ branching ratio [83]. Following these lines, the prediction

$$\text{BR}(B_s \to K^+K^-) = (35 \pm 7) \times 10^{-6} \tag{340}$$

was obtained in Refs. [83, 200] from the CP-averaged $B_d \to \pi^\mp K^\pm$ branching ratio. On the other hand, the CDF Collaboration announced recently the observation of the $B_s \to K^+K^-$ channel, with the following branching ratio [254]:

$$\text{BR}(B_s \to K^+K^-) = (33 \pm 5.7 \pm 6.7) \times 10^{-6}\,, \tag{341}$$

which is in excellent accordance with (340). For other recent analyses of the $B_s \to K^+K^-$ decay, see Refs. [255, 256].

In addition to the $B_s \to K^+K^-$, $B_d \to \pi^+\pi^-$ and $B_s \to D_s^\pm K^\mp$, $B_d \to D^\pm\pi^\mp$ strategies discussed above, other U-spin methods for the extraction of γ were also proposed, using $B_{s(d)} \to J/\psi K_{\rm S}$ or $B_{d(s)} \to D_{d(s)}^+ D_{d(s)}^-$ [142], $B_{d(s)} \to K^{0(*)}\bar{K}^{0(*)}$ [119, 244], $B_{(s)} \to \pi K$ [257], or $B_{s(d)} \to J/\psi\eta$ modes [258]. In a very recent paper [259], two-body decays of charged B mesons were also considered.

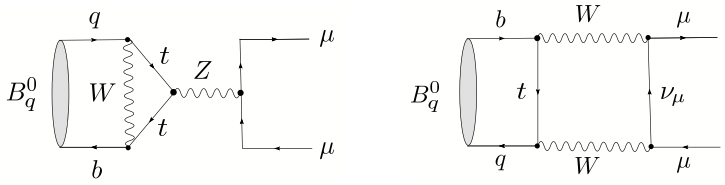

Fig. 39: Feynman diagrams contributing to $B_q^0 \to \mu^+\mu^-$ ($q \in \{s, d\}$)

10.5 $B_s^0 \to \mu^+\mu^-$ and $B_d^0 \to \mu^+\mu^-$

Let us finally have a closer look at the rare decay $B_s^0 \to \mu^+\mu^-$, which we already encountered briefly in Section 8.4. As can be seen in Fig. 39, this decay and its B_d-meson counterpart $B_d^0 \to \mu^+\mu^-$ originate from Z^0-penguin and box diagrams in the SM. The corresponding low-energy effective Hamiltonian is given as follows [67]:

$$\mathcal{H}_{\rm eff} = -\frac{G_{\rm F}}{\sqrt{2}}\left[\frac{\alpha}{2\pi\sin^2\Theta_{\rm W}}\right] V_{tb}^* V_{tq}\eta_Y Y_0(x_t)(\bar{b}q)_{\rm V-A}(\bar{\mu}\mu)_{\rm V-A} + \text{h.c.}\,, \tag{342}$$

where α denotes the QED coupling and $\Theta_{\rm W}$ is the Weinberg angle. The short-distance physics is described by $Y(x_t) \equiv \eta_Y Y_0(x_t)$, where $\eta_Y = 1.012$ is a perturbative QCD correction [260]– [262], and the Inami–Lim function $Y_0(x_t)$ describes the top-quark mass dependence. We observe that only the matrix element $\langle 0|(\bar{b}q)_{\rm V-A}|B_q^0\rangle$ is required. Since here the vector-current piece vanishes, as the B_q^0 is a pseudoscalar meson, this matrix element is simply given by the decay constant f_{B_q}. Consequently, we arrive at a very favourable situation with respect to the hadronic matrix elements. Since, moreover, NLO QCD corrections were calculated, and long-distance contributions are expected to play a negligible role [260], the $B_q^0 \to \mu^+\mu^-$ modes belong to the cleanest rare B decays. The SM branching ratios can then be written in the following compact form [37]:

$$\begin{aligned}\text{BR}(B_s \to \mu^+\mu^-) &= 4.1\times 10^{-9} \\ &\times \left[\frac{f_{B_s}}{0.24\,\text{GeV}}\right]^2\left[\frac{|V_{ts}|}{0.040}\right]^2\left[\frac{\tau_{B_s}}{1.5\,\text{ps}}\right]\left[\frac{m_t}{167\,\text{GeV}}\right]^{3.12}\end{aligned} \tag{343}$$

$$\begin{aligned}\text{BR}(B_d \to \mu^+\mu^-) &= 1.1\times 10^{-10} \\ &\times \left[\frac{f_{B_d}}{0.20\,\text{GeV}}\right]^2\left[\frac{|V_{td}|}{0.008}\right]^2\left[\frac{\tau_{B_d}}{1.5\,\text{ps}}\right]\left[\frac{m_t}{167\,\text{GeV}}\right]^{3.12}\end{aligned} \tag{344}$$

The most recent upper bounds (95% C.L.) from the CDF Collaboration read as follows [263]:

$$\text{BR}(B_s \to \mu^+\mu^-) < 1.0\times 10^{-7}, \quad \text{BR}(B_d \to \mu^+\mu^-) < 3.0\times 10^{-8}\,, \tag{345}$$

while the D0 Collaboration finds the following (95% C.L.) upper limit [264]:

$$\text{BR}(B_s \to \mu^+\mu^-) < 3.7\times 10^{-7}\,. \tag{346}$$

Using again relation (310) and neglecting the tiny corrections entering at the λ^2 level, we find that the measurement of the ratio

$$\frac{\text{BR}(B_d \to \mu^+\mu^-)}{\text{BR}(B_s \to \mu^+\mu^-)} = \left[\frac{\tau_{B_d}}{\tau_{B_s}}\right]\left[\frac{M_{B_d}}{M_{B_s}}\right]\left[\frac{f_{B_d}}{f_{B_s}}\right]^2\left|\frac{V_{td}}{V_{ts}}\right|^2 \tag{347}$$

would allow an extraction of the UT side R_t. Since the short-distance function Y cancels, this determination works not only in the SM, but also in the NP scenarios with MFV [137]. This strategy is complementary to that offered by the ratio $\Delta M_s/\Delta M_d$ discussed in the context of (306). If we look

at this expression in the MFV case, where $\rho_s/\rho_d = 1$, and (347), we see that the following relation is implied [265]:

$$\frac{\mathrm{BR}(B_s \to \mu^+\mu^-)}{\mathrm{BR}(B_d \to \mu^+\mu^-)} = \left[\frac{\tau_{B_s}}{\tau_{B_d}}\right]\left[\frac{\hat{B}_{B_d}}{\hat{B}_{B_s}}\right]\left[\frac{\Delta M_s}{\Delta M_d}\right] , \tag{348}$$

which holds again in the context of MFV models, including the SM. Here the advantage is that the dependence on $(f_{B_d}/f_{B_s})^2$ cancels. Moreover, we may also use the data for the mass differences ΔM_q to reduce the hadronic uncertainties of the SM predictions of the $B_q \to \mu^+\mu^-$ branching ratios [265]:

$$\mathrm{BR}(B_s \to \mu^+\mu^-) = (3.35 \pm 0.32) \times \times 10^{-9} \tag{349}$$

$$\mathrm{BR}(B_d \to \mu^+\mu^-) = (1.03 \pm 0.09) \times 10^{-10} , \tag{350}$$

where (349) is another application of the recent ΔM_s measurement at the Tevatron [237].

The current experimental upper bounds in (345) and (346) are still about two orders of magnitude away from these numbers. Consequently, should the $B_q \to \mu^+\mu^-$ decays be governed by their SM contributions, we could only hope to observe them at the LHC [147]. On the other hand, since the $B_q \to \mu^+\mu^-$ transitions originate from FCNC processes, they are sensitive probes of NP. In particular, the branching ratios may be dramatically enhanced in specific NP (SUSY) scenarios, as was recently reviewed in Ref. [118]. Should this actually be the case, these decays may already be seen at Run II of the Tevatron, and the e^+e^- B factories could observe $B_d \to \mu^+\mu^-$. Let us finally emphasize that the experimental bounds on $B_s \to \mu^+\mu^-$ can also be converted into bounds on NP parameters in specific scenarios. In the context of the constrained minimal supersymmetric extension of the SM (CMSSM) with universal scalar masses, such constraints were recently critically discussed by the authors of Ref. [266].

11 Conclusions and outlook

CP violation is now well established in the B-meson system, thereby complementing the neutral K-meson system, where this phenomenon was discovered more than 40 years ago. The data of the e^+e^- B factories have provided valuable insights into the physics of strong and weak interactions. Concerning the former aspect, which is sometimes only considered as a by-product, the data give us important evidence for large non-factorizable effects in non-leptonic B-decays, so that the challenge for a reliable theoretical description within dynamical QCD approaches remains, despite interesting recent progress. As far as the latter aspect is concerned, the description of CP violation through the KM mechanism has successfully passed its first experimental tests, in particular through the comparison between the measurement of $\sin 2\beta$ with the help of $B_d^0 \to J/\psi K_{\rm S}$ and the CKM fits. However, the most recent average for $(\sin 2\beta)_{\psi K_{\rm S}}$ is now somewhat on the lower side, and there are a couple of puzzles in the B-factory data. It will be very interesting to monitor these effects, which could be first hints for physics beyond the SM, as the data improve. Moreover, it is crucial to refine the corresponding theoretical analyses further, to have a critical look at the underlying working assumptions and to check them through independent tests, and to explore correlations with other flavour probes.

Despite this impressive progress, there are still regions of the B-physics landscape left that are essentially unexplored. For instance, $b \to d$ penguin processes are now entering the stage, since lower bounds for the corresponding branching ratios that can be derived in the SM turn out to be very close to the corresponding experimental upper limits. Indeed, we have now evidence for the $B_d \to K^0\bar{K}^0$ and $B^\pm \to K^\pm K$ channels, and the first signals for the radiative $B \to \rho\gamma$ transitions were reported, representing one of the hot topics of the summer of 2005. These modes have now to be explored in much more detail, and several other decays are waiting to be observed.

Another very interesting aspect of future studies is the B_s-meson system. Although the mass difference ΔM_s was measured in the spring of 2006 at the Tevatron, many features of B_s physics are still essentially unexplored. Concerning the measurement of ΔM_s, NP may actually be hiding in this

quantity, but is currently obscured by parameter uncertainties. The smoking-gun signal for NP in B_s^0–$\bar{B}_s^0$ mixing would be the observation of sizeable CP violation in $B_s^0 \to J/\psi\phi$ and similar decays. Since there are various specific extensions of the SM where such effects arise (also when taking the ΔM_s constraints into account), we may hope that the LHC will detect them. Moreover, the B_s-meson system allows several determinations of the angle γ of the UT in an essentially unambiguous way, which are another key ingredient for the search of NP, and offers further tests of the SM through strongly suppressed rare decays. After new results from Run II of the Tevatron, the promising physics potential of the B_s-meson system can be fully exploited at the LHC, in particular by the LHCb experiment.

These studies can be nicely complemented through the kaon system, which governed the stage of CP violation for more than 35 years. The future lies now in rare decays, in particular on the $K^+ \to \pi^+\nu\bar{\nu}$ and $K_{\rm L} \to \pi^0\nu\bar{\nu}$ modes; there is a proposal to measure the former channel at the CERN SPS, and efforts to explore the latter at KEK/J-PARC in Japan. Furthermore, flavour physics offers several other exciting topics. Important examples are top-quark physics, the D-meson system, the anomalous magnetic moment of the muon, electric dipole moments and flavour violation in the charged lepton and neutrino sectors.

The established neutrino oscillations as well as the evidence for dark matter and the baryon asymmetry of the Universe tell us that the SM is incomplete, and specific extensions usually contain also new sources of flavour and CP violation, which may manifest themselves at the flavour factories. Fortunately, the LHC is expected to go into operation in the autumn of 2007. This new accelerator will provide insights into electroweak symmetry breaking and, we hope, also give us direct evidence for physics beyond the SM through the production and subsequent decays of NP particles in the ATLAS and CMS detectors. It is obvious that there should be a very fruitful interplay between these 'direct' studies of NP, and the 'indirect' information provided by flavour physics[5]. I have no doubt that an exciting future is ahead of us!

Acknowledgements

I would like to thank the students for their interest in my lectures, the discussion leaders for their efforts to complement them in the discussion sessions, and the local organizers for hosting this exciting School in Kitzbühel. I am also grateful to my collaborators for the fun we had working on many of the topics addressed in these lectures.

References

[1] J.H. Christenson *et al.*, Phys. Rev. Lett. **13** (1964) 138.

[2] V. Fanti *et al.* [NA48 Collaboration], Phys. Lett. **B465** (1999) 335;
A. Alavi-Harati *et al.* [KTeV Collaboration], Phys. Rev. Lett. **83** (1999) 22.

[3] J.R. Batley *et al.* [NA48 Collaboration], Phys. Lett. **B544** (2002) 97.

[4] A. Alavi-Harati *et al.* [KTeV Collaboration], Phys. Rev. **D67** (2003) 012005.

[5] B. Aubert *et al.* [BaBar Collaboration], Phys. Rev. Lett. **87** (2001) 091801;
K. Abe *et al.* [Belle Collaboration], Phys. Rev. Lett. **87** (2001) 091802.

[6] B. Aubert *et al.* [BaBar Collaboration], Phys. Rev. Lett. **93** (2004) 131801;
Y. Chao *et al.* [Belle Collaboration], Phys. Rev. Lett. **93** (2004) 191802.

[7] A.D. Sakharov, JETP Lett. **5** (1967) 24.

[8] V.A. Rubako and M.E. Shaposhnikov, Usp. Fiz. Nauk **166** (1996) 493; Phys. Usp. **39** (1996) 461;
A. Riotto and M. Trodden, Annu. Rev. Nucl. Part. Sci. **49** (1999) 35.

[9] For a recent review, see W. Buchmüller, R.D. Peccei and T. Yanagida, Annu. Rev. Nucl. Part. Sci. **55** (2005) 311.

[5] This topic is currently addressed in detail within a CERN workshop: `http://cern.ch/flavlhc`.

[10] N. Cabibbo, Phys. Rev. Lett. **10** (1963) 531.

[11] M. Kobayashi and T. Maskawa, Prog. Theor. Phys. **49** (1973) 652.

[12] M. Battaglia *et al.*, *The CKM Matrix and the Unitarity Triangle*, CERN 2003-002-corr. (CERN, Geneva, 2003) [hep-ph/0304132].

[13] For a recent review, see A.J. Buras and M. Jamin, JHEP **0401** (2004) 048.

[14] L. Wolfenstein, Phys. Rev. Lett. **13** (1964) 562.

[15] M. Jeitler, lecture given at this school, see these proceedings.

[16] L. Widhalm, lecture given at this school, see these proceedings.

[17] A.J. Buras and R. Fleischer, Adv. Ser. Direct. High Energy Phys. **15** (1998) 65.

[18] G. Branco, L. Lavoura and J. Silva, *CP Violation*, International Series of Monographs on Physics 103, Oxford Science Publications (Clarendon Press, Oxford, 1999).

[19] I.I. Bigi and A. I. Sanda, *CP Violation*, Cambridge Monographs on Particle Physics, Nuclear Physics and Cosmology (Cambridge University Press, Cambridge, 2000).

[20] K. Kleinknecht, Springer Tracts Mod. Phys. **195** (2003) 1.

[21] T. Mannel, Springer Tracts Mod. Phys. **203** (2004) 1.

[22] Y. Nir, hep-ph/0510413, lectures given at 3rd CERN–CLAF School of High Energy Physics, Malarguee, Mendoza, Argentina, 27 February to 12 March 2005.

[23] A.J. Buras, hep-ph/0505175, lectures given at 2004 European School of High-Energy Physics, Sant Feliu de Guíxols, Barcelona, Spain, 2004, R. Fleischer (Ed.), CERN-2006-003 (CERN, Geneva, 2006), p. 95.

[24] A. Ali, Int. J. Mod. Phys. **A20** (2005) 5080.

[25] M. Gronau, Nucl. Phys. Proc. Suppl. **156** (2006) 69.

[26] A. Höcker and Z. Ligeti, hep-ph/0605217.

[27] W. Buchmüller, lecture given at this school, see these proceedings.

[28] S.L. Glashow, Nucl. Phys. **22** (1961) 579;
S. Weinberg, Phys. Rev. Lett. **19** (1967) 1264;
A. Salam, in *Elementary Particle Theory*, Ed. N. Svartholm (Almqvist and Wiksell, Stockholm, 1968).

[29] S.L. Glashow, J. Iliopoulos and L. Maiani, Phys. Rev. **D2** (1970) 1285.

[30] S. Eidelman *et al.* [Particle Data Group], Phys. Lett. **B592** (2004) 1.

[31] H. Fritzsch and Z.-Z. Xing, Phys. Lett. **B413** (1997) 396.

[32] C. Jarlskog, Phys. Rev. Lett. **55** (1985) 1039; Z. Phys. **C29** (1985) 491.

[33] J. Bernabeu, G. Branco and M. Gronau, Phys. Lett. **B169** (1986) 243.

[34] J. Ellis, lecture given at this school (unpublished).

[35] L. Wolfenstein, Phys. Rev. Lett. **51** (1983) 1945.

[36] A.J. Buras, M.E. Lautenbacher and G. Ostermaier, Phys. Rev. **D50** (1994) 3433.

[37] A.J. Buras, hep-ph/0101336, lectures given at Erice International School of Subnuclear Physics: Theory and Experiment Heading for New Physics, Erice, Italy, 27 August to 5 September 2000.

[38] R. Aleksan, B. Kayser and D. London, Phys. Rev. Lett. **73** (1994) 18.

[39] C. Jarlskog and R. Stora, Phys. Lett. **B208** (1988) 268.

[40] L.L. Chau and W.-Y. Keung, Phys. Rev. Lett. **53** (1984) 1802.

[41] J. Charles *et al.* [CKMfitter Group], Eur. Phys. J. C **41** (2005) 1; for the most recent updates, see http://ckmfitter.in2p3.fr/.

[42] M. Bona *et al.* [UTfit Collaboration], JHEP **0507** (2005) 028; for the most recent updates, see http://utfit.roma1.infn.it/.

[43] G. Ecker, lecture given at this school, hep-ph/0604165.

[44] A. Khodjamirian, lectures given at the 2003 European School of High-Energy Physics, Tsakhkadzor, Armenia, 2003, A.G. Olshevskii (Ed.), CERN-2005-007 (CERN, Geneva, 2005), p. 173. [hep-ph/0403145].

[45] M. Lüscher, Annales Henri Poincaré **4** (2003) S197 [hep-ph/0211220].

[46] C. Davies, hep-lat/0509046, lectures given at 58th Scottish Universities Summer School in Physics (SUSSP58): A NATO Advanced Study Institute and EU Hadron Physics 13 Summer Institute, St. Andrews, Scotland, 22–29 August 2004.

[47] M. Lüscher, Proceedings of Science, 23rd International Symposium on Lattice Field, Dublin, 2005, PoS **LAT2005** (2006) paper 002.

[48] F. De Fazio, hep-ph/0010007.

[49] K. Ikado *et al.* [Belle Collaboration], hep-ex/0604018.

[50] D.G. Cassel, eConf **C0304052** (2003) WG501 [hep-ex/0307038].

[51] C. Davies, plenary talk at HEP2005 Europhysics Conference, Lisbon, Portugal, 21–27 July 2005, http://www.lip.pt/events/2005/hep2005/.

[52] C. Aubin *et al.*, Phys. Rev. Lett. **95** (2005) 122002.

[53] M. Artuso *et al.* [CLEO Collaboration], Phys. Rev. Lett. **95** (2005) 251801.

[54] N. Isgur and M.B. Wise, Phys. Lett. **B232** (1989) 113 and **B237** (1990) 527.

[55] M. Neubert, Phys. Rep. **245** (1994) 259.

[56] *The BaBar Physics Book*, eds. P. Harrison and H.R. Quinn, SLAC-R-504 (1998).

[57] M. Neubert, Phys. Lett. **B264** (1991) 455.

[58] M.E. Luke, Phys. Lett. **B252** (1990) 447.

[59] P. Gambino and N. Uraltsev, Eur. Phys. J. **C34** (2004) 181.

[60] O. Buchmüller and H. Flächer, Phys. Rev. **D73** (2006) 073008.

[61] Heavy Flavour Averaging Group [E. Barberio *et al.*], hep-ex/0603003;
online updates: http://www.slac.stanford.edu/xorg/hfag.

[62] M. Okamoto *et al.*, Nucl. Phys. Proc. Suppl. **140** (2005) 461;
E. Gulez *et al.*, Phys. Rev. **D73** (2006) 074502.

[63] A. Khodjamirian *et al.*, Phys. Rev. **D62** (2000) 114002;
P. Ball and R. Zwicky, JHEP **0110** (2001) 019; Phys. Rev. **D71** (2005) 014015; Phys. Rev. **D71** (2005) 014029; Phys. Lett. **B625** (2005) 225.

[64] E. Blucher *et al.*, hep-ph/0512039.

[65] F.J. Gilman and M.B. Wise, Phys. Rev. **D20** (1979) 2392;
G. Altarelli, G. Curci, G. Martinelli and S. Petrarca, Phys. Lett. **B99** (1981) 141;
A.J. Buras and P.H. Weisz, Nucl. Phys. **B333** (1990) 66.

[66] G. Buchalla, A.J. Buras and M.E. Lautenbacher, Rev. Mod. Phys. **68** (1996) 1125.

[67] A.J. Buras, hep-ph/9806471, lectures given at Summer School on Theoretical Physics: Probing the Standard Model of Particle Interactions, Les Houches, France, 28 July–5 September 1997.

[68] M. Bander, D. Silverman and A. Soni, Phys. Rev. Lett. **43** (1979) 242.

[69] R. Fleischer, Z. Phys. **C58** (1993) 483.

[70] A.J. Buras and R. Fleischer, Phys. Lett. **B341** (1995) 379.

[71] M. Ciuchini, E. Franco, G. Martinelli, M. Pierini and L. Silvestrini, Phys. Lett. **B515** (2001) 33;
C. Isola, M. Ladisa, G. Nardulli, T.N. Pham and P. Santorelli, Phys. Rev. **D65** (2002) 094005;
C.W. Bauer, D. Pirjol, I.Z. Rothstein and I.W. Stewart, Phys. Rev. **D70** (2004) 054015.

[72] R. Fleischer, Z. Phys. **C62** (1994) 81; Phys. Lett. **B321** (1994) 259 and **B332** (1994) 419.

[73] R. Fleischer, Int. J. Mod. Phys. **A12** (1997) 2459.

[74] N.G. Deshpande and X.-G. He, Phys. Rev. Lett. **74** (1995) 26 [E: ibid., p. 4099];
M. Gronau, O.F. Hernandez, D. London and J.L. Rosner, Phys. Rev. **D52** (1995) 6374.

[75] M. Neubert, B. Stech, Adv. Ser. Direct. High Energy Phys. **15** (1998) 294, and references therein.

[76] A.J. Buras and J.-M. Gérard, Nucl. Phys. **B264** (1986) 371;
A.J. Buras, J.-M. Gérard and R. Rückl, Nucl. Phys. **B268** (1986) 16.

[77] M. Beneke, G. Buchalla, M. Neubert and C. Sachrajda, Phys. Rev. Lett. **83** (1999) 1914; Nucl. Phys. **B591** (2000) 313; Nucl. Phys. **B606** (2001) 245.

[78] J.D. Bjorken, Nucl. Phys. (Proc. Suppl.) **B11** (1989) 325;
M. Dugan and B. Grinstein, Phys. Lett. **B255** (1991) 583;
H.D. Politzer and M.B. Wise, Phys. Lett. **B257** (1991) 399.

[79] H.-n. Li and H.L. Yu, Phys. Rev. **D53** (1996) 2480;
Y.Y. Keum, H.-n. Li and A.I. Sanda, Phys. Lett. **B504** (2001) 6;
Y.Y. Keum and H.-n. Li, Phys. Rev. **D63** (2001) 074006;
Y.Y. Keum and A.I. Sanda, eConf **C0304052** (2003) WG420.

[80] C.W. Bauer, D. Pirjol and I.W. Stewart, Phys. Rev. Lett. **87** (2001) 201806, Phys. Rev. **D65** (2002) 054022; C.W. Bauer, S. Fleming, D. Pirjol, I.Z. Rothstein and I.W. Stewart, Phys. Rev. **D66** (2002) 014017; C.W. Bauer, B. Grinstein, D. Pirjol and I.W. Stewart, Phys. Rev. **D67** (2003) 014010.

[81] A. Khodjamirian, Nucl. Phys. **B605** (2001) 558;
A. Khodjamirian, T. Mannel and B. Melic, Phys. Lett. **B571** (2003) 75.

[82] A.J. Buras, R. Fleischer, S. Recksiegel and F. Schwab, Phys. Rev. Lett. **92** (2004) 101804.

[83] A.J. Buras, R. Fleischer, S. Recksiegel and F. Schwab, Nucl. Phys. **B697** (2004) 133.

[84] M. Gronau and D. Wyler, Phys. Lett. **B265** (1991) 172.

[85] D. Atwood, I. Dunietz, A. Soni, Phys. Rev. Lett. **78** (1997) 3257; Phys. Rev. **D63** (2001) 036005.

[86] R. Fleischer and D. Wyler, Phys. Rev. **D62** (2000) 057503.

[87] M. Gronau, J.L. Rosner and D. London, Phys. Rev. Lett. **73** (1994) 21;
M. Gronau, O.F. Hernandez, D. London and J.L. Rosner, Phys. Rev. **D50** (1994) 4529.

[88] A.B. Carter and A.I. Sanda, Phys. Rev. Lett. **45** (1980) 952; Phys. Rev. **D23** (1981) 1567;
I.I. Bigi and A.I. Sanda, Nucl. Phys. **B193** (1981) 85.

[89] G. Cavoto *et al.*, hep-ph/0603019.

[90] R. Fleischer, Nucl. Phys. **B671** (2003) 459.

[91] A.J. Buras, R. Fleischer, S. Recksiegel and F. Schwab, Eur. Phys. J. **C45** (2006) 701.

[92] F. Abe *et al.* [CDF Collaboration], Phys. Rev. Lett. **81** (1998) 2432.

[93] D0 Collaboration, D0 Note 4539-CONF (August 2004).

[94] D. Acosta *et al.* [CDF Collaboration], Phys. Rev. Lett. **96** (2006) 082002.

[95] M. Masetti, Phys. Lett. **B286** (1992) 160.

[96] M.A. Ivanov, J.G. Körner and O.N. Pakhomova, Phys. Lett. **B555** (2003) 189.

[97] T. Inami and C.S. Lim, Prog. Theor. Phys. **65** (1981) 297 [E: ibid., p. 1772].

[98] A.J. Buras, hep-ph/0307203, lectures given at 41st International University School of Theoretical Physics: Flavour Physics (IUTP 41), Schladming, Styria, Austria, 22–28 February 2003.

[99] A.J. Buras, M. Jamin and P.H. Weisz, Nucl. Phys. **B347** (1990) 491;
J. Urban, F. Krauss, U. Jentschura and G. Soff, Nucl. Phys. **B523** (1998) 40.

[100] A.A. Penin and M. Steinhauser, Phys. Rev. **D65** (2002) 054006;
M. Jamin and B.O. Lange, Phys. Rev. **D65** (2002) 056005;
K. Hagiwara, S. Narison and D. Nomura, Phys. Lett. **B540** (2002) 233.

[101] P. Ball and R. Fleischer, hep-ph/0604249.

[102] S. Aoki *et al.* [JLQCD Collaboration], Phys. Rev. Lett. **91** (2003) 212001.
[103] A. Gray *et al.* [HPQCD Collaboration], Phys. Rev. Lett. **95** (2005) 212001.
[104] M. Okamoto, Proceedings of Science, 23rd International Symposium on Lattice Field, Dublin, 2005, PoS **LAT2005** (2005) paper 013.
[105] S. Laplace, Z. Ligeti, Y. Nir and G. Perez, Phys. Rev. **D65** (2002) 094040.
[106] M. Beneke, G. Buchalla, A. Lenz and U. Nierste, Phys. Lett. **B576** (2003) 173;
M. Ciuchini, E. Franco, V. Lubicz, F. Mescia and C. Tarantino, JHEP **0308** (2003) 031.
[107] B Oscillations Working Group: `http://lepbosc.web.cern.ch/LEPBOSC/`.
[108] V. M. Abazov *et al.* [D0 Collaboration], hep-ex/0603029.
[109] A. Abulencia *et al.* [CDF Collaboration], hep-ex/0606027.
[110] A. Lenz, hep-ph/0412007.
[111] A.S. Dighe, I. Dunietz and R. Fleischer, Eur. Phys. J. **C6** (1999) 647.
[112] D. Acosta *et al.* [CDF Collaboration], Phys. Rev. Lett. **94** (2005) 101803.
[113] V.M. Abazov *et al.* [D0 Collaboration], Phys. Rev. Lett. **95** (2005) 171801.
[114] I. Dunietz, Phys. Rev. **D52** (1995) 3048.
[115] R. Fleischer and I. Dunietz, Phys. Rev. **D55** (1997) 259.
[116] R. Fleischer and I. Dunietz, Phys. Lett. **B387** (1996) 361.
[117] I. Dunietz, R. Fleischer and U. Nierste, Phys. Rev. **D63** (2001) 114015.
[118] A.J. Buras, hep-ph/0402191.
[119] R. Fleischer, Phys. Rep. **370** (2002) 537.
[120] For reviews, see, for instance, A. Ali, hep-ph/0412128;
G. Isidori, AIP Conf. Proc. **722** (2004) 181;
M. Misiak, Acta Phys. Polon. **B34** (2003) 4397.
[121] R. Fleischer and T. Mannel, Phys. Lett. **B506** (2001) 311.
[122] R. Fleischer, G. Isidori and J. Matias, JHEP **0305** (2003) 053.
[123] R. Fleischer and T. Mannel, Phys. Lett. **B511** (2001) 240.
[124] T. Goto *et al.*, Phys. Rev. **D70** (2004) 035012.
[125] S. Jäger and U. Nierste, Eur. Phys. J. **C33** (2004) S256.
[126] M. Ciuchini, E. Franco, A. Masiero and L. Silvestrini, eConf **C0304052** (2003) WG307 [J. Korean Phys. Soc. **45** (2004) S223].
[127] P. Ball, S. Khalil and E. Kou, Phys. Rev. **D69** (2004) 115011.
[128] P. Ko, J. Korean Phys. Soc. **45** (2004) S410.
[129] E. Gabrielli, K. Huitu and S. Khalil, hep-ph/0504168.
[130] P. Ball, J.M. Frere and J. Matias, Nucl. Phys. **B572** (2000) 3;
P. Ball and R. Fleischer, Phys. Lett. **B475** (2000) 111.
[131] A.J. Buras, M. Spranger and A. Weiler, Nucl. Phys. **B660** (2003) 225;
A.J. Buras, A. Poschenrieder, M. Spranger and A. Weiler, Nucl. Phys. **B678** (2004) 455;
K. Agashe, G. Perez and A. Soni, Phys. Rev. Lett. **93** (2004) 201804, Phys. Rev. **D71** (2005) 016002.
[132] V. Barger, C.W. Chiang, J. Jiang and P. Langacker, Phys. Lett. **B596** (2004) 229.
[133] S.R. Choudhury, N. Gaur, A. Goyal and N. Mahajan, Phys. Lett. **B601** (2004) 164;
A.J. Buras, A. Poschenrieder and S. Uhlig, Nucl. Phys. **B716** (2005) 173.
[134] W.S. Hou, M. Nagashima and A. Soddu, Phys. Rev. Lett. **95** (2005) 141601.
[135] A.J. Buras, P. Gambino, M. Gorbahn, S. Jäger and L. Silvestrini, Phys. Lett. **B500** (2001) 161.
[136] G. D'Ambrosio, G.F. Giudice, G. Isidori and A. Strumia, Nucl. Phys. **B645** (2002) 155.

[137] A.J. Buras, Acta Phys. Polon. **B34** (2003) 5615.
[138] K. Agashe, M. Papucci, G. Perez and D. Pirjol, hep-ph/0509117.
[139] For a review, see A.A. Petrov, Nucl. Phys. (Proc. Suppl.) **B142** (2005) 333.
[140] For a review, see M. Pospelov and A. Ritz, Ann. Phys. **318** (2005) 119.
[141] For a recent analysis, see P.H. Chankowski, J.R. Ellis, S. Pokorski, M. Raidal and K. Turzynski, Nucl. Phys. **B690** (2004) 279.
[142] R. Fleischer, Eur. Phys. J. **C10** (1999) 299.
[143] B. Aubert *et al.* [BaBar Collaboration], Phys. Rev. Lett. **94** (2005) 161803.
[144] K. Abe *et al.* [Belle Collaboration], BELLE-CONF-0569 [hep-ex/0507037].
[145] H. Boos, T. Mannel and J. Reuter, Phys. Rev. **D70** (2004) 036006.
[146] M. Ciuchini, M. Pierini and L. Silvestrini, Phys. Rev. Lett. **95** (2005) 221804.
[147] P. Ball *et al.*, hep-ph/0003238, in 1999 CERN Workshop on Standard Model Physics (and More) at the LHC, Geneva, 1999, L.M. Mangano and G. Altarelli (Eds.), CERN-2000-004 (CERN, Geneva, 2000), p. 305.
[148] R. Fleischer, Int. J. Mod. Phys. **A12** (1997) 2459.
[149] R. Fleischer and J. Matias, Phys. Rev. **D66** (2002) 054009.
[150] B. Aubert *et al.* [BaBar Collaboration], Phys. Rev. **D71** (2005) 032005.
[151] A. Bondar, T. Gershon and P. Krokovny, Phys. Lett. **B624** (2005) 1.
[152] M. Bona *et al.* [UTfit Collaboration], JHEP **0603** (2006) 080.
[153] R. Fleischer, Phys. Lett. **B562** (2003) 234; Nucl. Phys. **B659** (2003) 321.
[154] D. London and R.D. Peccei, Phys. Lett. **B223** (1989) 257;
N.G. Deshpande and J. Trampetic, Phys. Rev. **D41** (1990) 895 and 2926;
J.-M. Gérard and W.-S. Hou, Phys. Rev. **D43** (1991) 2909; Phys. Lett. **B253** (1991) 478.
[155] N.G. Deshpande and X.-G. He, Phys. Lett. **B336** (1994) 471.
[156] Y. Grossman and M.P. Worah, Phys. Lett. **B395** (1997) 241.
[157] V. Barger, C.W. Chiang, P. Langacker and H.S. Lee, Phys. Lett. **B598** (2004) 218.
[158] XXI International Symposium on Lepton and Photon Interactions at High Energies (LP '03), 11–16 August 2003, Fermilab, Batavia, IL, USA, `http://conferences.fnal.gov/lp2003/`.
[159] 32nd International Conference on High-Energy Physics (ICHEP '04), 16–22 August 2004, Beijing, China, `http://ichep04.ihep.ac.cn/`.
[160] XXII International Symposium on Lepton and Photon Interactions at High Energies (LP '05), 30 June–5 July 2005, Uppsala, Sweden, `http://lp2005.tsl.uu.se/ lp2005/`.
[161] B. Aubert *et al.* [BaBar Collaboration], Phys. Rev. **D71** (2005) 091102.
[162] K. Abe *et al.* [Belle Collaboration], BELLE-CONF-0569 [hep-ex/0507037].
[163] R. Fleischer, Phys. Lett. **B365** (1996) 399.
[164] D. London and A. Soni, Phys. Lett. **B407** (1997) 61.
[165] M. Gronau, Y. Grossman and J.L. Rosner, Phys. Lett. **B579** (2004) 331.
[166] M. Beneke, Phys. Lett. **B620** (2005) 143.
[167] R. Fleischer, Phys. Lett. **B459** (1999) 306.
[168] M. Gronau and D. London, Phys. Rev. Lett. **65** (1990) 3381.
[169] J.P. Silva and L. Wolfenstein, Phys. Rev. **D49** (1994) 1151.
[170] R. Fleischer and T. Mannel, Phys. Lett. **B397** (1997) 269.
[171] Y. Grossman and H.R. Quinn, Phys. Rev. **D58** (1998) 017504.
[172] J. Charles, Phys. Rev. **D59** (1999) 054007.
[173] M. Gronau, D. London, N. Sinha and R. Sinha, Phys. Lett. **B514** (2001) 315.

[174] B. Aubert *et al.* [BaBar Collaboration], Phys. Rev. Lett. **95** (2005) 151803.
[175] K. Abe *et al.* [Belle Collaboration], BELLE-CONF-0501 [hep-ex/0502035].
[176] R. Fleischer, Eur. Phys. J. **C16** (2000) 87.
[177] R. Fleischer and J. Matias, Phys. Rev. **D66** (2002) 054009.
[178] C.W. Bauer, I.Z. Rothstein and I.W. Stewart, Phys. Rev. Lett. **94** (2005) 231802.
[179] C.W. Bauer, I.Z. Rothstein and I.W. Stewart, hep-ph/0510241.
[180] R. Fleischer and T. Mannel, hep-ph/9706261.
[181] Y. Grossman, M. Neubert and A.L. Kagan, JHEP **9910** (1999) 029.
[182] A.J. Buras and R. Fleischer, Eur. Phys. J. **C16** (2000) 97.
[183] D. Cronin-Hennessy *et al.* [CLEO Collaboration], Phys. Rev. Lett. **85** (2000) 515.
[184] M. Beneke and M. Neubert, Nucl. Phys. **B675** (2003) 333.
[185] T. Yoshikawa, Phys. Rev. **D68** (2003) 054023.
[186] M. Gronau and J.L. Rosner, Phys. Lett. **B572** (2003) 43.
[187] S. Mishima and T. Yoshikawa, Phys. Rev. **D70** (2004) 094024.
[188] Y.L. Wu and Y.F. Zhou, Phys. Rev. **D71** (2005) 021701; Phys. Rev. **D72** (2005) 034037.
[189] C.W. Bauer, D. Pirjol, I.Z. Rothstein and I.W. Stewart, Phys. Rev. **D70** (2004) 054015.
[190] T. Feldmann and T. Hurth, JHEP **0411** (2004) 037.
[191] A.J. Buras and R. Fleischer, Eur. Phys. J. **C11** (1999) 93.
[192] M. Gronau, D. Pirjol and T.M. Yan, Phys. Rev. **D60** (1999) 034021 [E: **D69** (2004) 119901].
[193] A. Ali, E. Lunghi and A.Y. Parkhomenko, Eur. Phys. J. **C36** (2004) 183.
[194] C.W. Chiang, M. Gronau, J.L. Rosner and D.A. Suprun, Phys. Rev. **D70** (2004) 034020.
[195] G. Buchalla and A.S. Safir, Eur. Phys. J. **C45** (2006) 109.
[196] Y.Y. Keum and A.I. Sanda, eConf **C0304052** (2003) WG420.
[197] R. Fleischer and T. Mannel, Phys. Rev. **D57** (1998) 2752.
[198] R. Fleischer, Eur. Phys. J. **C6** (1999) 451.
[199] M. Neubert, JHEP **9902** (1999) 014.
[200] A.J. Buras, R. Fleischer, S. Recksiegel and F. Schwab, Acta Phys. Polon. **B36** (2005) 2015.
[201] M. Neubert and J.L. Rosner, Phys. Lett. **B441** (1998) 403; Phys. Rev. Lett. **81** (1998) 5076.
[202] B. Aubert *et al.* [BABAR Collaboration], Phys. Rev. **D71** (2005) 111102.
[203] M. Gronau, Y. Grossman and J.L. Rosner, Phys. Lett. **B579** (2004) 331.
[204] A.J. Buras, and L. Silvestrini, Nucl. Phys. **B546** (1999) 299;
A.J. Buras, G. Colangelo, G. Isidori, A. Romanino, and L. Silvestrini, Nucl. Phys. **B566** (2000) 3; A.J. Buras, T. Ewerth, S. Jäger and J. Rosiek, Nucl. Phys. **B714** (2005) 103.
[205] G. Buchalla, G. Hiller and G. Isidori, Phys. Rev. **D63** (2001) 014015;
D. Atwood and G. Hiller, hep-ph/0307251.
[206] A.J. Buras, R. Fleischer, S. Recksiegel and F. Schwab, Eur. Phys. J. **C32** (2003) 45.
[207] C. Bobeth, M. Bona, A.J. Buras, T. Ewerth, M. Pierini, L. Silvestrini and A. Weiler, Nucl. Phys. **B726** (2005) 252.
[208] E. Baracchini and G. Isidori, Phys. Lett. **B633** (2006) 309.
[209] A.J. Buras, F. Schwab and S. Uhlig, TUM-HEP-547, hep-ph/0405132.
[210] H.R. Quinn, Nucl. Phys. Proc. Suppl. **37A** (1994) 21.
[211] R. Fleischer, Phys. Lett. **B341** (1994) 205.
[212] A.J. Buras, R. Fleischer and T. Mannel, Nucl. Phys. **B533** (1998) 3.
[213] M. Ciuchini, E. Franco, G. Martinelli and L. Silvestrini, Nucl. Phys. **B501** (1997) 271;

M. Ciuchini, E. Franco, G. Martinelli, M. Pierini and L. Silvestrini, Phys. Lett. **B515** (2001) 33;
C. Isola, M. Ladisa, G. Nardulli, T.N. Pham and P. Santorelli, Phys. Rev. **D65** (2002) 094005;
C.W. Bauer, D. Pirjol, I.Z. Rothstein and I.W. Stewart, Phys. Rev. **D70** (2004) 054015.

[214] R. Fleischer and S. Recksiegel, Eur. Phys. J. **C38** (2004) 251.

[215] P. Ball and R. Zwicky, Phys. Rev. **D71** (2005) 014015.

[216] B. Aubert *et al.* [BaBar Collaboration], BABAR-CONF-04-044 [hep-ex/0408080];
B. Aubert *et al.* [BaBar Collaboration], BABAR-PUB-05-035 [hep-ex/0507023].

[217] K. Abe *et al.* [Belle Collaboration], BELLE-CONF-0524 [hep-ex/0506080].

[218] A.K. Giri and R. Mohanta, JHEP **0411** (2004) 084.

[219] B. Grinstein and D. Pirjol, Phys. Rev. **D62** (2000) 093002.

[220] R. Fleischer and S. Recksiegel, Phys. Rev. **D71** (2005) 051501(R).

[221] A. Ali, E. Lunghi and A.Y. Parkhomenko, Phys. Lett. **B595** (2004) 323.

[222] S.W. Bosch and G. Buchalla, JHEP **0501** (2005) 035.

[223] P. Ball and V.M. Braun, Phys. Rev. **D58** (1998) 094016.

[224] B. Aubert *et al.* [BaBar Collaboration], Phys. Rev. Lett. **94** (2005) 011801.

[225] K. Abe *et al.* [Belle Collaboration], BELLE-CONF-0401 [hep-ex/0408137].

[226] K. Abe *et al.*, BELLE-CONF-0520 [hep-ex/0506079].

[227] For the press release of the Belle collaboration about the observation of the $b \to d$ penguins, see `http://belle.kek.jp/hot/lp05_press.html`.

[228] B. Grinstein, Y. Grossman, Z. Ligeti and D. Pirjol, Phys. Rev. **D71** (2005) 011504.

[229] A. Ali, P. Ball, L.T. Handoko and G. Hiller, Phys. Rev. **D61** (2000) 074024;
M. Beneke, T. Feldmann and D. Seidel, Nucl. Phys. **B612** (2001) 25;
A. Ali and A.S. Safir, Eur. Phys. J. **C25** (2002) 583.

[230] T. Hurth and T. Mannel, Phys. Lett. **B511** (2001) 196.

[231] A. Drutskoy (Belle Collaboration), hep-ex/0605110.

[232] O. Schneider, talk at the Flavour in the Era of the LHC Workshop, 7–10 November 2005, CERN, `http://cern.ch/flavlhc`.

[233] M. Carena *et al.*, hep-ph/0603106.

[234] M. Ciuchini and L. Silvestrini, hep-ph/0603114.

[235] L. Velasco-Sevilla, hep-ph/0603115.

[236] M. Endo and S. Mishima, hep-ph/0603251.

[237] M. Blanke, A.J. Buras, D. Guadagnoli and C. Tarantino, hep-ph/0604057.

[238] Z. Ligeti, M. Papucci and G. Perez, hep-ph/0604112.

[239] J. Foster, K.I. Okumura and L. Roszkowski, hep-ph/0604121.

[240] K. Cheung, C.W. Chiang, N.G. Deshpande and J. Jiang, hep-ph/0604223.

[241] Y. Grossman, Y. Nir and G. Raz, hep-ph/0605028.

[242] P. Ball and R. Zwicky, JHEP **0604** (2006) 046.

[243] A.S. Dighe, I. Dunietz, H. Lipkin and J.L. Rosner, Phys. Lett. **B369** (1996) 144.

[244] R. Fleischer, Phys. Rev. **D60** (1999) 073008.

[245] Y. Nir and D.J. Silverman, Nucl. Phys. **B345** (1990) 301.

[246] G.C. Branco, T. Morozumi, P.A. Parada and M.N. Rebelo, Phys. Rev. **D48** (1993) 1167.

[247] M. Smizanska (ATLAS Collaboration), private communication.

[248] T. Speer (CMS Collaboration), private communication.

[249] R. Aleksan, I. Dunietz and B. Kayser, Z. Phys. **C54** (1992) 653.

[250] I. Dunietz and R.G. Sachs, Phys. Rev. **D37** (1988) 3186 [E: **D39** (1989) 3515];
I. Dunietz, Phys. Lett. **B427** (1998) 179;
D.A. Suprun, C.W. Chiang and J.L.Rosner, Phys. Rev. **D65** (2002) 054025.

[251] G. Wilkinson, talk at CKM 2005, 15–18 March 2005, San Diego, CA, USA,
`http://ckm2005.ucsd.edu/WG/WG5/thu2/Wilkinson-WG5-S3.pdf`.

[252] G. Balbi *et al.*, CERN-LHCb/2003-123 and 124;
R. Antunes Nobrega *et al.* [LHCb Collaboration], Reoptimized LHCb Detector, Design and Performance, Technical Design Report 9, CERN/LHCC 2003-030.

[253] A. Khodjamirian, T. Mannel and M. Melcher, Phys. Rev. **D68** (2003) 114007.

[254] A. Abulencia [CDF Collaboration], hep-ex/0607021.

[255] A.S. Safir, JHEP **0409** (2004) 053.

[256] S. Baek, D. London, J. Matias and J. Virto, JHEP **0602** (2006) 027.

[257] M. Gronau and J.L. Rosner, Phys. Lett. **B482** (2000) 71.

[258] P.Z. Skands, JHEP **0101** (2001) 008.

[259] A. Soni and D.A. Suprun, Phys. Lett. **B635** (2006) 330.

[260] G. Buchalla and A.J. Buras, Nucl. Phys. **B548** (1999) 309.

[261] G. Buchalla and A.J. Buras, Nucl. Phys. **B400** (1993) 225.

[262] M. Misiak and J. Urban, Phys. Lett. **B451** (1999) 161.

[263] CDF Collaboration, CDF Public Note 8176 (2006) [`http://www-cdf.fnal.gov`].

[264] D0 Collaboration, D0note 4733-CONF (2005) [`http://www-d0.fnal.gov`].

[265] A.J. Buras, Phys. Lett. **B566** (2003) 115.

[266] J.R. Ellis, K.A. Olive and V.C. Spanos, Phys. Lett. **B624** (2005) 47.